AD-A078 461 DAEDALEAN ASSOCIATES INC WOODBINE MD F/G 11/5
ENGINEERING FEASIBILITY OF INTERNAL FRICTION DAMPING AS A NONDE--ETC(U)
FEB 79 D C FRESCH , L L YEAGER DOT-CG-828271-A

UNCLASSIFIED USCG-D-51-79 NL

1 OF 3
AD
A078461

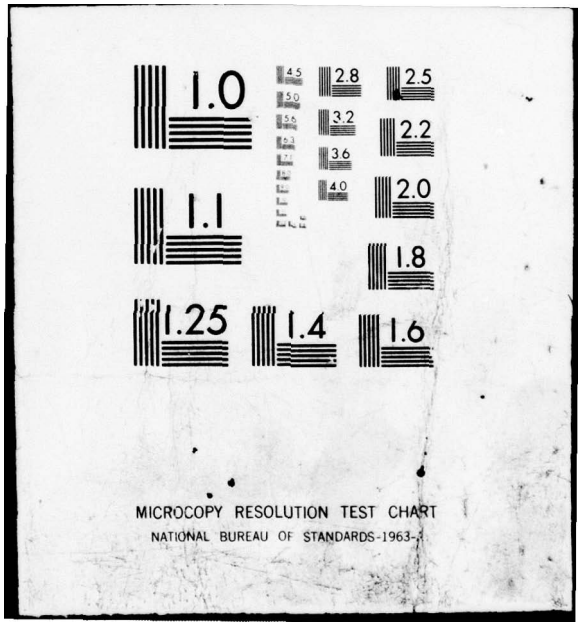
1.0
1.1
1.25
1.4
1.6
1.8
2.0
2.2
2.5
2.8
3.2
3.6
4.0
4.5
5.0
5.6
MICROCOPY RESOLUTION TEST CHART
NATIONAL BUREAU OF STANDARDS-1963-A

Report No. CG-D-51-79

ENGINEERING FEASIBILITY OF INTERNAL FRICTION DAMPING AS A NONDESTRUCTIVE EVALUATION TECHNIQUE FOR SYNTHETIC ROPES

David C. Fresch
Larry L. Yeager
and
A. P. Thiruvengadam

DAEDALEAN ASSOCIATES, INC.
SPRINGLAKE RESEARCH CENTER
WOODBINE, MD. 21797

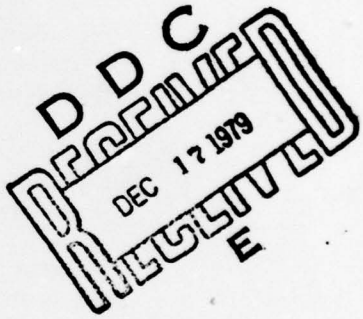

June 28, 1979

FINAL REPORT

Prepared for

U.S. DEPARTMENT OF TRANSPORTATION
United States Coast Guard
Office of Research and Development
Washington, D.C. 20590

NOTICE

This document is disseminated under the sponsorship of the Department of Transportation in the interest of information exchange. The United States Government assumes no liability for its contents or use thereof.

The contents of this report do not necessarily reflect the official view or policy of the Coast Guard; and they do not constitute a standard, specification, or regulation.

This report, or portions thereof may not be used for advertising or sales promotion purposes. Citation of trade names and manufacturers does not constitute endorsement or approval of such products.

Technical Report Documentation Page

1. Report No.	2. Government Accession No.	3. Recipient's Catalog No.
(18) US CG-D-51-79 (19)		(11)

4. Title and Subtitle (6)

ENGINEERING FEASIBILITY OF INTERNAL FRICTION DAMPING AS A NONDESTRUCTIVE EVALUATION TECHNIQUE FOR SYNTHETIC ROPES

5. Report Date: 28 February, 1979

6. Performing Organization Code:

7. Author(s) (10): David C. Fresch, Larry L. Yeager and A. P. Thiruvengadam

8. Performing Organization Report No.:

9. Performing Organization Name and Address:
DAEDALEAN ASSOCIATES, Inc.
Springlake Research Center
15110 Frederick Road
Woodbine, Maryland 21797

10. Work Unit No. (TRAIS): 784712.1.3

11. Contract or Grant No. (15): DOT-CG-828271-A

12. Sponsoring Agency Name and Address:
Department of Transportation
U. S. Coast Guard
Washington, D. C. 20590
(12) 232

13. Type of Report and Period Covered (9): Final Report

14. Sponsoring Agency Code: G-DOE-4

15. Supplementary Notes:

16. Abstract

This report discusses the technical feasibility of applying an internal friction damping, nondestructive evaluation technique for synthetic ropes. Applications for synthetic ropes include mooring lines, towing hawsers and lines for single point moorings (SPM) in deep water ports (DWP). The theory of internal friction damping is presented as it has been historically applied to metallic materials. The report then discusses the methodology for application of the internal friction damping technique to synthetic rope material and construction. The experimental apparatus and specific laboratory technique as applied to six inch and eight inch circumference rope is next discussed in detail. The report then discusses the experimental results and relates the test results to feasibility of employing the test technique as a guideline device for rope deterioration/performance. The report also relates this discussion to characteristics of the ropes tested under both wet and dry conditions. The experimental results section concludes with a comparison of the effect of the internal friction damping for various synthetic rope failure mechanisms. The report ends with specific conclusions and recommendations for further investigation into large synthetic rope testing and inspection for the ultimate feasibility determination for the potential development of DWP hawser performance hardware.

17. Key Words	18. Distribution Statement
Deep Water Ports, Synthetic Ropes, Nondestructive Testing, Internal Friction, Rope Testing, Hawser, Hawser Testing, In-situ Hawser Performance Testing.	Document is available to the public through the National Technical Information Service, Springfield, Virginia, 22151.

19. Security Classif. (of this report)	20. Security Classif. (of this page)	21. No. of Pages	22. Price
Unclassified	Unclassified	225	

Form DOT F 1700.7 (8-72) Reproduction of completed page authorized

WU → 390758

CREDITS AND ACKNOWLEDGEMENTS

This report has been prepared under the auspices of the Materials Division of the Springlake Research Center of DAEDALEAN ASSOCIATES, Incorporated.

Dr. A. P. Thiruvengadam was the Principal Investigator.

David C. Fresch was the Project Engineer. The electronic instrumentation was developed by Cushing Daniel, III and assistance was provided by John Myracle. Laurence Olver and Bruce Jachowski were responsible for data generation and fabrication of the rope support and tensioning apparatus. The electrohydraulic loading device was initially designed and fabricated by Frederick Franz. Data reduction was performed by Laurence Olver, Bruce Jachowski, Ray Brasfield and Brent Davis.

Larry Yeager is the Technical Director of the Materials Division.

The authors wish to acknowledge the organizations who have provided new and used rope samples for test under the program. New rope sections were obtained from Samson Ocean Systems, Inc.; American Manufacturing Co. Inc.; Columbia Cordage Co.; and Southwestern Cordage Co. The used rope sections were obtained from Harbour Towing Inc.; Curtis Bay Towing Co.; McCallister Drydock Co.; U.S.C.G. Curtis Bay Station and U.S. Navy, Cheatham Annex.

TABLE OF CONTENTS

LIST OF SYMBOLS

A	Cross sectional area	(in^2)
A_o	Amplitude of decay signal at reference cycle	
A_n	Amplitude of decay signal at n^{th} cycle	
B	Damping force	($lb/sec/in^2$)
C	Specific heat	($BTU/lb/^0F$)
c	Concentration	
D	Thermal diffusion coefficient	(in^2/sec)
d	Effective grain boundary thickness	(in)
E	Modulus of elasticity	(lb/in^2)
E*	Complex modulus	(lb/in^2)
E'	Real portion of complex modulus	(lb/in^2)
E''	Viscous portion of complex modulus	(lb/in^2)
$\|E^*\|$	Dynamic modulus	(lb/in^2)
f	Frequency	(Hz)
H	Activation energy	(BTU/mole)
h	Specimen thickness	(in)
I	Moment of inertia	(in^4)
j	Imaginary number	
L	Length	(in)
l	Unsupported length	(in)
m	Grain size	(in)
N	Atomic lengths	(A^o)
P	Interatomic spacing	(in)

R	Universal gas constant	(BTU/mole.^{o}R)
R	Radius of a circle	(in)
r	Radius of gyration	(in)
s	Density of disordered groups	(numbers)
T	Temperature	(^{0}R)
W	Energy	(in-lb)
Y	$\Delta W/W \times 10^{-4}$	(nondimensional)
α	Damping coefficient	(nondimensional)
β	Thermal expansion coefficient	(lb/in/^{0}F)
Δ	Incremental change	(nondimensional)
γ	Frequency parameter	(rad/sec)
ε_o	Maximum strain experienced during test	(in/in)
η	Viscosity	(lb-sec/in^2)
σ	Maximum stress applied	(lb/in^2)
τ	Relaxation time	(sec)
ϕ	Phase lag angle	(degrees)
ω	Angular frequency	(rad/sec)

LIST OF TABLES

LIST OF FIGURES

ENGINEERING FEASIBILITY OF INTERNAL FRICTION DAMPING AS A NONDESTRUCTIVE EVALUATION TECHNIQUE FOR SYNTHETIC ROPES

SYNOPSIS

One of the major requirements for the safe operation, maintenance and inspection of single point mooring hawsers used in deepwater ports is the development of a simple and reliable nondestructive evaluation technique that can be used in-service under the conditions of the ocean environment. Conventional nondestructive techniques including x-ray, ultrasonic, magnetic particle, dye penetrant and acoustic emission are not suitable for this application for various reasons discussed in this report.

A relatively new technique called Internal Friction Damping has been recently developed and has been successfully used in several applications including pressure vessels, drill string pipes and aircraft wheels. Further developments are underway to extend this technique to wire ropes in mining applications, LNG tankers for maritime industry, offshore towers for the offshore industry and nuclear power plant components for the nuclear energy industry. Because of the unique advantages offered by this technique for the inspection of SPM hawsers used in deepwater ports, the U. S. Coast Guard initiated a preliminary investigation to examine the technical feasibility of extending the internal friction technique for synthetic ropes. This program was initiated as a recommended extension to previous USCG deepwater port programs and was evaluated as a technical feasibility program because of the unique application to synthetic rope materials.

A laboratory test facility was developed for investigating the various aspects and the experimental problems associated with the synthetic ropes were resolved. The results of this program

clearly indicate that the internal friction nondestructive evaluation technique is applicable to synthetic ropes of both six inch circumference and eight inch circumference. There is also evidence to suggest that the measurement of the internal friction will not only detect impending failure, but can also be correlated to the remaining strength of the rope. Three different materials including nylon, Dacron and polypropylene were evaluated using three different constructions of rope. Both new and used ropes were studied using two different sizes. The results of these investigations show that this technique can be successfully extended to full-size SPM hawsers in-service.

However, further work is needed to accomplish this goal. For example, engineering considerations such as the specific rope construction design, various synthetic materials of fabrication, preload, in-service deterioration, failure mechanisms, water absorption, and environmental degradation including ultraviolet damage need to be evaluated before this technique can be used in the field. Detailed recommendations to meet this objective are also included in this report.

ENGINEERING FEASIBILITY OF INTERNAL FRICTION DAMPING AS A NONDESTRUCTIVE EVALUATION TECHNIQUE FOR SYNTHETIC ROPES

EXECUTIVE SUMMARY

The "Deepwater Ports Act of 1974" (Public Law 93-627, 1975) enacted legislation which authorized the Department of Transportation (DOT) to license the construction and operation of deepwater ports off the coast of the United States. Pursuant to the Deepwater Ports Act, the United States Coast Guard (USCG) conducted research in technical areas relating to deepwater port design, construction and operation. The purpose of the research was to utilize technology in order to minimize any adverse environmental impacts.

A major requirement for the deepwater port construction and operation is the design of the mooring system. Therefore, a primary aspect of the research program was the development of a report entitled, "Guidelines for Deepwater Port Single Point Mooring Design." (1)* This study investigated and provided guidelines for establishing design mooring loads for single point moorings (SPM) and the design of the SPM for load retention. Within the scope of the report, additional areas of investigation were recommended in order to develop nondestructive means of determining new rope strength because "A reliable means of determining the breaking strength of new large diameter synthetic rope by nondestructive testing as part of in-plant inspection is needed."(1) Moreover, the report further recommended that means and practices for determining used-rope strength be developed because

*Numbers in parentheses refer to references at the end of this report.

"There is also a need for a method of quickly, easily and reliably determining the strength of used rope through the inspection and nondestructive testing in the field." (1)

Therefore, in order to assist further in the charter of the Deepwater Ports Project (DWP) and to address the recommendation of the SPM guidelines study, DAEDALEAN ASSOCIATES, Inc. (DAI), under contract to the USCG, has conducted an initial technical feasibility study regarding the application of a nondestructive evaluation technique for detecting incipient failure and in-service deterioration of synthetic ropes. The rationale and motivating force for the initiation of this feasibility program lies in the fact that presently there does not exist a nondestructive evaluation system which can evaluate synthetic rope specimens subject to field service and field degradation. Current technology for rope evaluation consists of establishing engineering load carrying estimates which are obtained from cyclic loading and failure tests. Service loads are established by applying a factor of safety criteria to the load carrying test results. Synthetic rope rejection is decided by time in service and the rejection criteria is completely unrelated to load cycles of field service conditions. Presently, SPM hawsers are replaced at the Port Managers discretion, but typically semi-annually in accordance with SPM forum recommendations.(2) There are no established in-service standards for the specification of hawsers and marine towing or mooring lines, and existing field classification is sporadic and varies widely from port to port and from user to user. Therefore, many ropes are prematurely discarded or permitted in-service loads that exceed their safe load carrying capacity because of the established rejection criteria based solely upon time in-service. A nondestructive test technique which could detect

material degradation resulting from in-service conditions and at the same time influence safety criteria, establish safety standards and alleviate large inventory requirements would be beneficial to the industry.

Historically, nondestructive testing is a means of evaluating the formation and growth of cracks in homogeneous materials and/or structures. Most nondestructive testing to date has been performed on metallic materials with acoustic emission (AE) and ultrasonic test (UT) techniques being widely employed. An additional nondestructive evaluation (NDE) technique has been developed recently which utilizes the internal friction damping (IFD) properties of the material and measures the dynamic response of the structure. When a material deteriorates in service, the internal structure of the material changes and affects the damping properties. Because internal friction is an inherent material property for synthetic materials and elastomers as well as metallic materials, and because of the basic application problems that exist in applying AE and UT to synthetic ropes; a comparison of the IFD-NDE technique to AE and UT would conclude that the design and construction of the rope would preclude any reasonable responses from AE and UT inputs. For example, the rough texture and numerous rope strand interfaces with corresponding void spaces would be identified as crack initiation locations with UT. Moreover, the coupling pressure for AE would have to circumferentially contact the rope for adequate output response. Therefore, any anomaly in the rope surface would produce erroneous AE results. The IFD-NDE technique utilizes input and output transducers that need not contact the synthetic rope and therefore are not sensitive to coupling pressure. This major advantage of the IFD-NDE technique regarding a coupling method that is insensitive to pressure simplifies the test technique and increases the reliability of inspection without causing variation in data reproducibility. Similar comparisons

and conclusions can be made regarding the advantages of IFD when evaluated with AE and UT in regard to the signal to noise ratio; the input signal to output signal ratio; the effect of specimen geometry on the inspection technique; and the frequency of test in relation to the ability to locate material flaws and degradation. Of all the existing NDE techniques, IFD alone holds the possibility for defining the extent of rope deterioration in-service and for establishing inspection standards. Therefore, this program specifically addresses the feasibility of evaluating the IFD-NDE technique to synthetic rope samples.

Application of the IFD-NDE technique involves monitoring the vibrational response of test material or specimen. The specimen is vibrated at a resonant frequency, excitation source is removed, and the natural decay of the vibration is monitored. As a material experiences degradation from fatigue, abrasion, etc., the properties of the material change which causes a higher rate of energy absorption. This change is reflected in an increase in the measured internal friction damping values. The changes in the internal friction are recorded as a function of the fatigue or stress cycle history, allowing the characterization of impending material degradation and failure (crack) site formation.

Various failure modes can be observed by monitoring changes in the internal friction of the material. These include stress cracking, corrosion fatigue, hydrogen embrittlement and cyclic fatigue cracking. A prediction capability of the technique arises from the changes that occur in the specific damping capacity as the material undergoes deterioration. When the $\Delta W/W^*$ values move outside a statistical confidence bandwidth

---

*$\Delta W/W$ is the specific damping capacity. It is the change in system energy per cycle per total initial system energy.

about the baseline data, a failure mechanism can be said to be at work and that incipient failure has been initiated with the formation of crack sites.

The instrumentation package employs commercially available electronic equipment that is sensitive to amplitude and frequency analysis. The input, or source of excitation, is normally a voice-coil type mini-shaker or an electro-magnetic field transducer. These transducers vibrate the specimen and provide the input signal to the material. The output response is the natural decay of the vibration which is processed through a frequency analyzer. This allows for selective filtering of the signal and/or signal gain if a very low output signal is obtained. The decay response of the material, after the excitation source is removed, is monitored on an oscilloscope or strip chart level recorder. The level recorder automatically provides a permanent record by virtue of its operation while a Polaroid ™ photograph serves as the record for the oscilloscope display. Data is reduced by measurement of the amplitude change in signal, and the specific damping capacity ($\Delta W/W$) is calculated according to an established set of equations. A portable mini-computer is currently being phased into the data processing operation, utilizing an Analog to Digital (A/D) convertor and will replace the oscilloscope/level recorder and hand reduction process. This capability will provide immediate specific damping capacity values, and will therefore produce "in-situ" information concerning the extent of rope deterioration.

Adoption of this technique for commerical and industrial use is taking place (or being aided) through various technology transfer applications. The demonstrated record of prior experience in applying the IFD-NDE technique to various metallic structures and components has provided base line data and field service results for: 1) Bar test specimens for pressure vessel base material; 2) Pressure vessels for hydrostatic tests;

3) The Ocean Simulation Facility Hyperbaric Chamber in Panama City, Florida and U. S. Navy Submarine Fluid Dynamics Simulation Facility in Annapolis, Md.; 4) Nuclear reactor materials and components for the Nuclear Regulatory Commission, Westinghouse Electric Corp. (Advanced Reactor Division), General Electric Corp. (Nuclear Reactor Division), and the Electric Power Research Institute; 5) Drill string pipe for geothermal and offshore drilling applications for Tom Brown Drilling Co.; 6) Model offshore tower structures for the Interior Dept., U. S. Geological Survey; 7) Laboratory application to wire rope for the Bureau of Mines and Department of Energy. These programs include laboratory data and field application of the IFD-NDE technique to homogeneous metallic materials for the majority of the work performed.

An outline of the phase progression for a previous program can serve as an example for interested agencies to follow.

Specifically, a three phase program for the Civil Engineering Laboratory (CEL) has been completed successfully utilizing the IFD-NDE technique. Initial phase of the program involved feasibility testing of uniform bar test samples of representative steel types, used in the construction of CEL pressure vessels. These were 1" x 1" x 12" bars of A514 and A537 steel. A major point of this study was the indication of a weld type mismatch to the base metal. Following the successful feasibility study concerning the bar test specimens, a second phase was completed. Eight inch diameter by 37 inch long pressure vessels of similar material as the bar specimens, were evaluated. Pressure cycling of these vessels was monitored by the IFD-NDE technique. Successful completion of these tests prompted the application to two larger (18" diameter 60" long) pressure vessels. Prediction of early failure in these vessels was accomplished. CEL then granted an extension for a third phase of the program. This phase involved

the in-situ evaluation of two hyperbaric chambers at the Ocean Simulation Facility (OSF) in Panama City, Florida and the Submarine Fluid Dynamics Simulation Facility (SFDSF) in Annapolis, Md. Subsequent field data indicated satisfactory conditions at the OSF, however a crack was correctly identified at the SFDSF facility.

The above results indicate that the technical feasibility and field use of the IFD technique has been successfully demonstrated on numerous occasions for homogenous metallic materials. Based on these test results and the applicability of the test technique, the feasibility of evaluating non-homogenous viscoelastic materials was initiated.

Furthermore, in order to identify a technical feasibility program for applying the IFD-NDE technique as a detection system for measuring degradation and impending failure of hawsers, mooring lines and towing lines, the following overall objectives were identified as the Program Plan:

- Evaluate the feasibility of applying the IFD-NDE technique to synthetic ropes.
- Generate the required base line engineering data for prototype synthetic rope specimens.
- Design and develop the necessary apparatus including individual subsystems for full scale rope evaluation.
- Field test the prototype system under actual in-service operating conditions in order to demonstrate the associated performance and reliability of the equipment and technique.

The tasks required to meet these objectives must be divided into several phases. A logical approach would require Phase I to establish technical feasibility, identify system limitations, and address laboratory data generation for existing rope sizes and construction. Phase II would address an application of the test procedure for detecting impending failure

under cyclic loading for full scale rope sections. Phase III would address the in-service test and evaluation of the system for field performance.

This report addresses the initial phase (Phase I) for technical feasibility evaluation and laboratory data generation. The purpose of the initial phase of this program is to characterize the technical feasibility and applicability of the IFD-NDE technique for six inch and eight inch circumference synthetic ropes commonly used in port operations.

This is the first application of a NDE technique to synthetic ropes. Within the confines of the test matrix, it was realized that all possible scenarios for even one application could not be pursued. The approach taken was that of determining technical feasibility of applying the IFD-NDE technique to six and eight inch circumference synthetic ropes, with the promise of future use for evaluating degradation in large diameter hawsers. Moreover, it was not the purpose of the report nor was it within the scope of the program to develop particular standards for rope deterioration, but rather to assess the generic feasibility of the concept for the specific non-metallic area of synthetic ropes. The test matrix and resulting test data was designed in order to measure general rope performance as related to the specific damping capacity measurement. The major failure mechanisms for synthetic ropes such as abrasion, ultraviolet deterioration, long term immersion in water and oil, were addressed only from the standpoint of the general performance of the rope. Therefore, the cumulative contribution of these failure modes was measured, and there was no attempt made to identify the specific contribution for each failure mode on the specific damping capacity measurements. The initial phase consisted of modifying the existing equipment and technique in order to generate the required engineering data for typical synthetic rope samples

obtained from rope manufacturers and from field service. This report presents the data generated and conclusions developed as a result of the study.

The rationale for employing six inch and eight inch synthetic ropes for this initial feasibility program is found in the fact that:

- There exists an abundance of accummulated breaking strength data for these rope sizes;
- These rope sizes have current widespread availability and use as towing and mooring lines;
- The materials of construction are the same materials used in the fabrication of the SPM hawsers.

The test matrix for this program consisted of rope specimens of two sizes: six inch circumference and eight inch circumference. Three strand twisted, eight strand plaited, and double braided constructions were evaluated for nylon, Dacron ™ and polypropylene materials. Samson Ocean Systems, Inc.; American Manufacturing Co., Inc.; Columbia Cordage Co.; and Southwest Cordage Co. supplied the new rope specimens for the various construction and material combinations. Six inch and eight inch circumference rope specimens of the various materials and construction types were paired with like materials, sizes and construction types for used rope specimens. Twenty-four new rope samples were obtained, representing 17 different types (i.e.; size, material and fabrication) of rope. However, lack of availability for various types of used rope necessitated this study being confined to eight matched pairs of new and used rope specimens. Therefore, eight of these 17 different types were paired with used ropes of the same types, giving a total of 16 rope specimens which were evaluated. The matched pairs were tested under both dry and laboratory wet (saturated for 24 hours in synthetic seawater) conditions. Table ES-1 shows the size, construction and materials of fabrication for the ropes tested.

TABLE ES-1: CLASSIFICATION OF MATCHED PAIRS OF NEW AND USED SYNTHETIC ROPE SPECIMENS

SIZE / CONSTR. / MATERIAL	6" CIRCUMFERENCE 3 STRAND TWISTED	8" CIRCUMFERENCE 3 STRAND TWISTED	8" CIRCUMFERENCE DOUBLE BRAIDED
NYLON	NEW USED	NEW USED	NEW USED
POLYPROPYLENE	NEW USED	NEW USED	
DACRON™		NEW USED	NEW USED
POLY-DAC*	NEW USED		

*POLY-DAC: POLYPROPYLENE WITH OUTER FIBERS OF EACH STRAND MADE OF DACRON

The test procedure consisted of applying a tensile load on the rope specimen and vibrating the rope under tension. The natural decay of the vibration was measured and the data was translated into the specific damping capacity. The initial rope specimens were three foot lengths. However, difficulty was encountered in producing vibration in three foot lengths of the six inch and eight inch circumference rope specimens because of the low length to radius of gyration (l/r) ratio. Therefore, the test apparatus was modified in order to vibrate six foot length of rope. This provided l/r ratios of approximately 100 and these sections were easily vibrated. The test results indicated that the synthetic rope specimens could be induced to vibrate at a natural resonant frequency and the associated specific damping capacity could be measured.

The test procedure for the six foot specimens correlated the measured specific damping capacity ($\Delta W/W$) to the applied tensile load on the rope specimen. The $\Delta W/W$ value varied as the tension on the rope was increased in the range of 1% to 10% of breaking strength. When the tension was increased in the range of 15% to 20% of breaking strength, great variability was noticed in the measured $\Delta W/W$ values. Therefore, these early results prompted a more thorough investigation using three new six inch circumference, three strand nylon rope specimens. Tests conducted on these ropes indicated that the factor causing the variability of $\Delta W/W$ values was the length of time for which the particular tension level had been maintained.

The rope specimens exhibited a range of linear elastic behavior which approximated the working load range. Further investigation on the time dependent behavior of the measured specific damping capacity resulted in determining that when the rope tension was increased from zero and held at a constant

value within the working load range, the $\Delta W/W$ value decreased over time until a stable value was obtained after 60 to 100 minutes (Figure ES-1). Of considerable importance to the program was the fact that the stable specific damping capacity values remained at an essentially constant level throughout the range of linear elastic behavior.

Noting that the measured specific damping capacity is independent of the level of tension (Figure ES-2), above some minimum tension, resulted in important test ramifications. These results indicate that:

1. The specific damping capacity measurements agree with the theoretical understanding of the viscoelastic behavior of the synthetic rope.
2. The independence of the measurement eliminated the need to test every rope specimen at a multitude of tension levels and therefore allowed more rope sections to be investigated under this program than would have been otherwise possible.
3. There were occasions during the course of the program when the fundamental frequency was very close to the 60 Hz power frequency, causing difficulty in data analysis because of interference and "beating" of the driven resonance and the 60 Hz noise provided by the electrohydraulic tensioning apparatus. Knowing that $\Delta W/W$ was independent of the level of tension allowed the tension on the rope specimens to be increased or decreased in order to change the resonant frequency significantly to allow the 60 Hz noise interference to be electronically filtered.

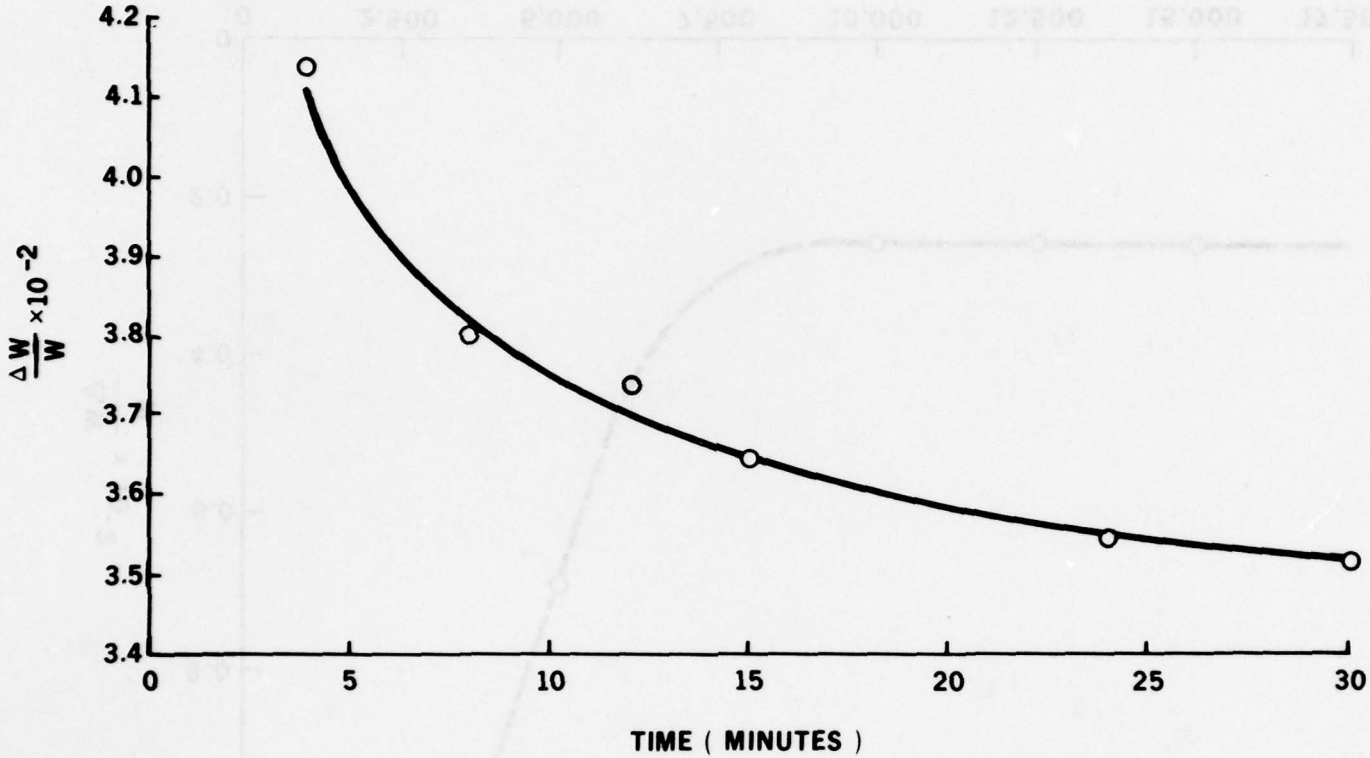

FIGURE ES-1 SPECIFIC DAMPING CAPACITY $\left(\frac{\Delta W}{W}\right)$ VS. LENGTH OF TIME UNDER LOAD OF 11,250 POUNDS FOR A NEW 6" CIRCUMFERENCE, 3 STRAND NYLON ROPE SPECIMEN

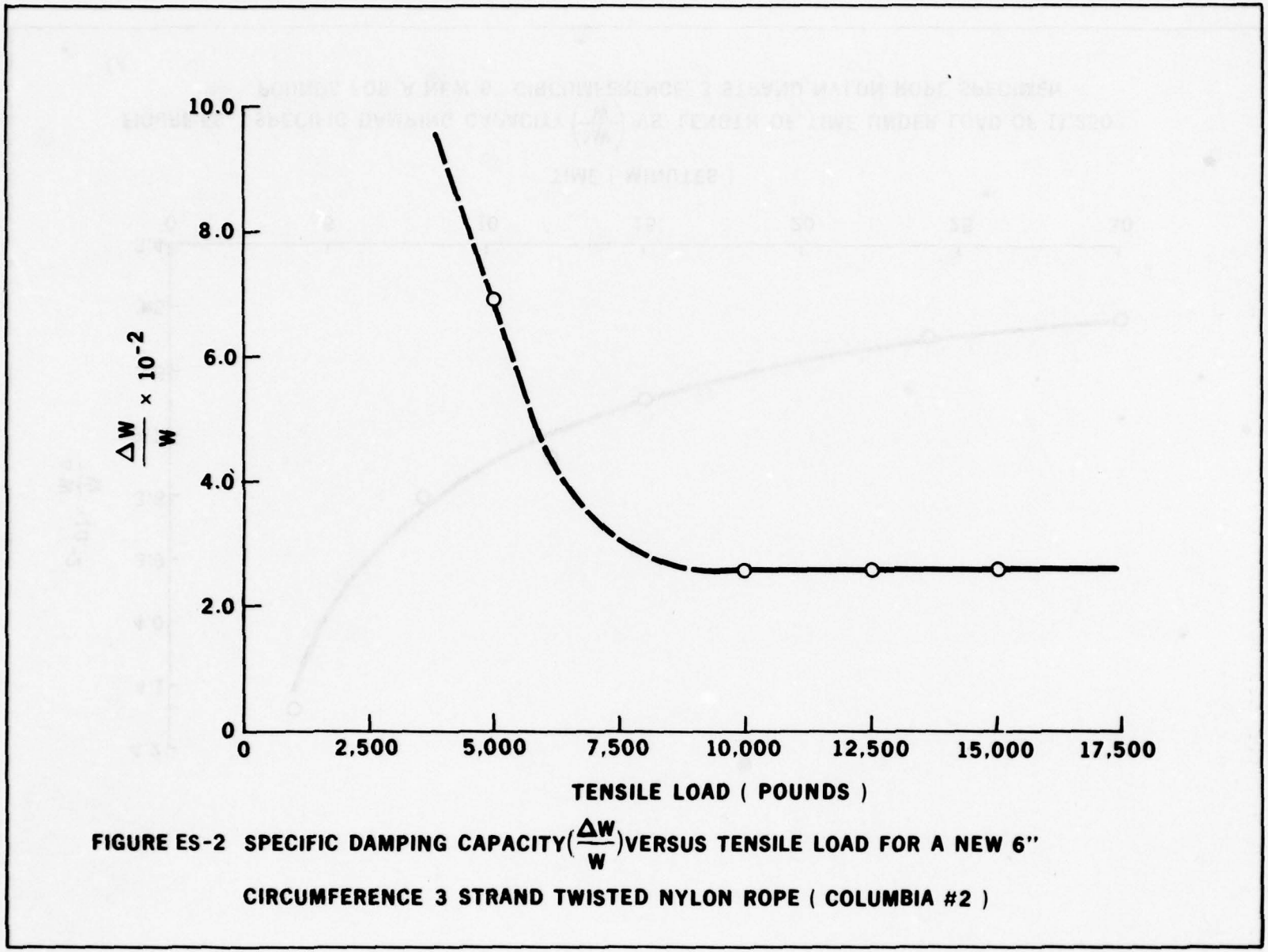

FIGURE ES-2 SPECIFIC DAMPING CAPACITY($\frac{\Delta W}{W}$)VERSUS TENSILE LOAD FOR A NEW 6" CIRCUMFERENCE 3 STRAND TWISTED NYLON ROPE (COLUMBIA #2)

4. For possible future field applications, a precise level of tension will not be required so long as the tension is approximately constant and is within the range of linear elasticity.

It was also found that rope specimens which had experienced stresses in excess of the elastic limit during early testing exhibited specific damping capacity values 20% higher than a similar virgin specimen. This is a preliminary indication of the ability of the internal friction damping NDE technique to detect material degradation in synthetic ropes.

Within the confines of the test matrix, comparisons were made of the specific damping capacity values on dry and laboratory wet rope specimens. For polypropylene ropes, the measured specific damping capacity was lower when tested wet than when tested dry. It is hypothesized that because the polypropylene ropes are constructed of hard, nonabsorbent, monofilament fibers, the water acts as a lubricant, reducing the friction between the fibers and consequently reducing the damping. When nylon rope specimens were tested under the laboratory wet condition, the associated values were always higher than when tested dry. Dacron™ rope specimens also exhibited a general increase in $\Delta W/W$ values when tested wet. Used Dacron™ ropes showed a larger difference between wet and dry values than did new ropes of the same type. Furthermore, Poly-Dac specimens (three strand polypropylene with Dacron™ outer fibers) exhibits a 40% to 60% increase when tested in the laboratory wet condition as opposed to dry.

The results of the test program which compared the new and used specimens are provided in the following findings:

1. Three of the matched pairs contained used specimens which showed no visible signs of deterioration. Measurement of the specific

damping capacity also indicated no evidence of material deterioration.

2. The six inch circumference three strand nylon rope specimen appeared to be work hardened but showed no difference in specific damping capacity over the new specimen. Two new specimens which had been overstressed consistently gave 20% higher $\Delta W/W$ values than a virgin specimen when tested under both dry and laboratory wet conditions.
3. Two of the matched pairs contained used rope specimens which showed visible deterioration with numerous abrasions and cut and broken strands. Specific damping capacity values for the used specimens were between two and three times greater than for the new specimens. Both used specimens subsequently failed under load testing.
4. Comparison of the percent change in $\Delta W/W$ from new to used rope sections with the percentage of original breaking strength at which the used ropes failed, indicated that a correlation between normalized specific damping capacity versus the percentage of rating breaking strength for abraded ropes. Test results for the comparison between new and used eight inch circumference, three strand polypropylene specimens were inconclusive.
5. The measurements of specific damping capacity for the six inch circumference, three strand Poly-Dac specimens showed an anomaly in that the first used specimen tested showed no difference in $\Delta W/W$ from the new specimen.

Visually, the specimen was only moderately abraded however, it failed under a load of 20,000 pounds when fatigue cycling was attempted.

After completing the testing of the eight matched pairs of ropes, a six inch circumference, three strand nylon rope was subjected to stress cycling using a tensile load in excess of the upper limit of the range of linear elasticity. Subsequent testing yielded a $\Delta W/W$ value approximately twice that of the virgin specimen.

Based on the test results of the program, this report concluded that monitoring the dynamic response of synthetic ropes as a function of the work-cycle history is a viable, nondestructive technique for detecting impending failure and material degradation due to fatigue and abrasion. The results of this program are an important milestone in accomplishing the overall objective of utilizing the internal friction damping nondestructive evaluation (IFD-NDE) technique in order to detect impending failure and/or deterioration of SPM hawsers, mooring, towing and other marine lines.

The results of this program indicate that the IFD-NDE technique is applicable to synthetic ropes of both six inch circumference and eight inch circumference. Applicability has been demonstrated for all three materials of fabrication and constructions. Moreover, the initial test results also indicate a probable correlation between specific damping capacity and remaining strength of the rope specimen (Figure ES-3).

As a result of the tests, this report concludes that:

1. The measured specific damping capacity is dependent upon the length of time that a constant tensile load has been maintained. The measured specific damping capacity decreases over time until the rope specimen

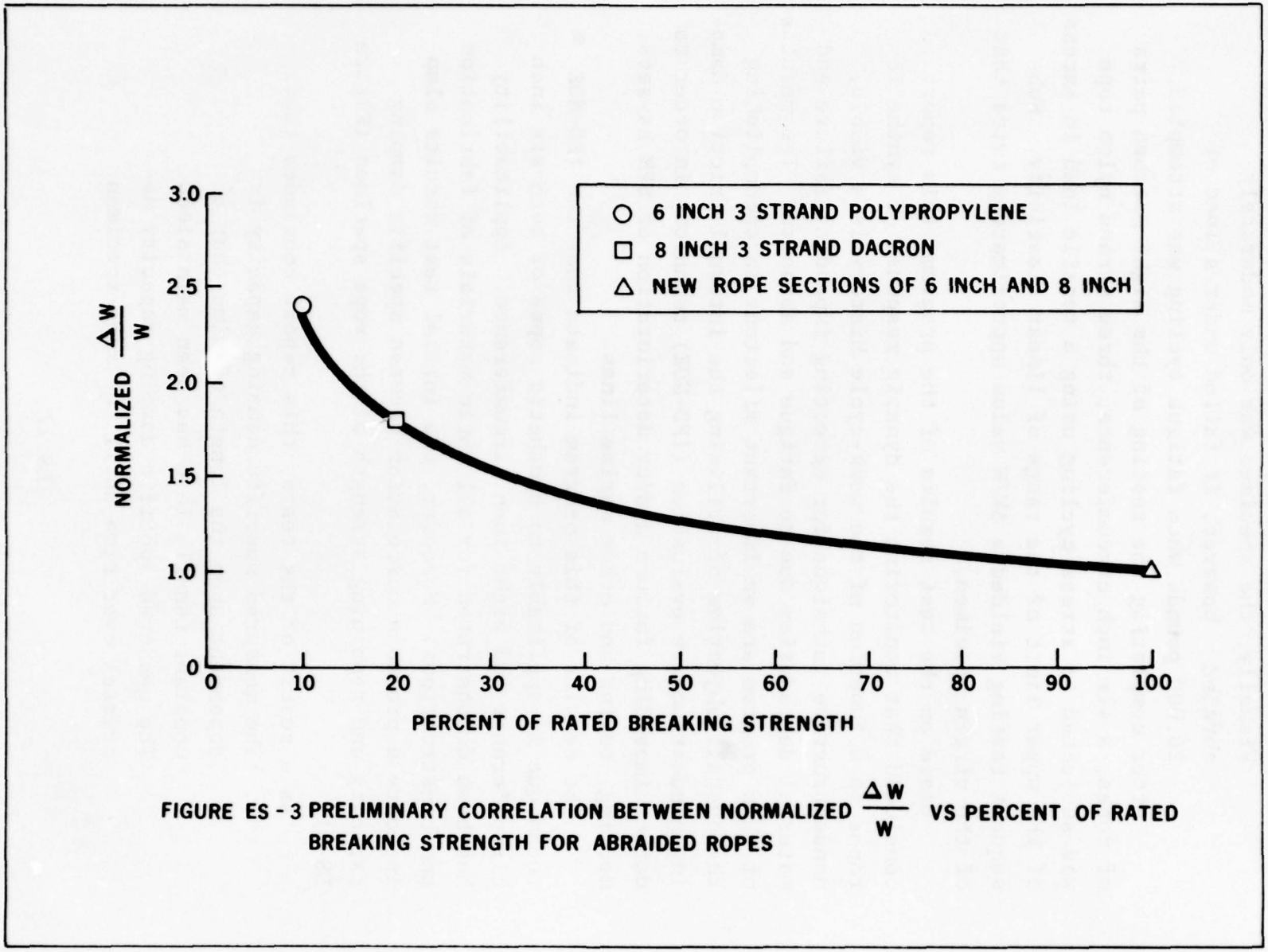

FIGURE ES - 3 PRELIMINARY CORRELATION BETWEEN NORMALIZED $\frac{\Delta W}{W}$ VS PERCENT OF RATED BREAKING STRENGTH FOR ABRAIDED ROPES

reaches equilibrium, at which time a stable minimum value of specific damping capacity is obtained.

2. Proper utilization of the technique for synthetic ropes requires the tension to be maintained in the linear elastic range, as tension levels below this range will lead to inaccurate measurements of $\Delta W/W$ and tension levels above this range cause permanent deformation of the specimen.
3. A minimum ratio between unsupported length of rope and radius of gyration of the rope cross-section (l/r) of approximately 100 is needed in order to produce the stable vibration necessary to utilize the internal friction damping technique.
4. The input signal strength and the output signal strength are not critical, thereby eliminating the need for precise positioning of the transducers.

This report also makes several general conclusions concerning measurement of specific damping capacity for dry specimens versus saturated specimens. These conclusions are enumerated below and discussed in detail in Section 4.4 of the report. However, it must be realized that these conclusions are qualitative in nature and are general conclusions based on a limited number of tests and on an associated limited data base. More specific quantitative conclusions will be possible after additional testing is accomplished.

1. Saturated polypropylene ropes generally have a lower measured specific damping capacity than the same ropes tested dry.
2. Saturated nylon and Dacron™ ropes generally

have a higher measured specific damping capacity than the same ropes dry.

3. It is feasible to conduct the technique under either condition, as the eight inch three strand Dacron™ specimen which experienced failure had significantly higher specific damping capacity values than the new specimen under both conditions.
4. Correlation of specific damping capacity to remaining strength appears to be immediately feasible for dry rope specimens.
5. Correlation of specific damping capacity to remaining strength for saturated specimens appears to be feasible. However, further investigation is necessary in order to quantify all the effects of water saturation such that meaningful correlations can be made.

In reviewing the above listed conclusions, the application of the IFD-NDE technique to the synthetic ropes is seen to be feasible. However, the conclusions are limited, stemming from the lack of a representative data base. Because of these limitations and the results of the application of the technique to synthetic materials, the following further work is recommended as a continuation of this initial feasibility program:

1. Additional data needs to be acquired to determine the feasibility of correlating synthetic rope conditions to remaining useful life.
2. Additional data is required to refine the length to radius of gyration constraint indicated in the results.

3. A prototype design and working model of a field test machine is required to implement the field IFD-NDE technique.
4. The acquisition of a field data base would be required in any future work to be performed.
5. Other vibrational modes, materials, constructions and tests should be performed on laboratory specimens to define adequately the entire range of expected results for specific damping capacity measurements.
6. Specific and major failure mechanisms of ropes, sections, lines, and hawsers should be adequately defined for the purpose of establishing quantitative failure guidelines.

In order to develop the internal friction damping technique to full utilization for synthetic materials, other work outside the scope of the present program would be required. This includes:

1. Fatigue cycle monitoring of full size hawsers would accelerate the transfer of this technology to the SPM hawser safety program. The preliminary correlation made under this program between remaining strength and specific damping capacity should be refined. This work would permit a correlation to be made between specific damping capacity and remaining useful life for full size hawsers subject to cyclic fatigue. The inclusion of environmental degradation in the test matrix via exposure to ultraviolet radiation, salt water immersion, etc. of certain samples would permit quantifying the effects on the specific damping capacity value of the various environmental forces.

This work may be expedited through interaction with Coordinated Equipment Company in California, as Coordinated Equipment has the apparatus for fatigue cycling full scale hawsers.

2. Acquisition of field data to acquire adequate information on all Coast Guard approved lines, ropes, braces and hawsers, as well as spliced sections, eye splices, etc. This information would allow the determination of standard regions of safe operation for these lines, based on the correlations which could be made to specific damping capacity.
3. Feasibility studies are suggested where other synthetic materials are used in marine applications. Some areas where feasibility studies should be performed are floating hoses used in conjunction with SPM systems, hovercraft skirts, buoy mooring lines, composite structural materials. Investigations should also be conducted to determine the feasibility of utilizing the internal friction damping technique as an aid to quality control at the point of manufacture for various items used in the marine industry.

In conclusion, the successful contribution of the IFD-NDE technique to the investigation for a nondestructive test technique applied to synthetic materials has been defined. Specifically, the first study of applying the technique to six inch and eight inch circumference synthetic rope specimens has shown feasibility of application to synthetic ropes. Rope specimens have been found to have characteristic repeatable specific damping capacity values, which are affected by degradation due to fatigue and abrasion. Based upon the test data, the technique is applicable not only to small and medium

size hawsers, but also full size SPM hawsers. Further work leading to utilizing this technique for full size SPM hawsers has been recommended and is strongly suggested. This technique may also be applicable to many other synthetic materials, both for field evaluation of items in-service and for quality control of newly manufactured items.

All of the objectives of the synthetic rope feasibility study have been met. Ropes of various synthetic materials, constructions and sizes have been tested, both dry and in the saturated laboratory wet condition. The data was analyzed and specific damping capacity values were correlated to the visible condition of the ropes. Differences between new and used ropes of similar size, material and construction were noted. Differences between the values obtained in the dry and laboratory wet conditions were also noted.

Conclusions have been drawn from the results. Where firm conclusions could not be made but trends were noted, these were discussed and the work needed to arrive at firm conclusions was identified. Recommendations for further work needed to bring the IFD-NDE technique to full utilization in the evaluation of synthetic ropes and hawsers have been made. Recommendations for further work in related areas and for feasibility studies for other synthetic material marine applications have also been made.

ENGINEERING FEASIBILITY OF INTERNAL FRICTION DAMPING AS A NONDESTRUCTIVE EVALUATION TECHNIQUE FOR SYNTHETIC ROPES

1.0 INTRODUCTION

The "Deepwater Ports Act of 1974" (Public Law 93-627, 1975) enacted legislation which authorized the Department of Transportation (DOT) to license the construction and operation of deepwater ports off the coast of the United States. Of primary concern to the licensor is that the licensee of the deepwater port can demonstrate the utilization of best available technology in order to minimize any adverse environmental impact. Pursuant to the Deepwater Ports Act, the United States Coast Guard (USCG) conducted research in technical areas relating to deepwater port design, construction, and operation.

A major requirement for deepwater port construction and operation is the design of the mooring system. Therefore, a primary aspect of the research program was the development of guidelines for deepwater port single point mooring design. (1) This study investigated and provided guidelines for establishing design mooring loads for single point moorings (SPM) and for the design of mooring components of SPM's. Within the scope of the report, additional areas of investigation were recommended in order to develop nondestructive means of determining new rope strength because, "A reliable means of determining the breaking strength of new, large diameter synthetic rope by nondestructive testing as part of in-plant inspection is needed." Moreover, the report further recommends that means and practices for determining used-rope strength be developed because, "There is also a need for a method of quickly, easily and reliably determining the strength of used rope through the inspection and nondestructive testing in the field." (1)

Therefore, in order to assist further in the mission of the Deepwater Ports Project (DWP), and to address the recommendations of the SPM guideline study, DAEDALEAN ASSOCIATES, Inc. (DAI) under contract to the USCG has conducted an initial technical feasibility study regarding the application of a nondestructive evaluation technique for detecting the incipient failure of synthetic ropes used in single point moorings of ships. The nondestructive evaluation technique utilizes the phenomenon of internal friction of the synthetic rope for detecting incipient failure modes. Under the present program, this technique has been utilized for the nondestructive evaluation of "as-received" rope sections and for "in-service" rope specimens with various degrees of degradation.

1.1 Background

Deepwater ports for very large crude carriers (VLCC) are an essential element to the solution of our nation's energy transportation needs. VLCC's increase the efficiency of oil transport by supplying larger quantities per ship as well as reducing the potential of critical oil shortage transportation occurrences to the United States.

1.1.1 SPM Definition

Following Exxon (1), an SPM system for tankers is defined; the SPM for tankers consists of an integrated mooring and cargo transfer system which incorporates either a cargo swivel concentric with the mooring system or a mooring swivel concentric with the cargo system so the tanker can freely swing around the mooring in response to the environment while simultaneously transferring cargo.

The single point mooring system is an ideal system for mooring VLCC's because, "The tanker is free to align itself into the environment at an SPM, minimizing mooring forces. Thus, the tanker can remain moored and continue transferring cargo in environments more severe than could be

tolerated at moorings, such as piers and multiple buoy berths, where the tanker is held in a fixed heading. One of the principle advantages of an SPM is it can be located offshore in uncongested deepwater instead of in protected, crowded harbors and bays." (1) Several SPM systems have been designed, including the catenary anchor leg mooring (CALM), the single anchor leg mooring (SALM) and the tower type SPM. Of these three principle types of SPM, the CALM is presently the most used. Figure 1 illustrates a typical CALM system.

A further advantage to the port operator of the SPM over multipoint mooring is a reduction in capital equipment cost resulting from the reduced amount of rope required for handling the ship.

1.1.2 SPM Hawser Replacement

Presently, SPM hawsers are replaced at the port manager's discretion, usually quarterly or semi-annually in accordance with SPM Forum Recommendations. (2) This is a preventive measure undertaken to reduce the possibility of a hawser failure. Hawser failures are most likely to occur during storms, when high seas and strong currents induce additional stresses on the hawser. Failure of the hawser could result in extensive damage to the deepwater port due to a collision between the ship and the mooring buoy. Hawser failure could also result in ecological damage due to an oil spill if the failure should occur during loading or unloading operations.

The capability to detect loss of mooring line integrity and impending failure of these lines using a nondestructive evaluation technique would avoid failures which result in the aforementioned damages. Moreover, such a technique would allow the hawsers to continue in service as long as the operational criteria for service is met. Proper utilization of such a technique would minimize the costs associated with both potential hawser failures and premature hawser replacement, and would assist the shipping and transportation industries in the application of state-of-the-art technology.

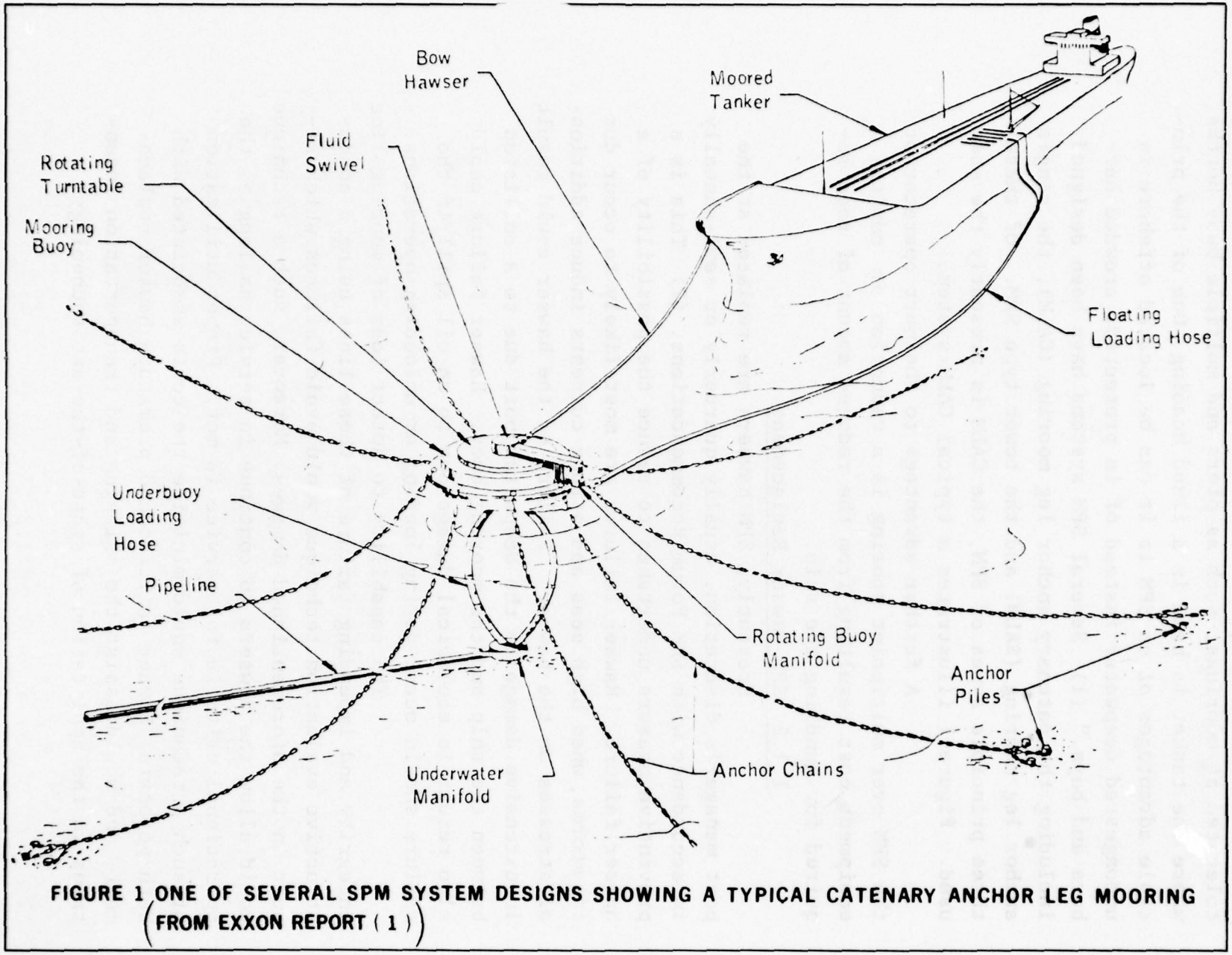

FIGURE 1 ONE OF SEVERAL SPM SYSTEM DESIGNS SHOWING A TYPICAL CATENARY ANCHOR LEG MOORING (FROM EXXON REPORT (1))

1.1.3 IFD-NDE Background

In order to present a chronological representation of laboratory test data to full scale application and field usage, the following three phase program regarding manned hyperbaric pressure chambers is discussed. Initially, bar specimens one inch square by twelve inches long were evaluated for the U. S. Navy, Naval Facilities Engineering Command (NAVFAC). These bar specimens were fatigued in flexure utilizing three point loading to a total of 10^5 cycles to fracture. The materials were ductile steel (A514 and A537) with yield stresses of 100KSI and 120KSI. Six bars were notched and welded while the remaining six bars were notched and did not contain any welds. Base line data was evaluated for all bars before fatigue cycling began. Data was obtained at convenient intervals throughout the load cycle history of the bar specimens. Measured IFD values indicated incipient crack formation in all 12 bars, with cracking being predicted from 60% to 90% of the ultimate load cycle life of the various bar combinations (i.e., welded A514, unwelded A537, etc.). An important conclusion from the applied testing enabled the identification of a mismatch of weld material to base material to be made. This conclusion was supported by test data and subsequently confirmed by NAVFAC personnel.

The Naval Civil Engineering Laboratory (CEL) extended the application of the IFD-NDE technique to pressure vessels of similar material as the bar specimens. Eight inch diameter by 37 inch long pressure vessels (.337 inch wall thickness) were constructed of Schedule 100-A53 steel. The vessels were notched along the longitudinal axis at the midspan so that failure would occur in approximately 10^4 load cycles. The pressure vessels were failed by applying pressure cycle loads of 3,000 psi; cycling the pressure between extremes of 50 psi and 3,000 psi. Base line data was collected and the fatigue cycling was initiated on the five pressure

vessels. In all cases the IFD-NDE technique predicted incipient failure of the pressure vessels. The results of the tests indicated that the prediction of failure could be correlated to the measured specific damping capacity. Moreover, the prediction of incipient crack formation occurred at 80% to 90% of the ultimate life of the pressure vessels. The logical extension of the IFD-NDE technique from thin walled pressure vessels was further confirmed by the results of thick walled pressure vessel tests.

Two additional pressure vessels 60 inches in length and 18 inches in inside diameter with a three inch wall thickness were evaluated utilizing the IFD-NDE technique. These vessels were evaluated with the previously established test procedure which resulted in a failure prediction at 2,000 pressure cycles for Vessel 1 and 10,000 pressure cycles for Vessel 2. The vessels failed after 3,000 and 14,000 cycles respectively although they were designed to rupture at approximately 100,000 cycles. The prediction of failure in the pressure vessels also indicated the location of the crack that was correct within three inches of the actual crack (well within the limitation of the instrumented quadrant of the vessel). The failure was caused by an end plate failure in a butt weld. The pressure vessel did not crack along the machined notch as it was designed to do.

The results of the previously reported programs led to the application of the IFD-NDE technique to two large and complex hyperbaric pressure chambers. Results of tests conducted on laboratory pressure vessels provided base line data on the Ocean Simulation Facility (OSF) pressure chamber in Panama City, Florida and the Submarine Fluid Dynamics Simulation Facility (SFDSF) in Annapolis, Md. The OSF has three major systems which consist of a main chamber 15 feet in diameter and 40 feet long, a transfer chamber 12 feet in diameter and 15 feet long, and five smaller connected

chambers measuring six feet in diameter and six feet long. Various on-site inspections including base line evaluation of the OSF pressure chamber have indicated no incipient crack formation has taken place. This result has been confirmed by frequent in-service inspection by the U. S. Navy Inspector General's proof load pressure cycle tests.

Additional IFD-NDE results were acquired on the SFDSF for both base line and in-service conditions. The results of field tests indicated that an incipient crack was forming near a relief valve weld. Subsequent hydrostatic tests at 110% of yield opened the crack and demonstrated the successful application of the IFD-NDE technique in isolating and predicting the crack formation.

In addition to the pressure chamber tests, various component parts (cap bolts, bypass lines, primary piping systems, etc.) of nuclear reactors have been evaluated and are in the process of being field tested utilizing the IFD-NDE technique. The nuclear industry's inspection procedures are required to identify incipient failures because of the inherent safety requirements of the system. The field service test conditions in the reactor environment require internal pressure of 1100 psig, 288°C fluid temperature with flow conditions of 2500 gpm and mechanical loading of 1370 psig for the calculated hoop stress in the feedwater pipe system. Moreover, the application of the IFD-NDE technique to drill string pipe, an offshore platform model and wire rope specimens, confirmed the expected results of incipient cracking, material degradation and failure detection. The drill string pipe program initially identified the correlation of measured specific damping capacity to a measure of time of use of the drill pipes. The internal friction damping values were recorded for numerous tests along with base line values and associated confidence limits. The generated data base enabled a mathematical model to be postulated that accounted for various individual and combined

forms of degradation and failure. The established failure criteria that was based on the accumulated data was then correlated to the internal friction damping measurements. Thus, the rejection criteria based on IFD measurements for individual and combined failure modes was established. This rejection criteria will be evaluated by field data and will confirm the failure mechanism model. A specification based on the failure mechanism model and the rejection criteria that utilizes the IFD measurements is being established for drill string pipe. This specification will enable the user to define adequately that time in the load cycle history of his drill pipe that the pipe can no longer function as it was intended. The evaluation and confirmation of the failure mechanism model through field testing is being performed at this time.

1.2 Objectives of Program

A complete research and development effort for the application of a nondestructive evaluation technique for detecting impending failure of SPM hawsers and mooring lines would be carried out in a three phase program. The following overall objectives are required in order to complete this program:

PHASE I

- Evaluate the feasibility of applying the IFD-NDE technique to synthetic ropes.
- Generate the required base line engineering data for the specific application to synthetic ropes used in marine scenarios, particularly as related to potential DWP usage.

PHASE II

Design and develop the necessary apparatus including individual subsystems for testing and evaluation in the field.

PHASE III

- Field test the prototype system under actual in-service operating conditions in order to evaluate and demonstrate the associated performance and reliability of the equipment and technique.

This document presents the final report for the initial phase of technical feasibility evaluation and laboratory data generation. The purpose of the initial phase of this program has been to answer specific questions regarding the feasibility and applicability of an internal friction damping nondestructive evaluation technique for six and eight inch circumference synthetic ropes commonly used in port operations. The initial phase consisted of modification of the existing equipment and technique, and then the generation of the required engineering data for typical synthetic rope samples obtained from both rope manufacturers and field service.

1.2.1 Task Statements

In order to address the purpose of the technical feasibility and laboratory data generation (Phase I), specific tasks were performed. The program contained the following seven tasks.

TASK I - Modify the internal friction damping instrumentation system for synthetic rope application.

TASK II - Procure synthetic rope samples from American Rope Manufacturing Co., Columbia Cordage Co., Southwestern Cordage Co., and Samson Ocean Systems, Inc.

TASK III - Obtain the specific damping capacity (internal friction damping) response of the "as manufactured" sections of six and eight inch circumference rope sections.

TASK IV - Obtain from port operators, tanker operators, and towing companies samples of used rope sections identical in material, construction and size to the "as manufactured" rope sections.

TASK V - Measure the specific damping capacity response of the used rope sections.

TASK VI - Analyze and correlate the specific damping capacity response for "as manufactured" rope sections and compare to used rope sections of the same size, construction and material.

TASK VII - Prepare a Technical Report and progress reports that reflect the salient accomplishments of the program at specified intervals.

This report presents the data generated and conclusions developed as a result of the study. Section 2 of the report discusses the theory and application of internal friction damping. Section 3 discusses the experimental apparatus and measuring technique. Section 4 is a discussion of the experimental results. The conclusions and recommendations are discussed in Sections 5 and 6.

1.3 Scope of the Program

The scope of the technical feasibility program has included six and eight inch circumference rope. The rope conditions were tested "as received" and after field service. Both laboratory wet* and dry conditions were evaluated. Three constructions (three strand twisted, eight strand braided and double braided) were analyzed and included in the overall scope of work. The three common materials of construction that were utilized were nylon, Dacron and polypropylene. The specific type of nylon used in each rope specimen is unknown.

Several different manufacturers provided the new rope sections. The used rope sections were obtained from several marine towing companies and related marine industries. Matched pairs of new and used rope were tested in regard to the material, the construction and the circumference. The ropes were tested in six foot sections under tensile loads which varied from 5% to 20% of the breaking strength. Nominal applied load to the six inch circumference rope was 10,000 pounds, and the associated applied load to the eight inch circumference rope was 20,000 pounds. Specific damping capacity measurements were made as a function of the established time dependency of the test interval. These measurements were used to evaluate the technical feasibility of utilizing the specific damping capacity for synthetic rope (hawsers) applications.

---

* Laboratory wet = Soaked for at least 24 hours in synthetic sea water solution.

2.0 THEORETICAL DEVELOPMENT OF INTERNAL FRICTION DAMPING

The theory presented in this chapter includes a discussion of internal friction damping on macroscopic and microscopic scales. The macroscopic view of internal friction damping is a relaxation process. The microscopic view considers the motion of dislocations which are pinned down by impurities and other dislocations. These two views are evaluated from the thermal diffusion coefficient and from the activation energy required to pass two dislocations over each other.

2.1 Internal Friction Damping of Materials

It is well known for over a century that materials manifest deviations from perfect elastic behavior even at small stress levels. Zener (3) called this behavior "anelasticity." Since real solids are never perfectly elastic, some of their mechanical energy is always converted into heat. The various mechanisms by which this occurs are collectively termed as internal friction damping. Moreover, real solids exhibit a hysteresis loop whereby the stress-strain curve for decreasing stresses does not exactly retrace its upward path. Even though the offset in the magnitude of the hysteresis loop is negligible for static loading, it is an important factor in the materials' dynamic response. In addition to hysteresis, viscoelastic materials exhibit mechanical relaxation by an asymptotic increase in strain resulting from the sudden application of a fixed stress; and conversely, by an asymptotic relaxation in stress whenever they are suddenly strained. This mechanical relaxation has an associated relaxation time, the direct result of which is the severe attenuation of vibrations whenever the imposed frequency has a period that approximates the relaxation time.

2.1.1 Specific Damping Capacity Definition

The most direct method for defining internal friction damping is by the specific damping capacity.

Precisely, the specific damping capacity, Y, is defined by:

$$Y \equiv \frac{\Delta W}{W} \qquad [1]$$

where:

ΔW = the energy dissipated in one cycle, and

W = the total energy of the cycle.

The mechanism by which the energy is dissipated may be any one of the following (4):

1. relaxation by thermal diffusion,
2. relaxation by atomic diffusion,
3. relaxation by magnetic diffusion,
4. relaxation by ordered distributions,
5. relaxation of preferential distributions,
6. stress relaxation along previously formed slip bands,
7. stress relaxation across grain boundaries, and
8. stress relaxation across twin interfaces.

2.1.2 Application of Internal Friction Damping

The phenomenon of internal friction damping of materials is used throughout the world to test authenticity of coins, the soundness of castings, the operating conditions of railroad wheels, and the quality of musical instruments and glassware by listening to the tone and duration of sound. (5) The study of internal friction damping has been very useful as a research tool in physical metallurgy, in vibration control of high speed missiles, planes, and vehicles, in fatigue of materials, and in the study of the mechanical properties of viscoelastic materials from the standpoint of theoretical and analytical verification. There are various technical terms to characterize this phenomenon: internal

friction damping, logarithmic decrement, hysteretic constant, viscosity, elastic phase constant, specific damping capacity, and so on. For the purposes of this report, internal friction damping describes the technique for utilizing the specific damping capacity of the synthetic rope. Internal friction damping measurements are a standard technique (6-11) for evaluating how energy is absorbed as a function of changing material variables. These material variables include the grain size, the chemical composition, interstitial elements, dislocations, precipitate particles, strain rate effects, etc. The study presented in this report is the first research undertaken to apply the internal friction damping nondestructive evaluation technique (IFD-NDE) to a nonlinear elastic material.

2.2 Macroscopic Evaluation of Internal Friction Damping

From the theory of elasticity based on Hooke's Law, a body is considered in equilibrium under the action of applied forces when the elastic deformations take on static values. Many solids do not depart seriously from this perfectly elastic behavior for small deformations and the obtained results agree well with the predictions from the elastic theory. Within the realm of Hooke's Law, the only differences between individual solids results from differences in their elastic constants and their densities. However, when solids are subjected to forces that are rapidly changing, the response to these forces must be considered in terms of the dynamic elastic properties of the material. (12)

Real solids are never perfectly elastic, so when they are set in vibration, some of the mechanical energy is always converted to heat. Thus, during vibrations, the natural oscillations of the specimen decay even if it is environmentally isolated. The various mechanisms by which this occurs are collectively termed as internal friction damping. The vibrational amplitude of a specimen should, in the absence of internal

friction damping, increase indefinitely when vibrating at its resonant frequency; but, in practice, this amplitude always assumes a finite value. Moreover, real solids exhibit a hysteresis loop whereby the stress-strain curve for decreasing stresses does not exactly retrace its upward path. Even though the magnitude of the hysteresis loop is negligible for static loading, it is an important factor in the materials' dynamic response. In addition to hysteresis, viscoelastic materials exhibit mechanical relaxation by an asymptotic increase in strain resulting from the sudden application of a fixed stress; and conversely, by an asymptotic relaxation in stress whenever they are suddenly strained. This mechanical relaxation has an associated relaxation time, the direct result of which is the severe attenuation of vibrations whenever the frequency of vibration has a period that approximately equals the relaxation time. As previously stated, the most direct method defining internal friction damping is the ratio $\Delta W/W$, where ΔW is the energy dissipated in one cycle and W is the total elastic energy of the cycle. This ratio is called the specific damping capacity and can be measured for a given response frequency of the specimen.

2.2.1 Internal Friction Damping as a Relaxation Process

For viscoelastic materials, it was shown by Zener (13) that internal losses are the contributing factor for internal friction damping; and therefore, the mechanism of internal friction damping is described herein as a relaxation process. For vibrations whose frequencies are comparable with the time required for the relaxation process, there is an irreversible conversion of mechanical energy into heat which appears as internal friction damping. Zener (14) has solved this heat transfer problem, and for vibrating strings the specific damping capacity is given by:

$$\frac{\Delta W}{W} = \frac{1}{2\pi} \cdot \left(\frac{TE\beta^2}{C}\right)\left(\frac{\omega\gamma}{\omega^2 + \gamma^2}\right) \qquad [2]$$

where $\gamma = (\pi/h)^2 D$, and D is the thermal diffusion coefficient. The maximum specific damping capacity occurs at frequency f_o which is obtained from equation [2] as:

$$f_o = \left(\frac{\pi}{2}\right)\left(\frac{D}{h^2}\right) \qquad [3]$$

The important physical interpretation of this work is that internal friction damping is a relaxation process. This process is governed by a characteristic time which corresponds to the "peak" frequency and is referred to as the relaxation time. Moreover, the internal friction damping resulting from the relaxation and diffusion process occurs whether or not the solid is homogeneous. Within any viscoelastic material, neighboring grains may have different crystallographic directions with respect to the direction of strain. Randall, Rose and Zener (15) have measured the internal friction damping in specimens of various grain sizes and found that, at the frequencies used, the maximum damping occurred when the size of the grain has an amplitude close to that predicted by equation [3].

2.2.2 Logarithmic Decrement

The specific damping capacity and associated dynamic response of the material is characterized by the damping coefficient or logarithmic decrement which can be expressed as:

$$\alpha = \left(\frac{1}{N}\right)\left(\ln \frac{A_o}{A_n}\right) \qquad [4]$$

where α is the damping coefficient, A_o is the vibrational amplitude of the reference cycle, and A_n is the vibrational amplitude after N cycles. From the determination of α, the

specific damping capacity ($\Delta W/W$) for materials is calculated from the following equation:

$$\frac{\Delta W}{W} = 1-e^{-2\alpha} \qquad [5]$$

2.3 Microscopic Evaluation of Internal Friction Damping

The macroscopic development of internal friction damping is a relaxation process. The microscopic evaluation determines the motion of dislocations that are pinned down by impurities and other dislocations. The microscopic evaluation is based on the mechanical behavior of grain boundary slip for viscoelastic materials.

2.3.1 Grain Boundary Interaction

Ke´ (16) used the ideas of internal friction damping as a relaxation and diffusion process in order to evaluate the mechanical behavior of grain boundaries for polycrystalline materials. By conducting experiments on the damping characteristics of pure materials, the corresponding internal friction damping produced by grain boundary slip was investigated. Moreover, Ke´ showed that internal friction damping could be related to grain boundaries behavior as a viscous material, and an elementary model for viscous slip along the grain boundary was constructed. The result of the model relates the coefficient of viscosity η of polycrystalline materials to their relaxation time τ as follows:

$$\eta = \left(\frac{d}{m}\right) E \cdot \tau \qquad [6]$$

where d is the effective grain boundary thickness, E is the Young's Modulus, and m is the grain size. Ke´ computed the coefficient of viscosity for pure aluminum by determining the elastic modulus from the natural frequency of vibration and by determining the relaxation time from internal friction damping measurements.

2.3.2 Disordered Groups

Another approach to the mechanism of viscous slip along the grain boundary was developed by Orowan (17), who considered disordered arrangements of atoms which are referred to as "disordered groups" or dislocations. By determining the stress distribution around the two critical atoms in the "disordered group", and by determining the shear process by which they can pass over one another, the following expression was obtained for the coefficient of viscosity of intercrystalline slip as:

$$\eta = \left(\frac{T}{s}\right) e^{H/RT} \qquad [7]$$

where the activation energy H is that which is required to pass the two critical atoms over each other, and s is the density of "disordered groups." By observing the viscous behavior of grain boundaries under small shearing stresses, King, Cahn, and Chalmers (18) showed that the mechanism of grain boundary slip in terms of "disordered groups" experimentally satisfied the mechanical behavior of the boundary.

2.3.3 Stress Relaxation Across Grain Broundary

Prior to Orowan's work, Ké (19) had considered the relaxation dependence of internal friction damping and of the modulus of elasticity for aluminum as a function of the frequency and the grain size of the specimen. It was demonstrated that the manifestations of internal friction damping can be expressed as a function of the parameter $(m \cdot f \cdot e^{H/RT})$, and a relationship was experimentally obtained for the specific damping capacity of aluminum as follows:

$$\frac{\Delta W}{W} \propto \left(m \cdot f \cdot e^{H/RT}\right) \qquad [8]$$

where H is the activation energy associated with the stress relaxation across the grain boundary arising from the viscous behavior of the grain boundaries.

2.3.4 Dislocation Density

A contributing factor to the internal friction damping results from the motion of dislocations which are "pinned down" by impurities, precipitates, and other dislocations. Internal friction damping for viscoelastic materials is sensitive to the amount of previous cold work and to the chemical composition of the material. (20) By peforming internal friction damping measurements made over several orders in magnitude range, Koehler (21) considered the effect of impurities on the logarithmic decrement. Viscoelastic specimens were subjected to external shearing stresses for a large range of frequencies and it was assumed that since diffusion is an extremely slow process at room temperature, the impurity atoms are completely unable to follow the alternating stress. The dislocations were, therefore, anchored to the impurity atoms; and it was further assumed that the portion of the line dislocation between two impurity atoms oscillates on its slip plane like a stretched string. Thus, the fewer the impurities, the longer is the string length. Koehler solved the governing differential equation relating the applied shearing stress tending to move the dislocation along its slip plane to the equation of motion of the pinned-down dislocation loop.

2.3.4.1 Dislocation Displacement

Koehler obtained expressions for the average displacement of a dislocation of a given length and for the shearing strain produced by this single loop in a cube of material of edge, L. Furthermore, from a consideration of a random distribution of atoms of solute along the dislocation line, an expression was obtained for the probability of finding two impurities separated by solvent atoms. The

probability is directly proportional to the concentration of impurities, c, along the dislocation line. Finally, the logarithmic decrement was calculated by obtaining expressions for the energy loss per cycle and the total vibrational energy in the cycle. The specific damping capacity was found to vary with concentration of impurities as:

$$\frac{\Delta W}{W} \propto \frac{NBp^3}{c^4 L^3 E} \qquad [9]$$

where p is the interatomic spacing, N is the number of atomic lengths of dislocation line, and B is the damping force acting on the dislocation. Experimental verification of equation [9] is found in the fact that internal friction damping measurements conducted on copper after 40 hours exposure at 1,000°C in a vacuum showed that the logarithmic decrement was one order of magnitude greater than the logarithmic decrement of copper after 20 hours exposure at 1,000°C in hydrogen at atmospheric pressure. This dislocation concentration was further increased when a small percent by weight of iron was added to copper during melting and exposed to the above vacuum anneal. The logarithmic decrement for the copper-iron alloy decreased two orders of magnitude as compared to initial copper measurements.

2.3.4.2 Pinning of Dislocation Lines

Further verification of the theory regarding the change in internal friction damping by the pinning of free lengths of dislocation lines by impurity atoms is presented by Thompson and Holmes. (22) Internal friction damping measurements were made on copper test specimens subjected to neutron bombardment. The investigators showed that the neutron damage adds to the effective impurity pinning already present through interstitial and vacancy atoms.

2.3.4.3 Relationship of Dislocation Density to Specific Damping Capacity

By eliminating the viscosity term from equations [6] and [7], the following expression is obtained:

$$\frac{d}{m} E_\tau = \frac{T}{s} e^{H/RT} \qquad [10]$$

substituting the exponential term into equation [8] gives:

$$\frac{\Delta W}{W} \propto \left(f \, dE_\tau \cdot \frac{s}{T} \right) \qquad [11]$$

At the "peak" frequencies, $\tau - 1/f_o \simeq f$. Therefore, $\tau f \simeq 1$ for frequencies in the vicinity of the "peak" amplitude frequency. Equation [11] then becomes:

$$\frac{\Delta W}{W} \propto \frac{dE}{T} \cdot s \qquad [12]$$

This shows that the specific damping capacity is proportional to the dislocation density, s, which is the number of disordered pairs or the disordered density of the material. The disordered density of a material increases as the number of load repetitions increase. Figure 2 (23) illustrates the increase in the dislocation density as a function of the number of load cycles (ln N).

For cyclic loading of rope materials, slip bands (arrays of dislocations) will widen on the tensile cycle by slip interference, producing cross-slip dislocation. On the relaxation cycle, dislocations at the edge of the bands are forced back through regions of relatively high defect density. Interactions between these dislocations and loops, point defects, and other dislocations effectively strain the existing structure so that nucleation of new slip lines is subsequently favored over widening of the old ones. Snowden and Grosskrentz (24) have investigated the dislocation structure by transmission electron microscopy. Figure 3 experimentally illustrates that the internal friction damping is closely correlated to the strain in the outer layers of the test specimen. This figure

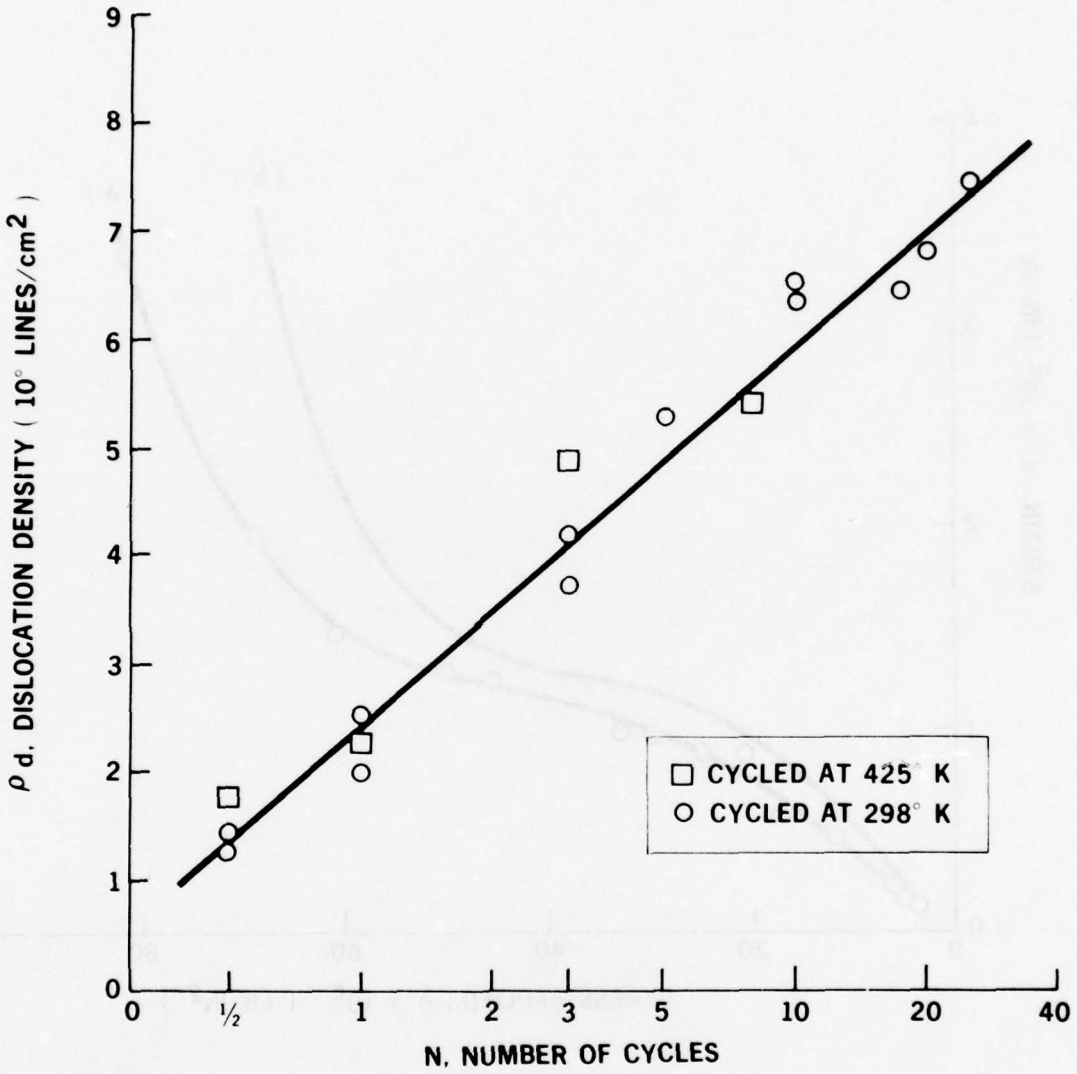

FIGURE 2 THE OVERALL DISLOCATION DENSITY, ρd, AS A FUNCTION OF THE NATURAL LOG OF THE NUMBER OF CYCLES, (LN N)

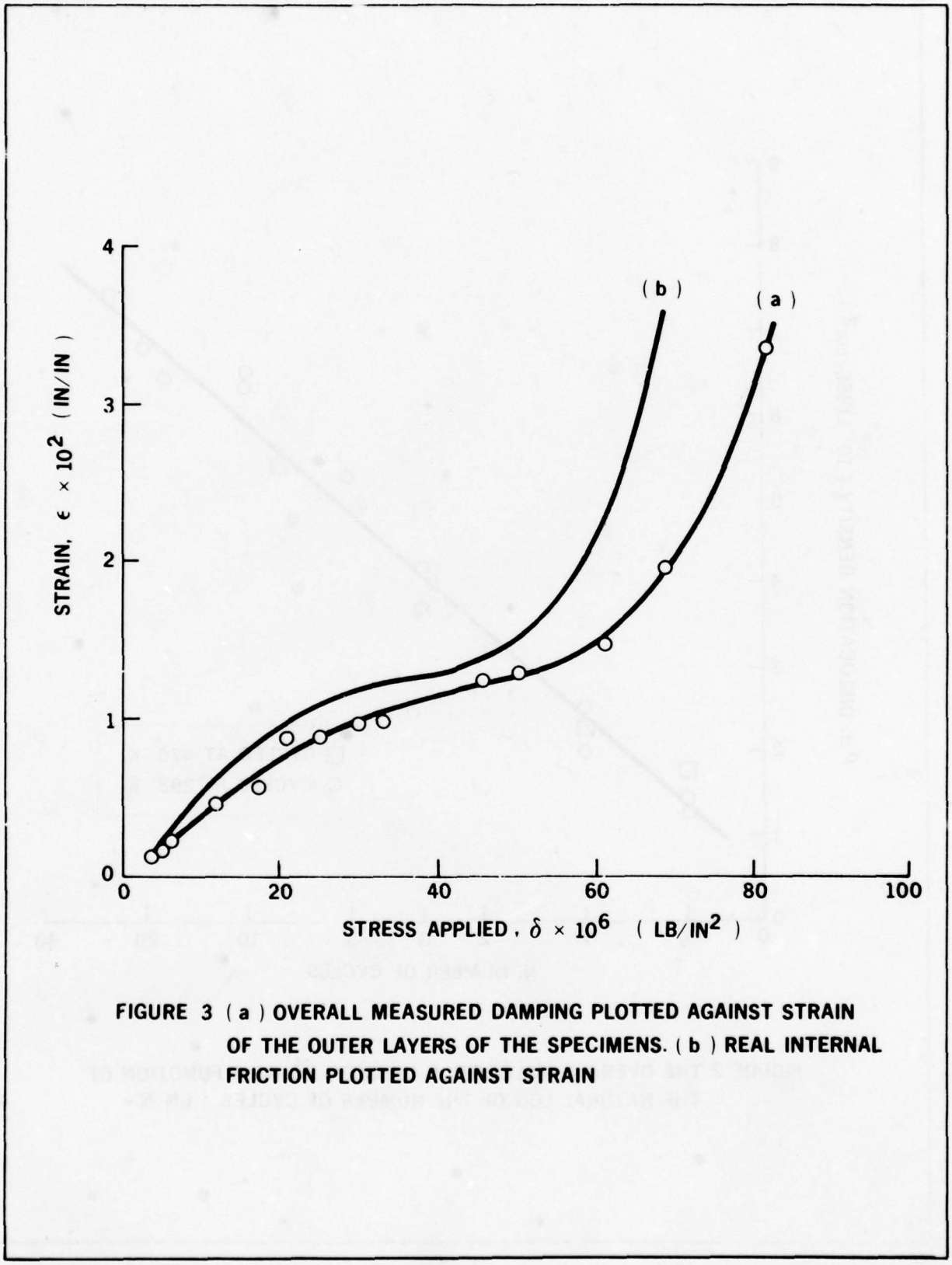

FIGURE 3 (a) OVERALL MEASURED DAMPING PLOTTED AGAINST STRAIN OF THE OUTER LAYERS OF THE SPECIMENS. (b) REAL INTERNAL FRICTION PLOTTED AGAINST STRAIN

also shows the close dependent relationship between the internal friction damping and the strain in the outer layer. Moreover, it was observed that tangles formed on separated primary slip planes after only a few loading cycles. With continued cycling, these tangles spread into unstrained zones parallel to the slip planes. Transition from initial hardening to saturation coincided with the formation of a rather loosely knit, but regular cell structure. This structure remains relatively stable throughout the bulk of the useful fatigue life of the material. Dislocations and dislocation debris from this cell structure interacted at strain centers in the material. When the so-called "dormant" phase (25) was over (i.e., when dislocations were no longer able to move freely due to increasing debris and new slip and dislocation climb would initiate the crack formation process), the crack initiation slowly grew (Stage I) with each strain increment; and then with increasing rapidity (Stage II), until the remaining cross-section fiber became small enough to break completely in a single tensile stroke. It is the defect distribution from the cell structure that is related to the specific damping capacity of the material. Moreover, corrosion fatigue stress accelerates failure because the corrosive media preferentially attacks the strain centers of the dislocation interactions and passivating films (26).

3.0 EXPERIMENTAL APPARATUS AND TECHNIQUES

This section details the experimental apparatus including the internal friction damping (IFD) nondestructive evaluation (NDE) instrumentation equipment necessary for data generation. The equipment necessary to generate the input response and monitor and analyze the output decay is discussed along with the necessary data reduction techniques.

The data analysis and reduction techniques are discussed along with the associated equipment, both hardware and software that are required for the application of the IFD-NDE technique to synthetic rope. Included is a discussion regarding the design and construction of the synthetic rope specimen support apparatus, the special mounting fixture, and the loading device. A schematic representation of the electronic equipment, the support apparatus for the rope specimens and the hydraulic loading device in shown in Figure 4.

3.1 Description of IFD-NDE Instrumentation

The internal friction damping technique requires an input pulse and an associated output signal. The specific damping capacity is determined from the resultant decay curve of the output signal. Representative damping decay curves indicating changes in the internal friction for incipient crack detection are shown in Figure 5.

3.1.1 Input Pulse

A continuous periodic signal at a specific frequency is supplied by an electronic oscillator which induces vibration into the synthetic rope specimen. In application, the technique uses the input of periodic excitation pulses. The input pulses are generated by a beat frequency oscillator gated through a tone burst generator to a permanent magnet vibration transducer. The beat frequency oscillator supplies a continuous periodic signal at a specific frequency and a tone burst generator is used to gate the

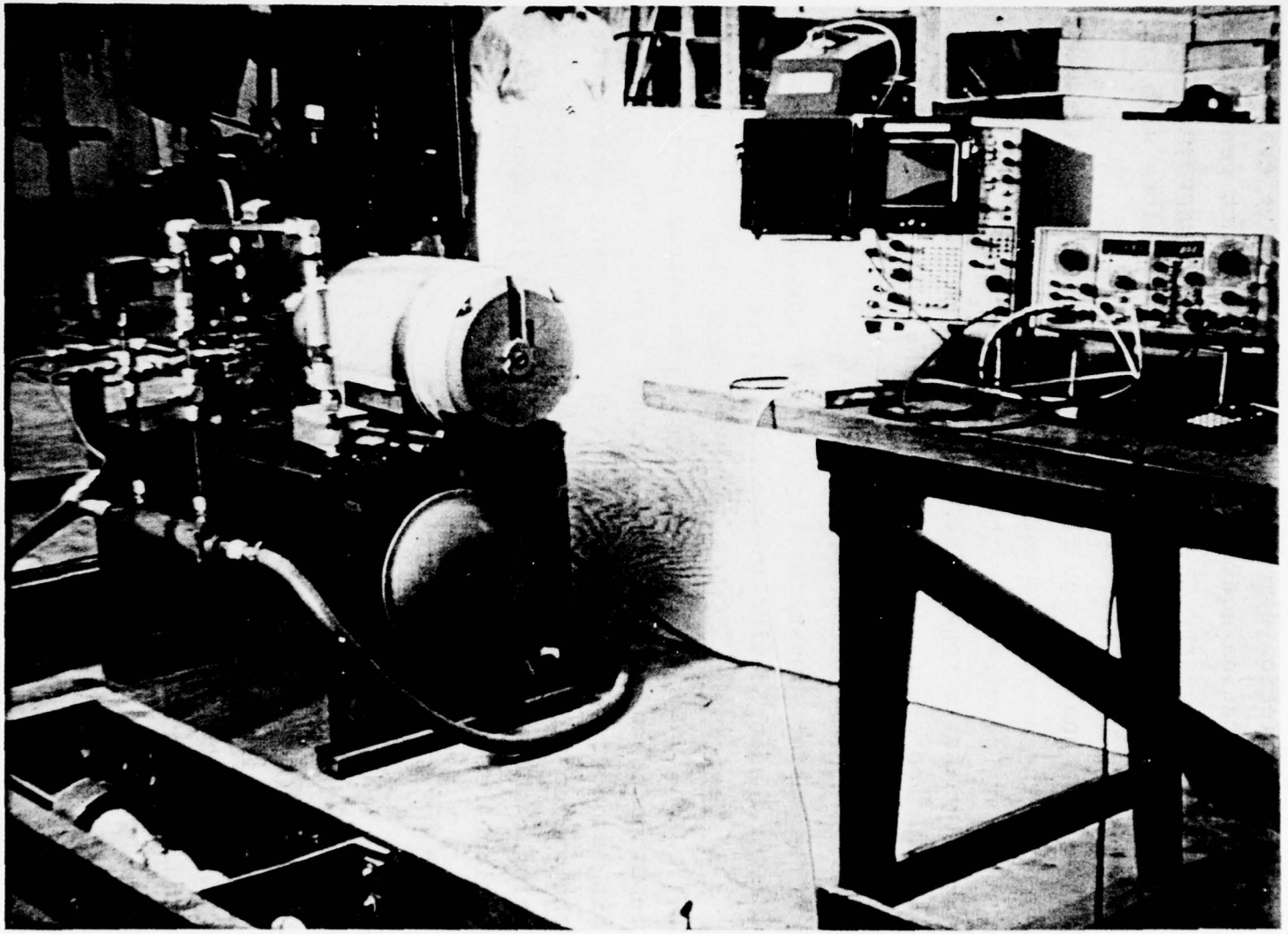

FIGURE 4 PHOTOGRAPHIC REPRESENTATION OF THE ELECTROHYDRAULIC APPARATUS, ELECTRONICS, AND ROPE SUPPORT MECHANISM FOR AXIALLY STRESSING SYNTHETIC ROPES IN TENSION

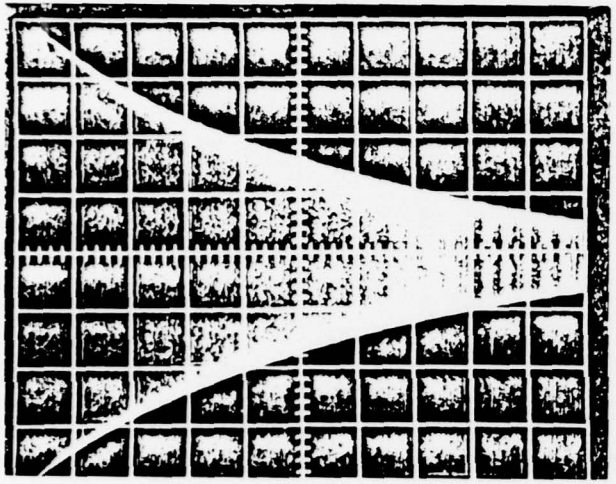

TYPICAL DECAY CURVE FOR INTERNAL FRICTION OF STEEL DAMPING

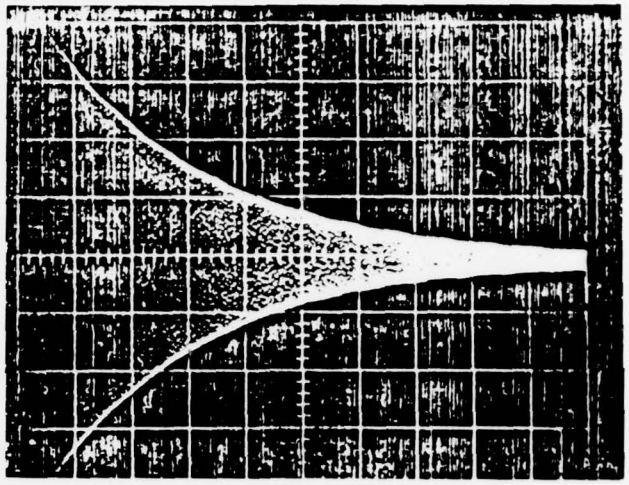

DECAY CURVE FOR INCIPIENT FAILURE DETECTION NOTE CHANGE IN ENVELOPE DECAY

FIGURE 5 REPRESENTATIVE DAMPING DECAY CURVES INDICATING CHANGES IN INTERNAL FRICTION DAMPING FOR INCIPIENT FAILURE DETECTION

signal from the oscillator into a series of discrete pulses. The generator controls the pulse duration and the time interval between pulses. The noncontact, magnetic, vibration input transducer converts the electrical pulses from the generator into mechanical vibrations. A gating device controls the duration of the input signal and simultaneously triggers the storage oscilloscope in order to record the vibrational decay.

3.1.2 Vibrational Response

The electronic signal provided by the oscilloscope is converted into mechanical vibration through the magnetic input transducer which produces a variation in the magnetic field on a steel disc attached to a rope. The vibrational response is measured by a noncontact magnetic output transducer. The output transducer converts the vibrational response of the rope to an electronic signal. The signal from the output transducer is filtered and amplified by an audio frequency analyzer and displayed on a storage oscilloscope. The specific damping capacity is determined from the decay curve of the input pulse. The magnetic output transducer converts the vibrational response of the specific component to an electrical signal. The output signal from the output transducer is filtered by an audio frequency analyzer and the output decay curve is displayed on a storage oscilloscope which is externally triggered by a synchronous output from the tone burst generator.

Measurements of the vibration decay are made between pulses with an output transducer. The generation of these pulses requires an oscillator coupled to a tone burst generator. On the pick-up side, the unit measures a wide range of damping levels, and various degrees of amplification in time and in signal strength. The amplification units will consist of a voltage amplifier for the amplitude of the received signal and an oscilloscope for the spread in time of the received signal.

The selection of the major components has to satisfy practical requirements to allow meaningful interpretation of results. Such design criteria require:

1. Frequency range: 20 - 20,000 Hz
2. High pick-up sensitivity
3. High signal/noise ratio
4. High accuracy of measurements
5. High amplification (100 dB)
6. Minimum harmonic distortion

A comparison of available off-the-shelf equipment led to the selection of several commercially available instruments.

3.2 Description of Instrumentation

A description of the electronic components and of the test apparatus is given in this section. The selected components are assembled as shown in Figure 6.

3.2.1 Beat Frequency Oscillator

The beat frequency oscillator is a precision signal generator covering the range of 20 - 20,000 Hz. It operates on the heterodyne principle using two high frequency oscillators, one of which resonates at a fixed frequency while the frequency of the other can be varied. The required audio frequency is then obtained by mixing these frequencies to produce a beat frequency. The purpose of the frequency oscillator within the test apparatus is to generate a continuous periodic signal that will be reduced, at a later stage, into a series of pulses.

3.2.2 Tone Burst Generator

The tone burst generator operates as a high quality fast switch that alternately interrupts and passes an input signal. The tone burst generator interrrupts a continuous tone into a series of bursts applied to the input. The instrument controls the burst duration and interval between

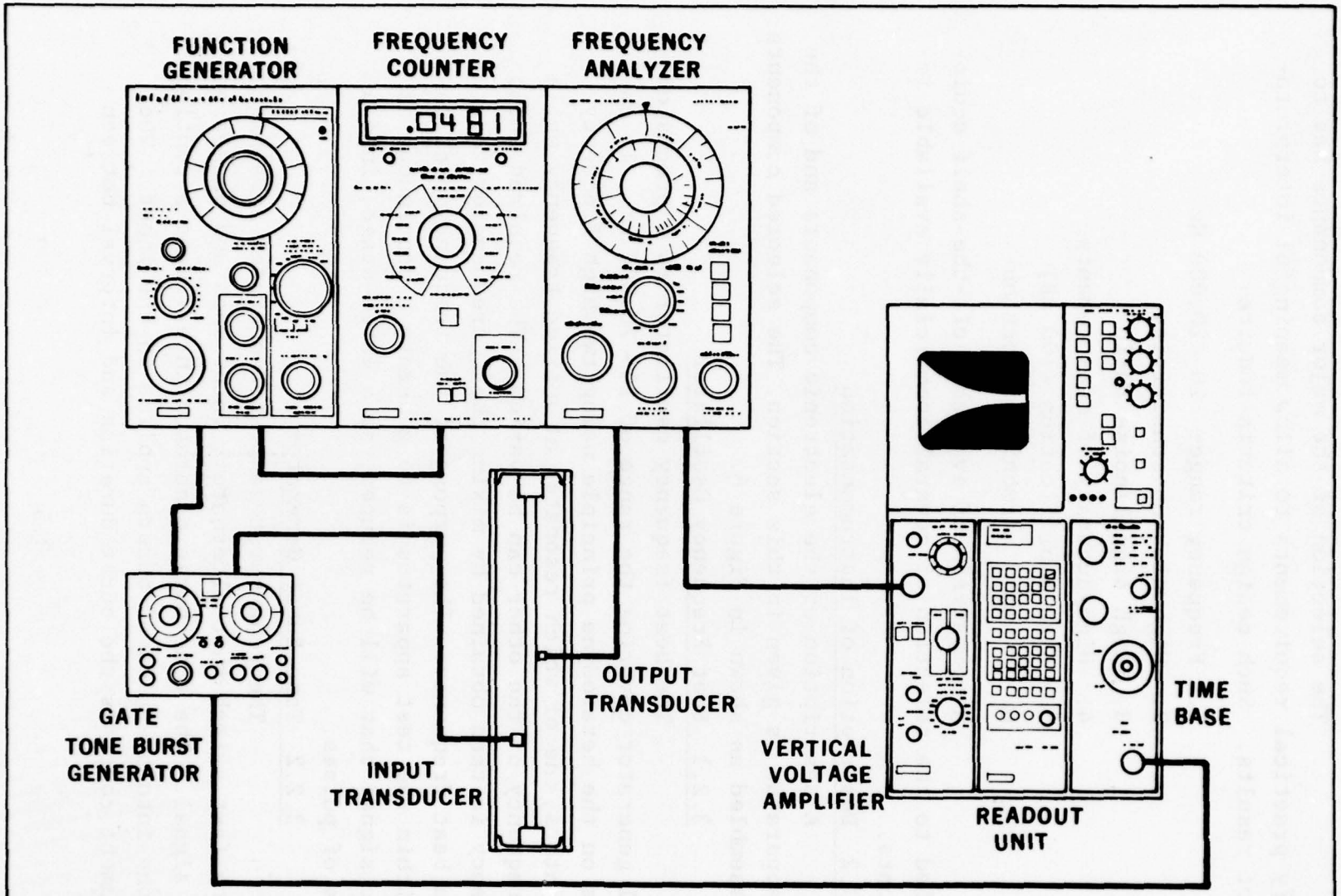

FIGURE 6 ILLUSTRATION SHOWING THE ELECTRONIC COMPONENTS AND TEST APPARATUS THAT COMBINE AS THE INTERNAL FRICTION DAMPING LABORATORY INSTRUMENTATION PACKAGE

bursts by counting the number of cycles or by actually timing the duration and interval. The purpose of the tone burst generator within the test apparatus is to reduce into pulses the continuous signal generated by the frequency oscillator. The tone burst generator controls the pulse duration and the time between pulses.

3.2.3 Magnetic Exciter and Output Transducer

The noncontact magnetic vibration transducer is a small vibration exciter covering the force range up to 7 Newtons (1.5 lbf). It has a wide frequency range with low cross-motion. The purpose of the exciter within the test apparatus is to convert the electrical pulses into mechanical vibrations. The AC signal generated by the oscillator passes through an internal coil which surrounds a magnetic pole, and induces a flux change in the magnetic field before the transducer. The magnetic output transducer is a variable reluctance device which can be used as a velocity sensitive vibration output transducer or as an electromagnetic vibration exciter. The output transducer consists of a cylindrical permanent magnet within a Teflon™ base coil. The winding combines high sensitivity with low internal impedance. Both coil and magnet are electrically isolated from the housing.

The magnetic output transducer responds to excitation of the synthetic rope under load by generating an AC output voltage proportional to the rope deflection. The purpose of the pickup within the test apparatus is to measure the vibrational response of the specimen when driven by the exciter. Synthetic ropes are not magnetic which required the use of μ discs (easily magnetized metal discs) to establish the input location and a similar output location. The use of these discs in no way altered the natural response of the synthetic rope.

3.2.4 Frequency Analyzer

The audio frequency analyzer has been designed expecially as a narrow band sound and vibration analyzer, and is of a constant percentage bandwidth type. It consists of an input amplifier, a weighting network, and a selective amplifier section (band pass filter). Its purpose within the test apparatus is to filter and amplify the output signal provided by the magnetic output transducer.

3.2.5 Storage Oscilloscope and Level Recorder

The storage oscilloscope is controlled by a voltage amplifier for the vertical axis and a time base for the horizontal axis. The voltage amplifier, amplifies the signal from the frequency analyzer, and allows vertical amplitude adjustment to the signal. The time base controls the sweep rate of the electron beam in the horizontal direction. The oscilloscope is externally triggered by the gating device so that the beam trace begins simultaneously with the interruption of the input signal to the input transducer. The trace continues as the vibration of the rope decays, recording the output amplitude as a function of time. A photograph is taken of the stored trace and later analyzed to yield the specific damping capacity value ($\Delta W/W$). An example of the decay curve as recorded by the storage oscilloscope is shown in Figure 7.

A second alternative for signal recordings is given by a level recorder combined with recording paper. The level recorder is designed to record the RMS, Average or Peak Level of an AC signal in the range from 2 Hz to 20 kHz. Recordings are made on preprinted line or frequency calibrated strip-chart paper as functions of either time or frequency. Its purpose within the test apparatus is to make a permanent recording of the output signal from the accelerometer.

3.2.6 Description of Test Assembly

The beat frequency oscillator generates a

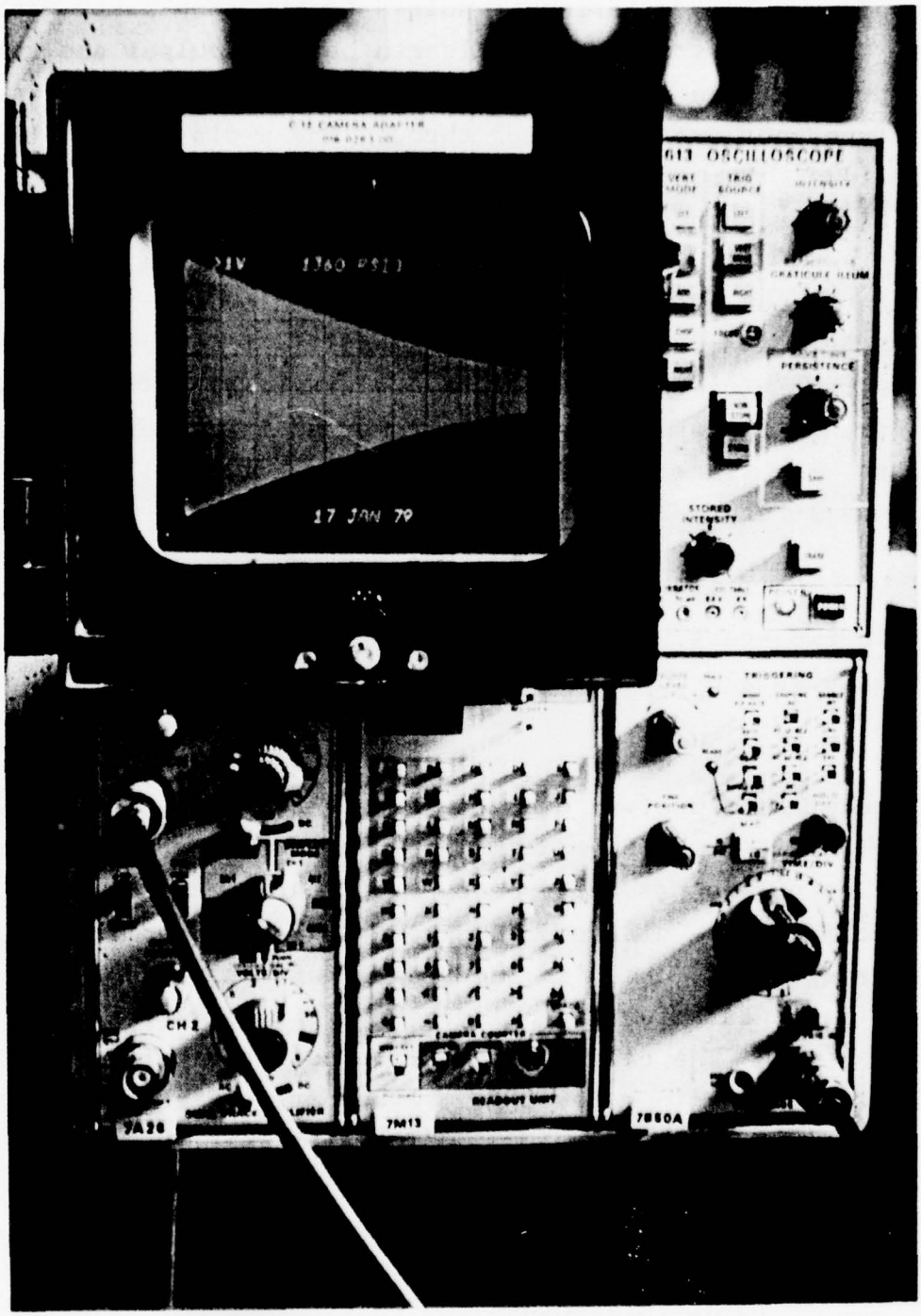

FIGURE 7 PHOTOGRAPH OF THE CATHODE RAY TUBE (CRT) DISPLAY OF THE OUTPUT DECAY INCLUDING SALIENT TEST PARAMETERS IDENTIFIED ON THE SCREEN.

sinusoidal signal of a predetermined frequency. This signal is transformed into a series of pulses by the tone burst generator. The generator sets the length between pulses and the pulse duration. The output from the tone burst generator drives an electromagnet exciter, which through the μ discs, vibrates the specimen. The amplitude of the vibrations are regulated by the beat frequency oscillator.

The vibrations within the specimen are picked up by the output electromagnet and amplified by a voltage amplifier. Before amplification, the signal is filtered to eliminate secondary vibration from the output signal. The voltage amplifier and filtering system are combined into the frequency analyzer. The signal is recorded on a storage oscilloscope or with a level recorder.

3.2.7 Instrumentation Calibration

The calibration of the test apparatus is performed in two steps. The driving signal is calibrated during the first step and the output decay signal is calibrated as a second step

To calibrate the driving signal, a continuous vibration of the specimen over the frequency range of the beat frequency oscillation is made. This procedure enables the determination of the natural frequency of the rope specimen, since each specimen has a different frequency. The pulsed input signal is generated to optimize the signal parameters (pulse amplitude, pulse duration and pulse periodicity).

The calibration of the output vibration decay for accurate recordings consists of two parts. First, the output signal amplitude is optimized using different levels of amplification. Then, the time spread of the vibration decay is set to occupy between 5 to 10 centimeters on the display of the oscilloscope.

At this point, the calibration of the experimental test apparatus is completed and a permanent recording

of the output signal can be performed. This permanent recording can be achieved either on the oscilloscope (storage memory) or on the level recorder (tracing of the decay slope on calibrated strip-chart paper). A complete discussion of the operation of the IFD instrumentation equipment can be found in Appendix A.

3.3 Design and Construction of Specimen Load Fixture

3.3.1 Support Frame

The initial rope support system allowed for testing of a three foot section of rope. The rope ends were epoxied into cylindrical end fittings. One end fitting was attached to the support frame; the other was attached to the hydraulic power cylinder. Using this system, the vibration of the three foot length of rope could not be monitored. The rope stiffness at this length was greater than the corresponding force of vibration being applied by the electromagnetic transducer. Therefore, further modification of the test apparatus was undertaken. The support frame was lengthened so that a six foot length of rope could be tested. Testing was initiated using this system, applying loads through the hydraulic power cylinder up to 1,700 pounds on the six inch circumference rope specimens and up to 3,400 pounds on the eight inch circumference samples. However, the following findings led to the design and construction of a complete new rope support and tensioning apparatus.

1. Resonant frequencies of the ropes were in the neighborhood of 20 Hz when loaded to the tensions given above. This is the lower limit of the frequency analyzer.
2. Specific damping capacities varied for the ropes tested when the tension was increased through the range of loading indicating that the load on the ropes

was insufficient to produce elastic behavior.

3. Actual working loads on the ropes beyond 1,700 pounds and 3,400 pounds, respectively, were not attainable because of failure of the epoxy which secured the ropes inside the cylindrical end fittings.
4. More meaningful data to actual field conditions could be generated if the specific damping capacity information was obtained with the rope samples under a load approximating in-service working loads; i.e., 10 to 17 percent of "breaking strength." (2)

3.3.2 Rope Support and Tensioning System

Because of these findings, a new rope support and tensioning system was designed and constructed. The elements of the new system allow loads up to 65,000 pounds to be applied. The major structural elements of the support system are two structural steel channels, 10 feet long, which are designated C8 x 11.5 (8" depth, 11.5#/ft.). These each have a cross-sectional area of 3.38 in^2, which allows a maximum load of 135,000 pounds under short column loading conditions. A reinforced steel plate at one end provides support for the nonmoving end of the rope and braces the two channels. A hydraulic power cylinder is mounted at the opposite end to load the rope specimens in tension. Two bridges are placed between the channels, six feet apart to control the length of rope being tested. Figure 8 schematically illustrates the rope support and tensioning apparatus. Figure 9 is a photographic view of the support system.

3.3.3 Hydraulic Power Cylinder

A hydraulic power cylinder was obtained which has a five inch diameter bore and 20 inch stroke. The long

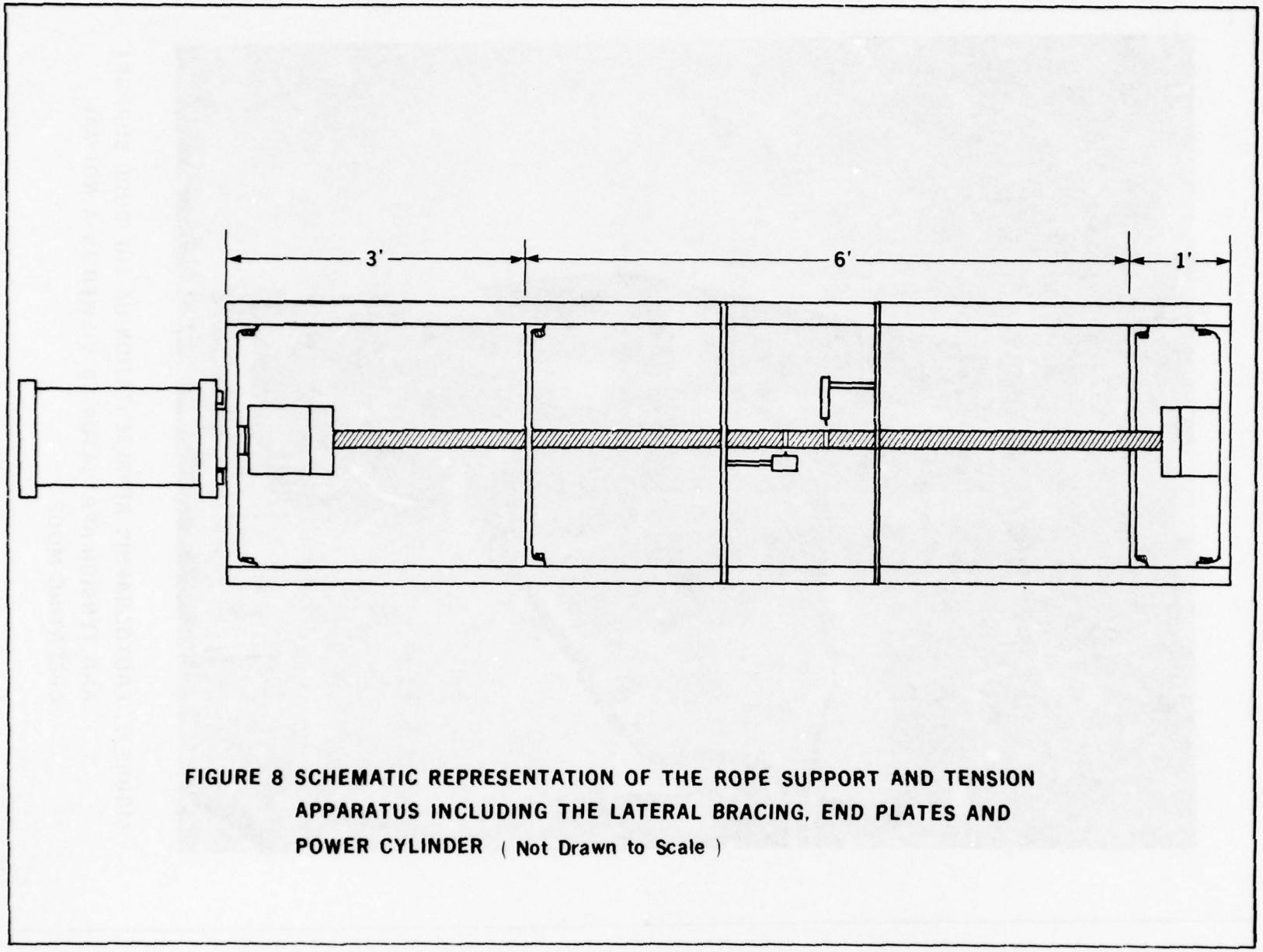

FIGURE 8 SCHEMATIC REPRESENTATION OF THE ROPE SUPPORT AND TENSION APPARATUS INCLUDING THE LATERAL BRACING, END PLATES AND POWER CYLINDER (Not Drawn to Scale)

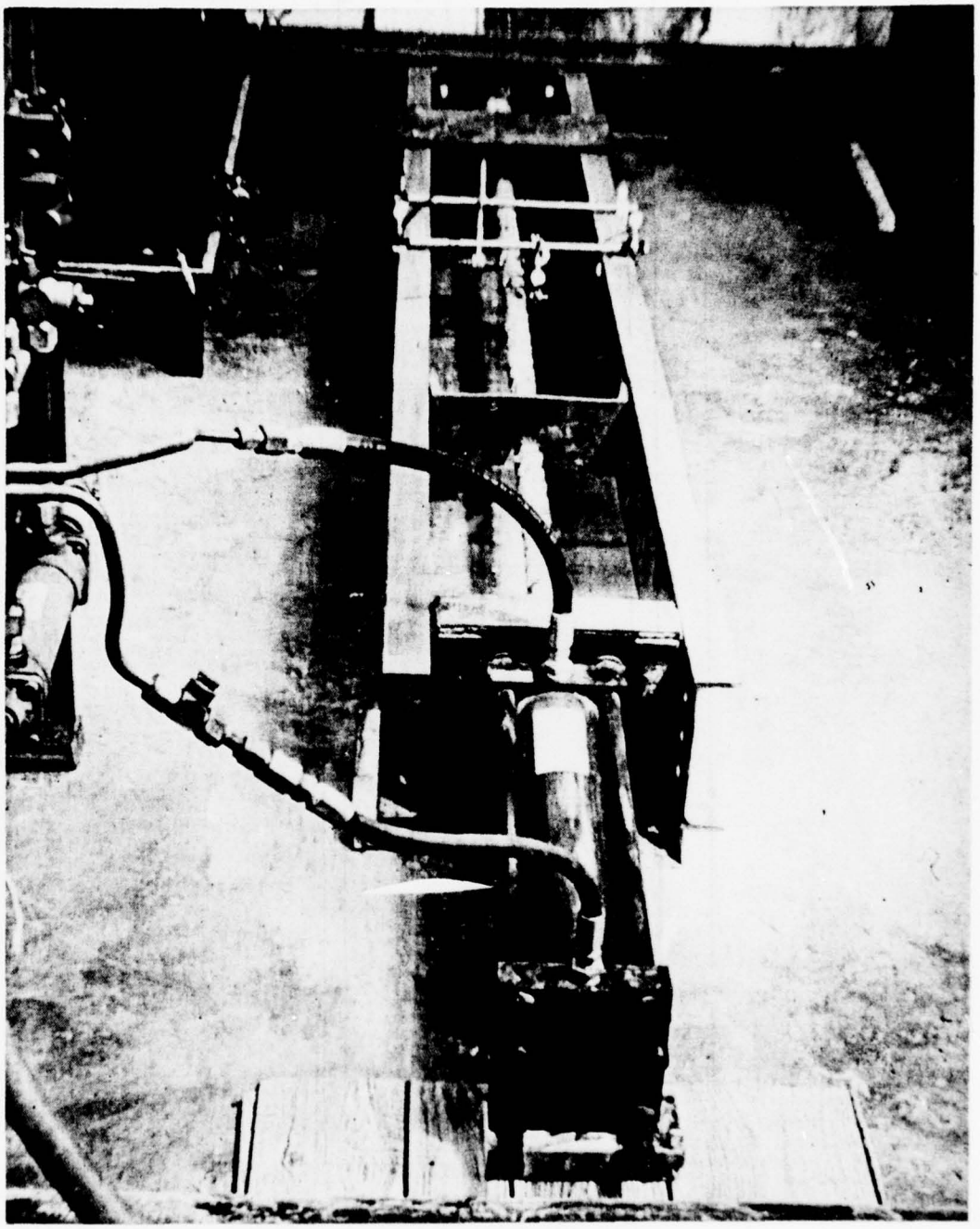

FIGURE 9 PHOTOGRAPHIC REPRESENTATION OF THE ROPE SUPPORT AND TENSION APPARATUS AS VIEWED IN A NORMAL OPERATING MODE

stroke minimizes repositioning of the cylinder as rope specimens elongate under load. The piston area for the cylinder under tensile load is 14.75 in^2, giving a maximum tensile load capability of 74,000 pounds at the rated static pressure. Directional control of the hydraulic cylinder is effected by a double acting directional valve which is activated by two solenoid relays. Figure 10 is a photographic view of the power cylinder attached to the base plate.

3.3.4 End Fittings

End fittings for the ropes were designed and fabricated, allowing high tensile forces to be applied without the ropes breaking loose from the end fitting device. The end fittings are similar in design to a reduced shear stress end fitting patented by the U. S. Navy under U. S. Patent Number 3,960,459. Figure 11 illustrates the Navy system. The modified design provides for the hawser to be imbedded in a conical plug of castable epoxy and surrounded by a steel member having a complimentary tapered surface. The steel member acts as the mold for the castable material. The tensile stress is distributed over the surface of the tapered plug, thereby preventing localized stress concentrations. This fitting design differs from the Navy fitting design in that the entire steel portion can be removed from the rope and re-used. Figures 12, 13 and 14 illustrate the end fitting design used in the present program. Figure 15 shows the photographic view of the end fitting.

3.4 Design and Construction of the Electrohydraulic Loading Device

Loading of the synthetic ropes to 20,000 psi tensile stress was accomplished with an electrohydraulic system as shown in Figure 16. The system is capable of a maximum pressure of 5,000 psi. The pressure is created by a gear type, constant displacement pump manufactured by the Robert Bosch Company. The pump hydraulic displacement is 8 gpm. The power for the

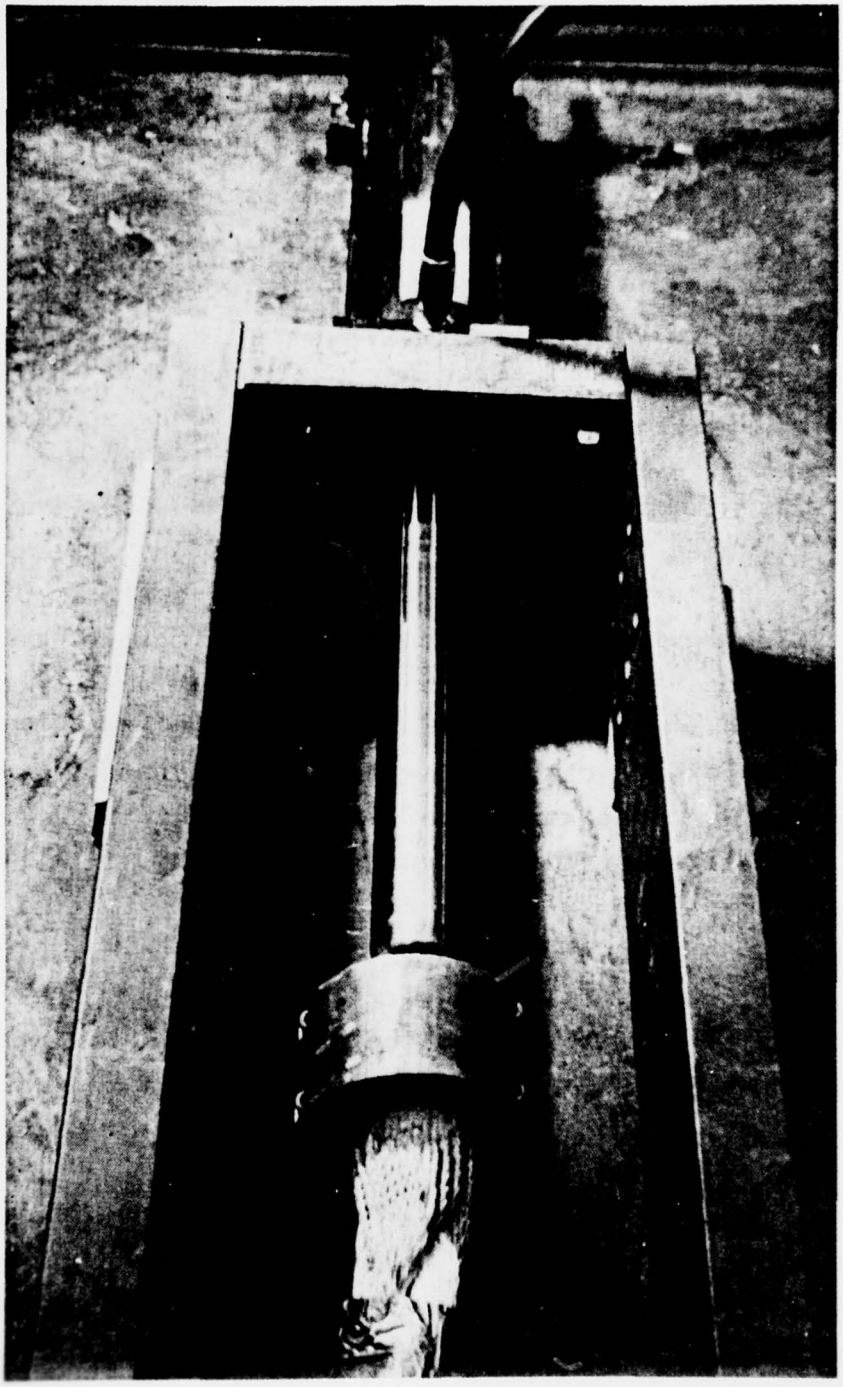

FIGURE 10 PHOTOGRAPHIC REPRESENTATION OF THE TWENTY INCH STROKE, HYDRAULIC POWER CYLINDER UTILIZED FOR APPLYING AN AXIAL TENSION LOAD TO THE SYNTHETIC ROPE SPECIMENS

U. S. PATENT
June 1, 1976
NO. 3,960,459

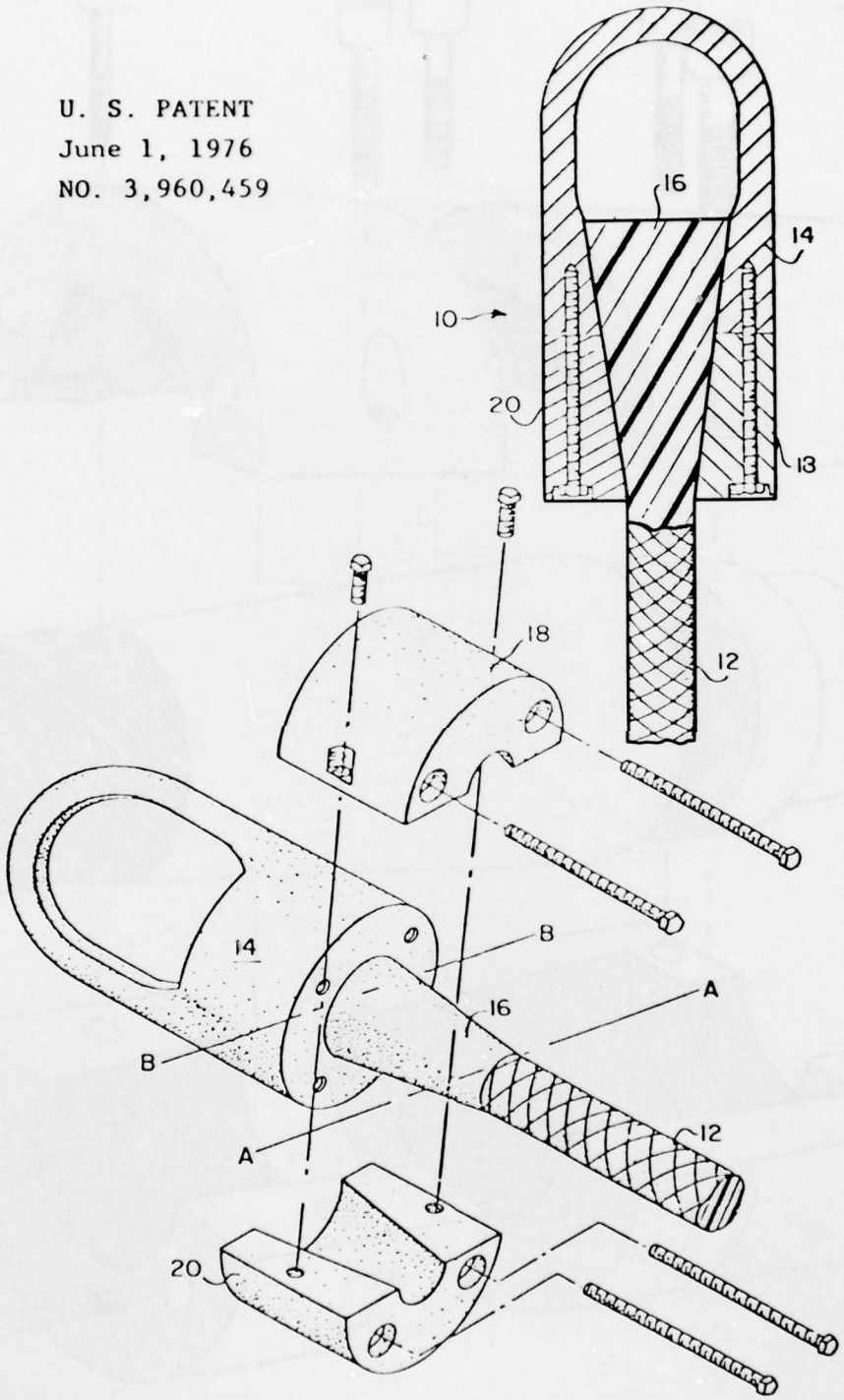

FIGURE 11 U.S. NAVY REDUCED SHEAR STRESS END FITTING

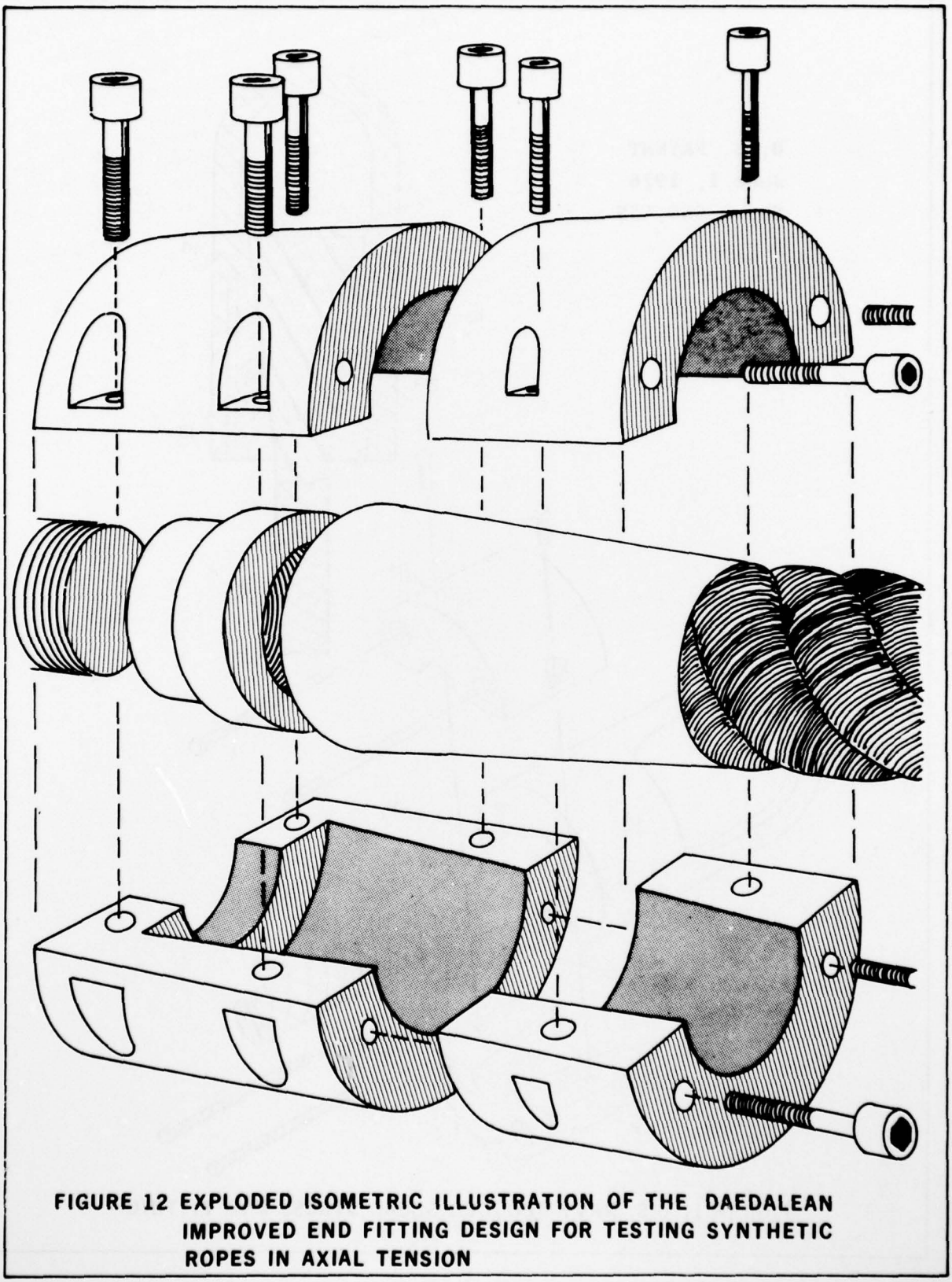

FIGURE 12 EXPLODED ISOMETRIC ILLUSTRATION OF THE DAEDALEAN IMPROVED END FITTING DESIGN FOR TESTING SYNTHETIC ROPES IN AXIAL TENSION

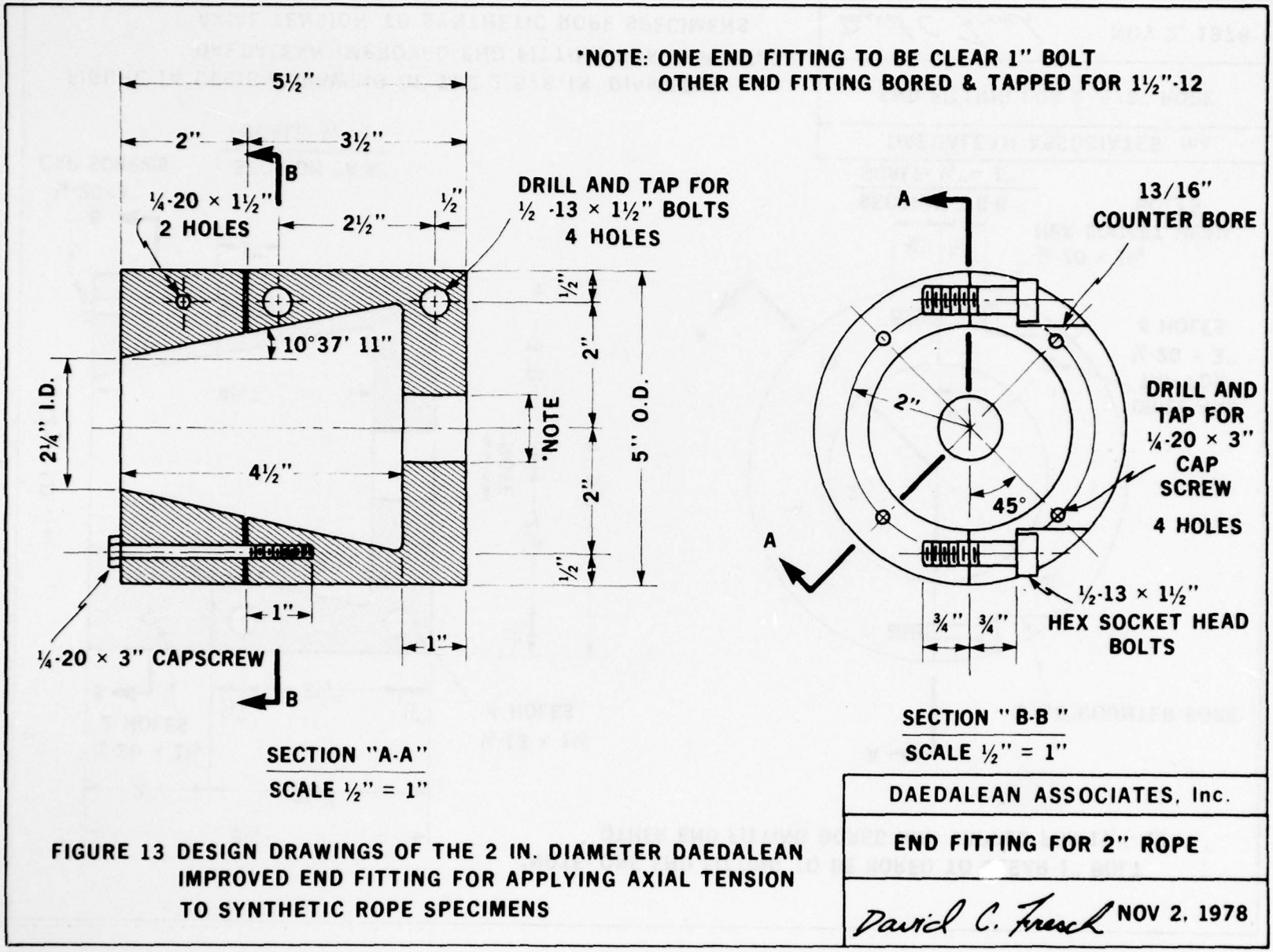

FIGURE 13 DESIGN DRAWINGS OF THE 2 IN. DIAMETER DAEDALEAN IMPROVED END FITTING FOR APPLYING AXIAL TENSION TO SYNTHETIC ROPE SPECIMENS

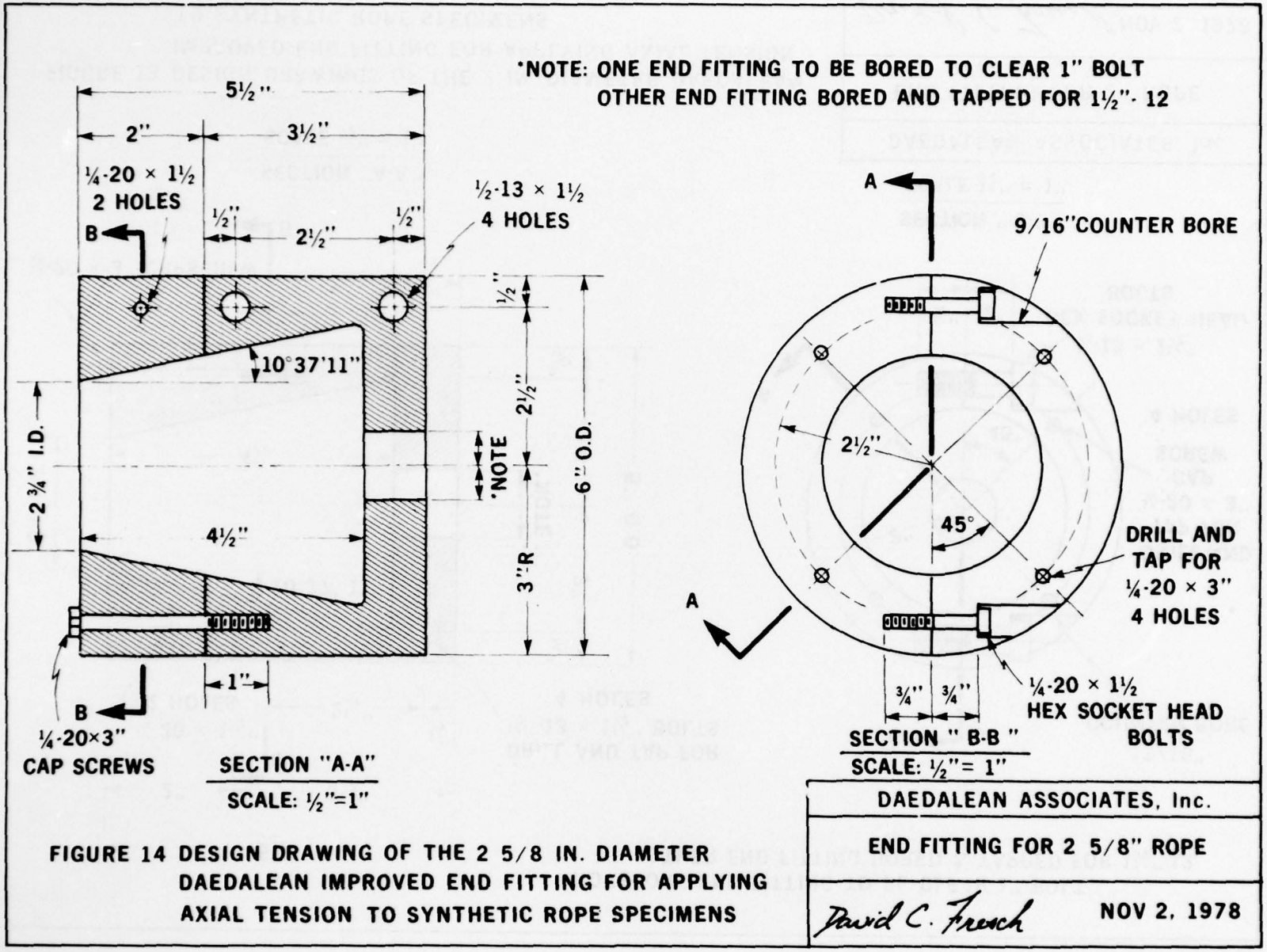

FIGURE 14 DESIGN DRAWING OF THE 2 5/8 IN. DIAMETER DAEDALEAN IMPROVED END FITTING FOR APPLYING AXIAL TENSION TO SYNTHETIC ROPE SPECIMENS

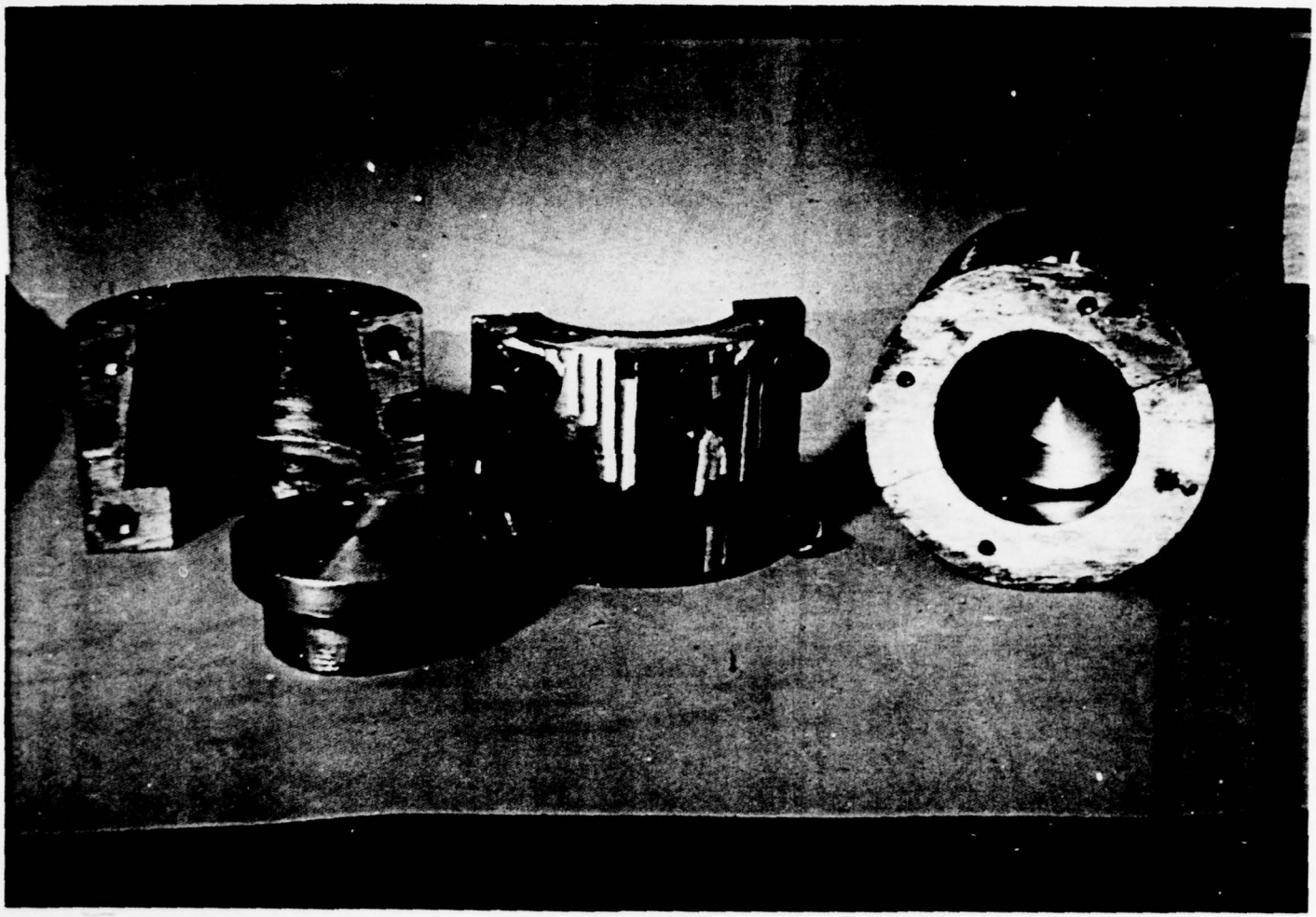

FIGURE 15 PHOTOGRAPHIC REPRESENTATION OF THE DAEDALEAN IMPROVED END FITTING FOR TESTING SYNTHETIC ROPES IN AXIAL TENSION

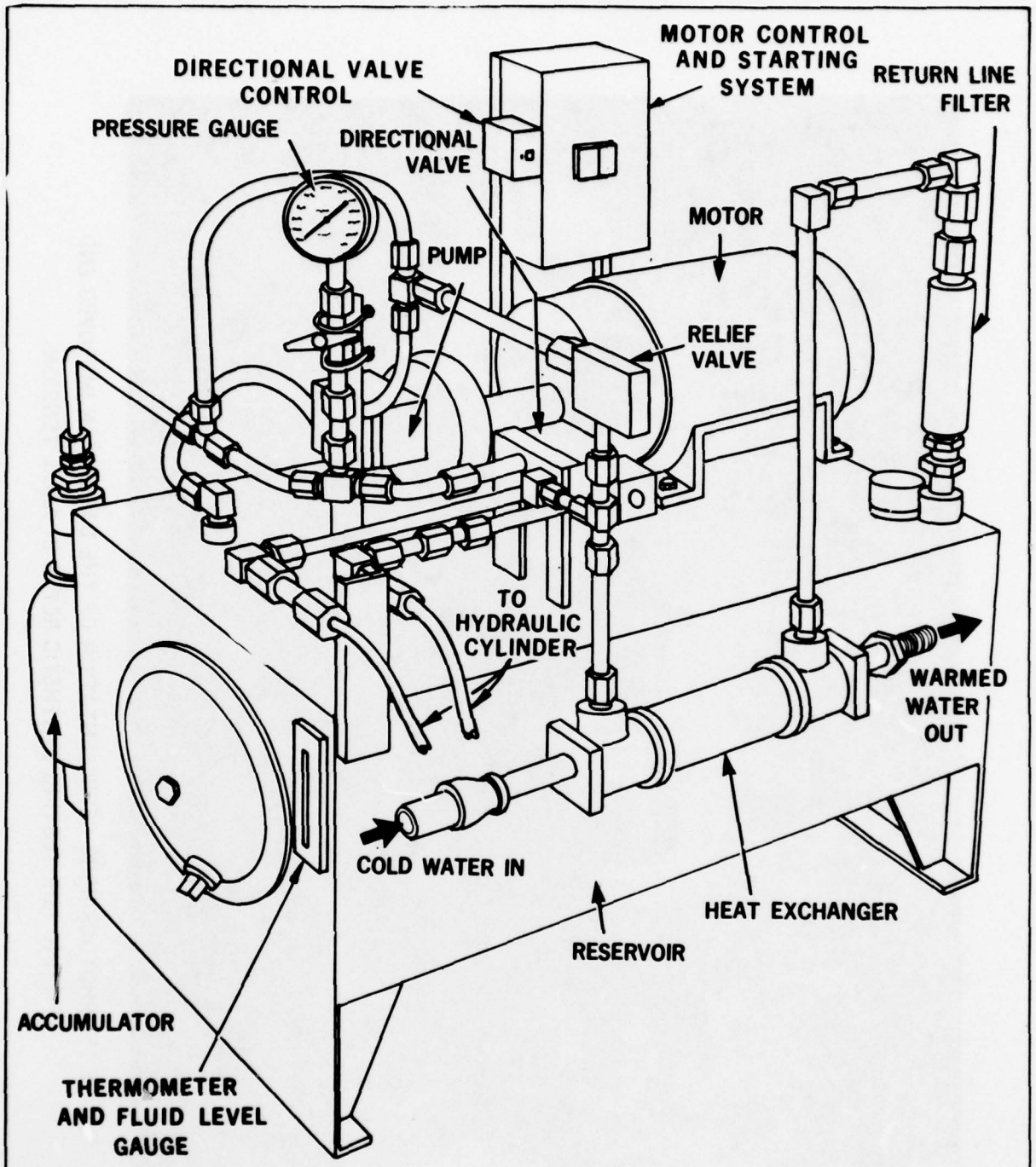

FIGURE 16 GRAPHICAL REPRESENTATION OF THE ELECTRO-HYDRAULIC APPARATUS FOR AXIALLY STRESSING SYNTHETIC ROPE IN TENSION

pump is supplied by a Reliance 30 hp electric motor operating on 440V - 3 phase current. Maximum internal pressure of the loading cylinder was controlled at 5,000 psi by a pilot actuated type relief valve.

A doubled-A directional valve allows flow reversal at the hydraulic loading cylinder by use of a double solenoid design. This is a three position valve; in Position 1, the hydraulic fluid flows into the hydraulic cylinder until 5,000 psi is reached. The hydraulic cylinder was filled at zero gauge pressure at the beginning of each loading interval. The pressurization time to 5,000 psi was five seconds. This is the time required to add the fluid needed in the hydraulic cylinder due to the fluid compressibility under high pressure. In Position 2, the valve is in neutral and 11 ports are open, allowing the fluid to dump from the pump back into the 40-gallon reservoir. In Position 3, the fluid flows from the hydraulic cylinder into the reservoir until zero pressure is reached.

All fluid returning to the reservoir passes through a Modine water cooled heat exchanger and a Gould Waterman 20μ in-line filter.

The entire pump assembly, including the motor, motor heater, starting relay, directional valve, filter, gauges, and heat exchanger is housed on the hydraulic reservoir tank. An internal immersible thermometer provides a constant determination of the operating temperature of the hydraulic fluid. The accumulator, also housed on the reservoir tank provides for a uniform pressure to be delivered to the hydraulic loading cylinder. The function of the accumulator would be to remove transient over-pressure surges from the system. Figure 17 is shown in the electrohydraulic loading apparatus complete with heat exchanger and other peripherals. A more complete viewing of the electrohydraulic loading device is shown in Figures 18 and 19, which illustrate the overall application of the loading device, the test fixture, and associated equipment.

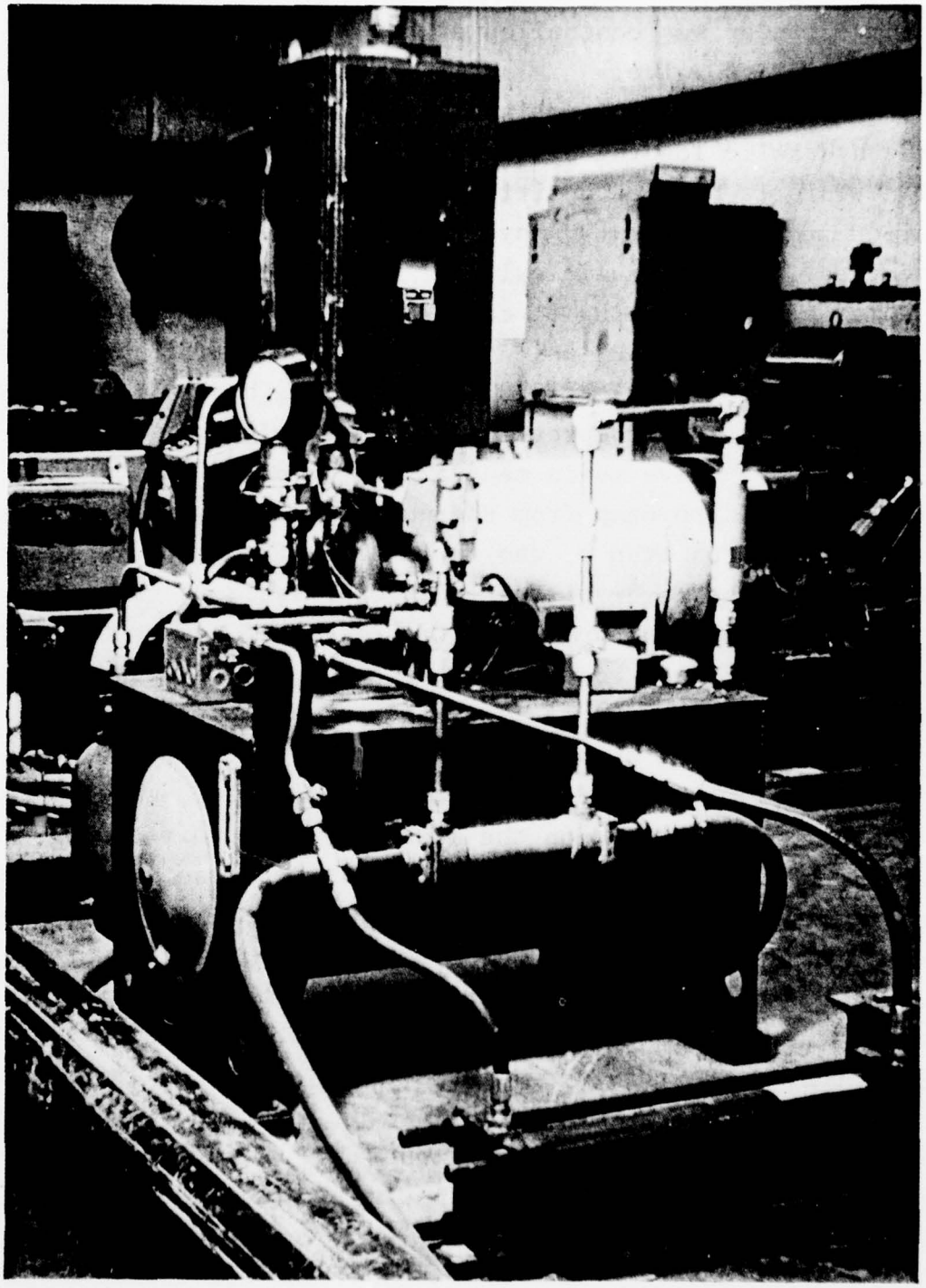

FIGURE 17. PHOTOGRAPHIC REPRESENTATION OF THE ELECTROHYDRAULIC LOADING APPARATUS INCLUDING PUMP, DIRECTIONAL VALVE AND RESERVOIR FOR SUPPLYING A MAXIMUM OF 5000 PSI PRESSURE TO THE POWER CYLINDER

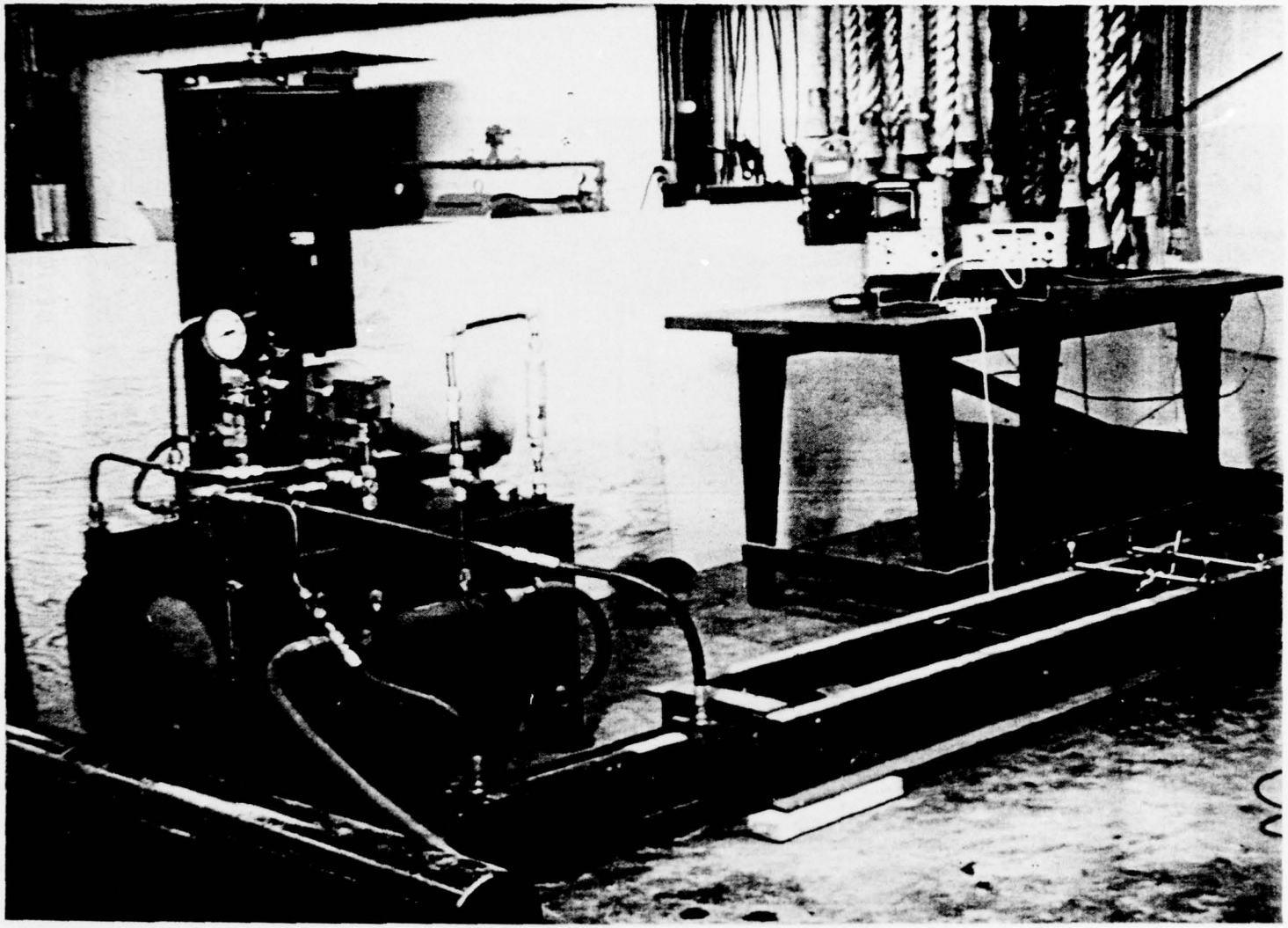

FIGURE 18 PHOTOGRAPHIC VIEW OF LOADING DEVICE, TEST FIXTURE AND ASSOCIATED EQUIPMENT FOR IFD-NDE TESTING OF SYNTHETIC ROPE

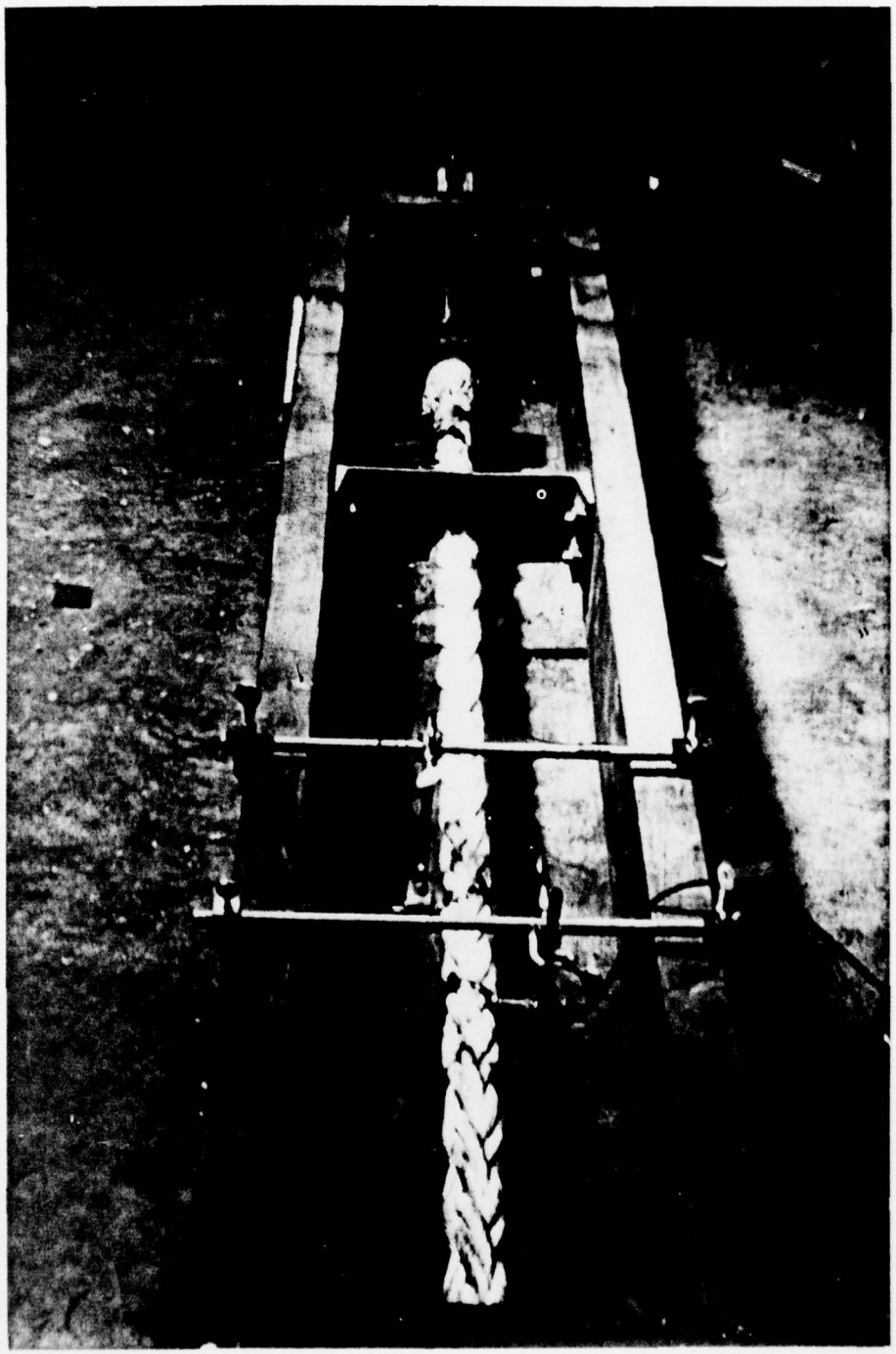

FIGURE 19 PHOTOGRAPHIC VIEW OF THE LOADING DEVICE, TEST FIXTURE, AND ASSOCIATED EQUIPMENT FOR IFD-NDE TESTING OF SYNTHETIC ROPES

3.5 Internal Friction Damping Technique Applied to Synthetic Rope Sections

The output responses and associated specific damping capacity measurements from the load tests performed on various sizes of synthetic ropes are presented in the results section of this report. The specific application of the instrumentation and technique to synthetic rope specimens was accomplished through the test apparatus described in Section 3.3 and Section 3.4.

3.5.1 Preparing Rope Section for Test

The ropes were sectioned to six foot lengths and the ends of the rope were then prepared for the application of the molded end caps. A two-part epoxy system was obtained from Fox Industries that could withstand the requirements of the load on the rope. The important characteristics of the epoxy included the bond strength and compressive strength. The bond strength must be sufficient to withstand the test tension which approximated 20,000 psi for large rope sections. The epoxy had the additional requirement for maintaining structural integrity throughout the entire range of tensile loads applied. This requirement was difficult to accomplish in that the synthetic ropes and the epoxy had different elastic moduli; however, there was only one recorded structural failure of the molded end fitting.

3.5.1.1 Casting End Sections

The next stage in preparing the rope for test was to cast the rope ends in epoxy which was positioned in the steel castings. The internal surfaces of the steel molds were sprayed with a silicon mold release for the purpose of preventing the hardened epoxy end fitting from adhering to the removable molds. The epoxy was injected into the mold to insure an adequate interface with the synthetic rope. After insuring that the molds were completely filled with the epoxy, they were permitted to cure for 48 hours to assure complete

curing. The ropes were then scheduled for testing in the electrohydaulic test apparatus.

3.5.2 Initiation of Rope Test

The synthetic rope specimens with the end epoxy fittings attached were tested in the electrohydraulic loading apparatus in a prescribed manner. The following description encompasses the test sequence from the point of curing the rope specimens to the point of adjusting the instrumentation system as described in Appendix A.

The construction of the electrohydraulic loading apparatus included the aspect of a movable base that contained the hydraulic cylinder. The cylinder was capable of a 20-inch stroke from deadhead to full extension. For some applications the 20-inch stroke was not sufficient to attain test tension as the synthetic rope tended to creep under load. For this reason, the cylinder block base was movable in multiples of 4 inches.

The rope sections with attached end fittings were inserted into the lower steel section of the mold which serves as the end cap attachment for the loading frame. The one end cap is directly attached to the end of the cylinder rod. The other steel end fitting is attached to the load frame by means of an attachment bolt. The rope specimen was then brought to proper test tension for data acquisition. The complete load frame, specimen preparation, and test technique is depicted in Figures 20 through 29. The detailed calibration of the equipment appears in Appendix A.

3.5.3 Specific Damping Capacity Measurements

Once the experimental apparatus has been positioned and the necessary adjustments have been performed on the instrumentation, the specific damping capacity measurements are made. The sinusoidal input frequency was maintained for a given rope specimen. It was determined that placing the rope specimen under tension required a settling time to elapse before

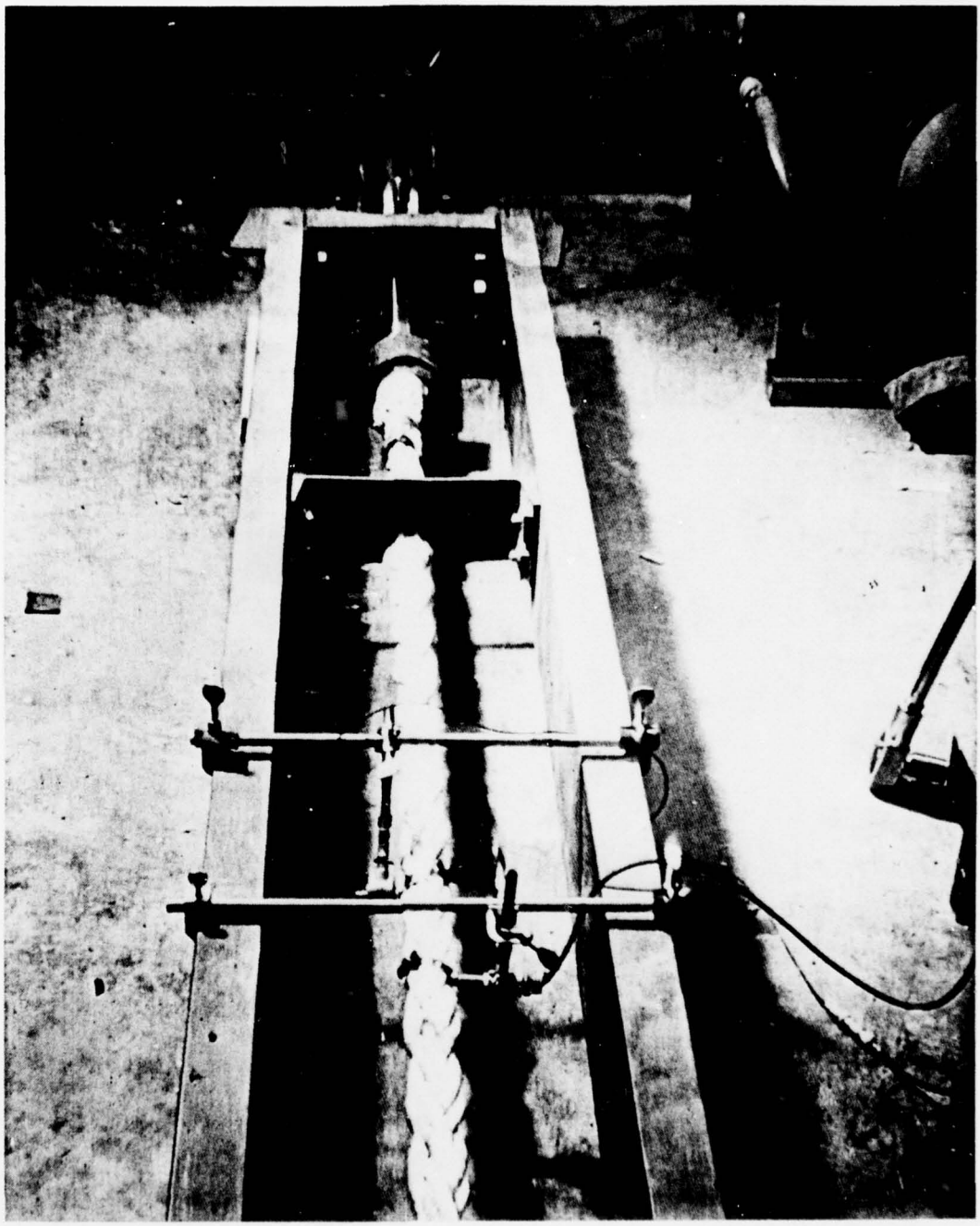

FIGURE 20 PHOTOGRAPHIC REPRESENTATION OF THE LOAD FRAME FOR APPLYING THE INTERNAL FRICTION DAMPING TO SYNTHETIC ROPES (OVERVIEW)

AD-A078 461 DAEDALEAN ASSOCIATES INC WOODBINE MD F/G 11/5
ENGINEERING FEASIBILITY OF INTERNAL FRICTION DAMPING AS A NONDE--ETC(U)
FEB 79 D C FRESCH , L L YEAGER DOT-CG-828271-A

UNCLASSIFIED USCG-D-51-79 NL

2 OF 3
AD
AD 78461

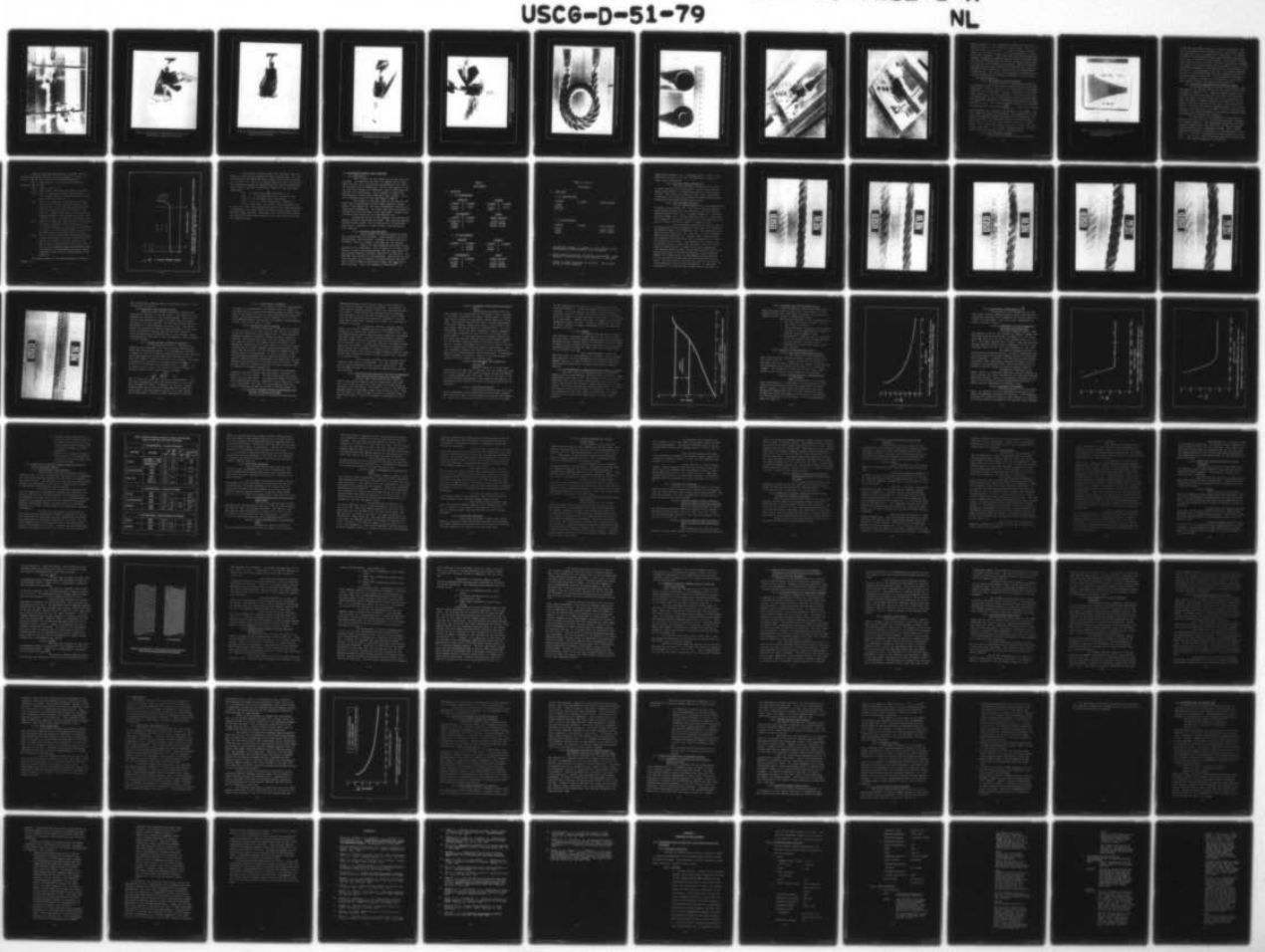


D
078

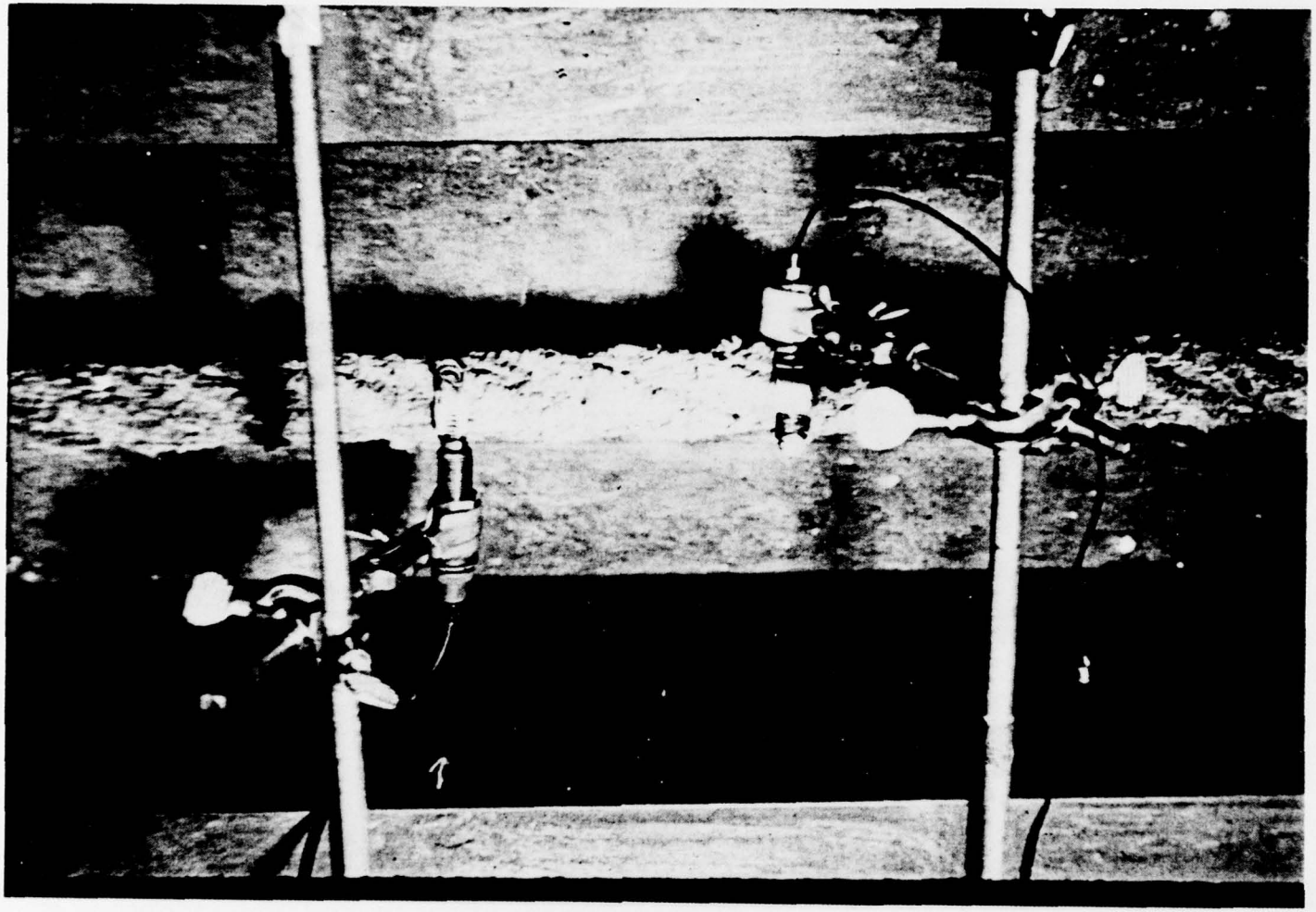

FIGURE 21 PHOTOGRAPHIC VIEW OF THE LOAD FRAME (TOP VIEW SHOWING INPUT & OUTPUT TRANDUCERS

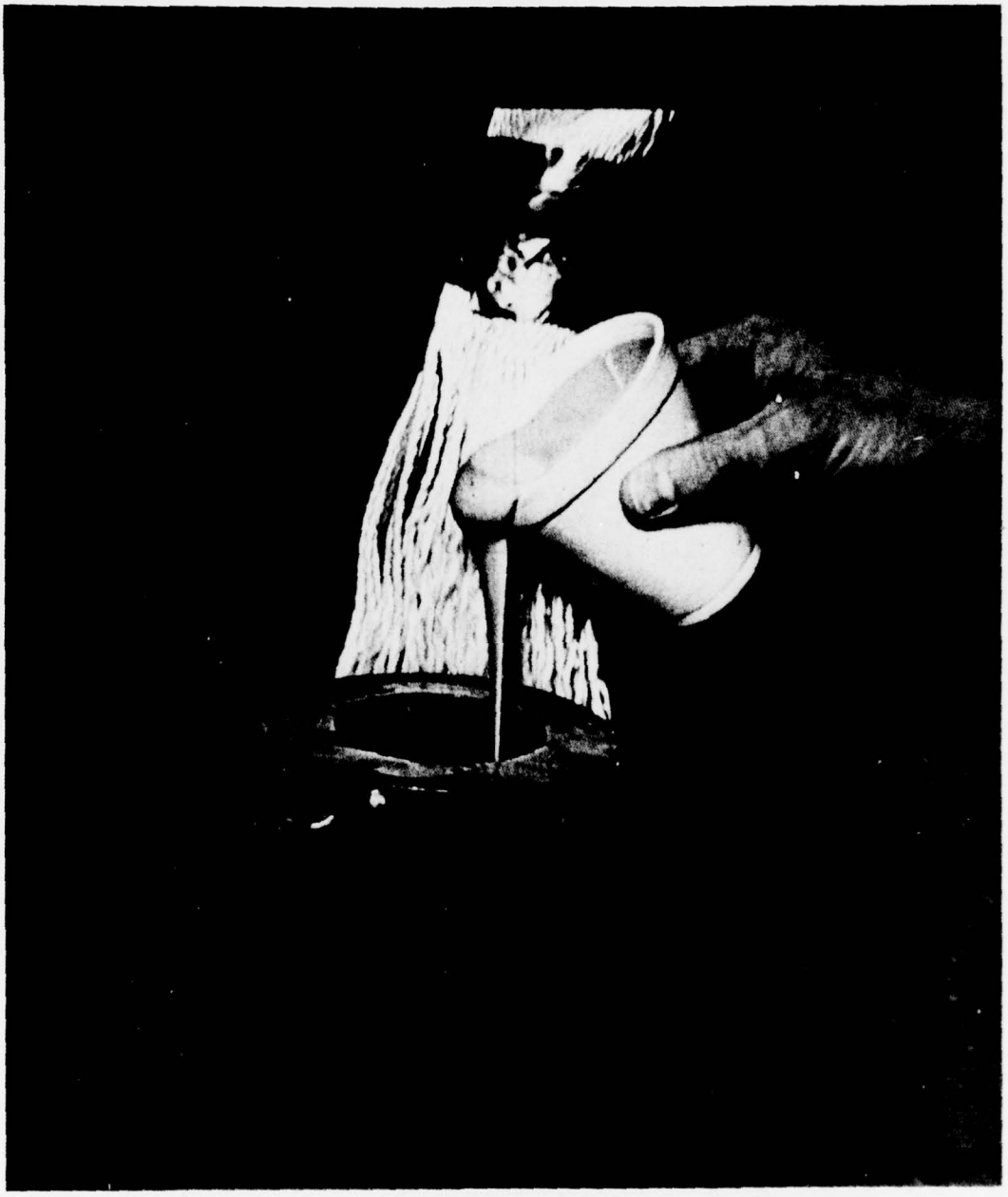

FIGURE 22 PHOTOGRAPHIC REPRESENTATION OF THE SPECIMEN PREPARATION (POURING EPOXY INTO MOLD)

FIGURE 23 PHOTOGRAPHIC REPRESENTATION OF SPECIMEN PREPARATION
(UNBRAIDED ROPE END IN MOLD)

FIGURE 24 PHOTOGRAPHIC VIEW OF SPECIMEN PREPARATION
(PRESSURIZED EPOXY INJECTION)

FIGURE 25 PHOTOGRAPHIC REPRESENTATION OF SPECIMEN PREPARATION
(COMPLETING MOLD WITH EPOXY FILLING)

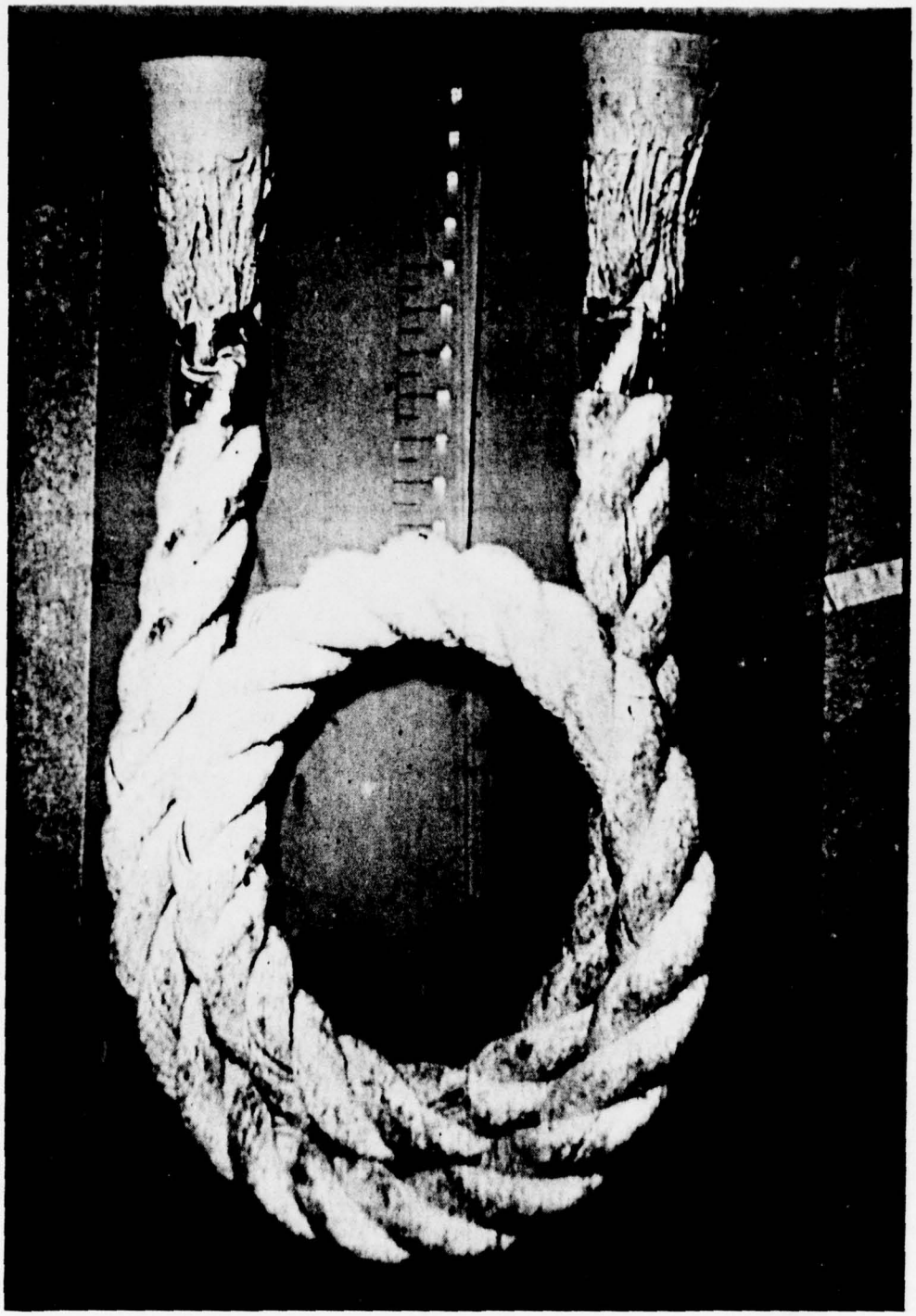

FIGURE 26 PHOTOGRAPHIC VIEW OF ROPE SECTION WITH EPOXY MOLD END FITTINGS

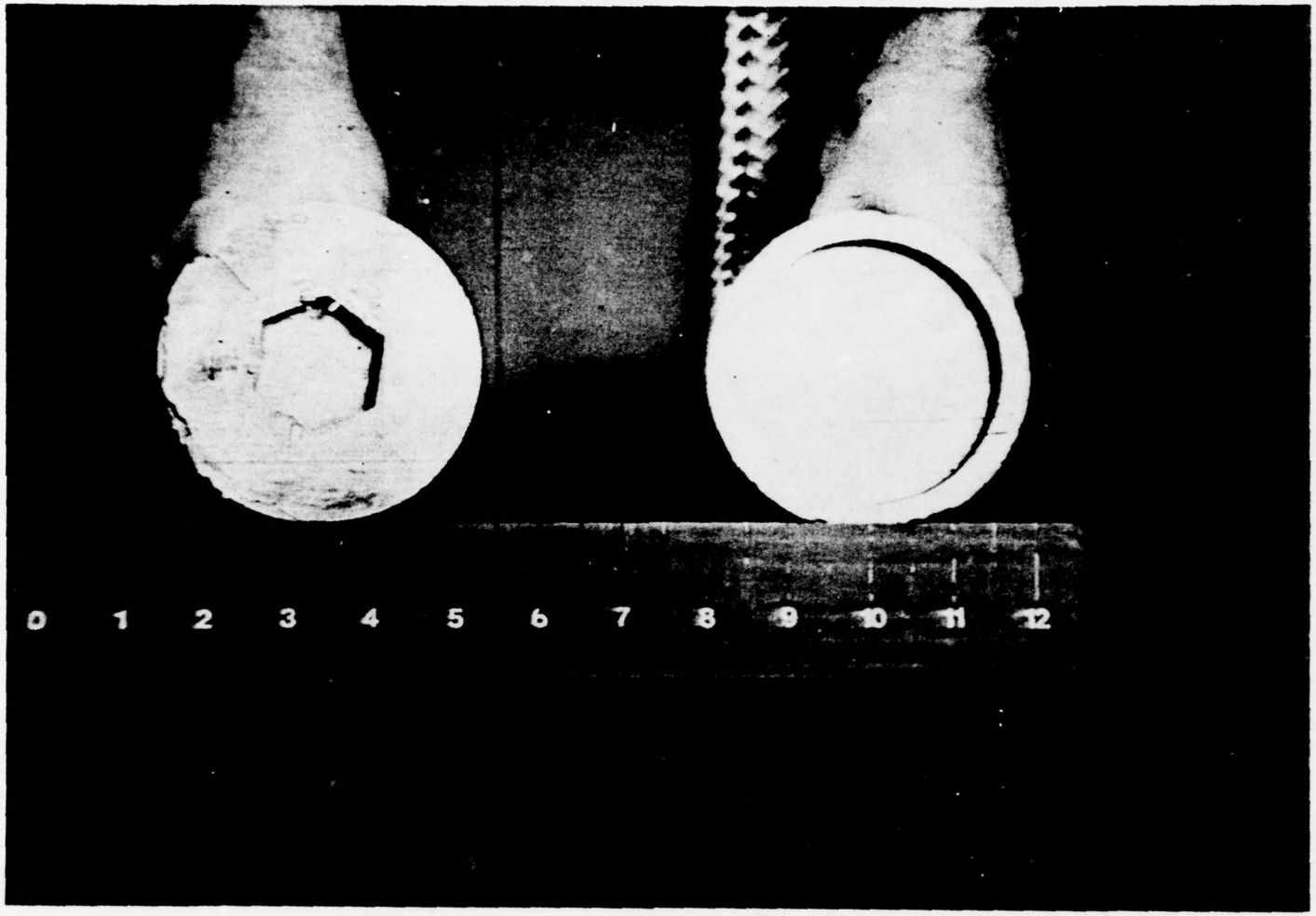

FIGURE 27 PHOTOGRAPHIC END VIEW OF EPOXY CASTING FOR ATTACHMENT INTO LOAD FRAME

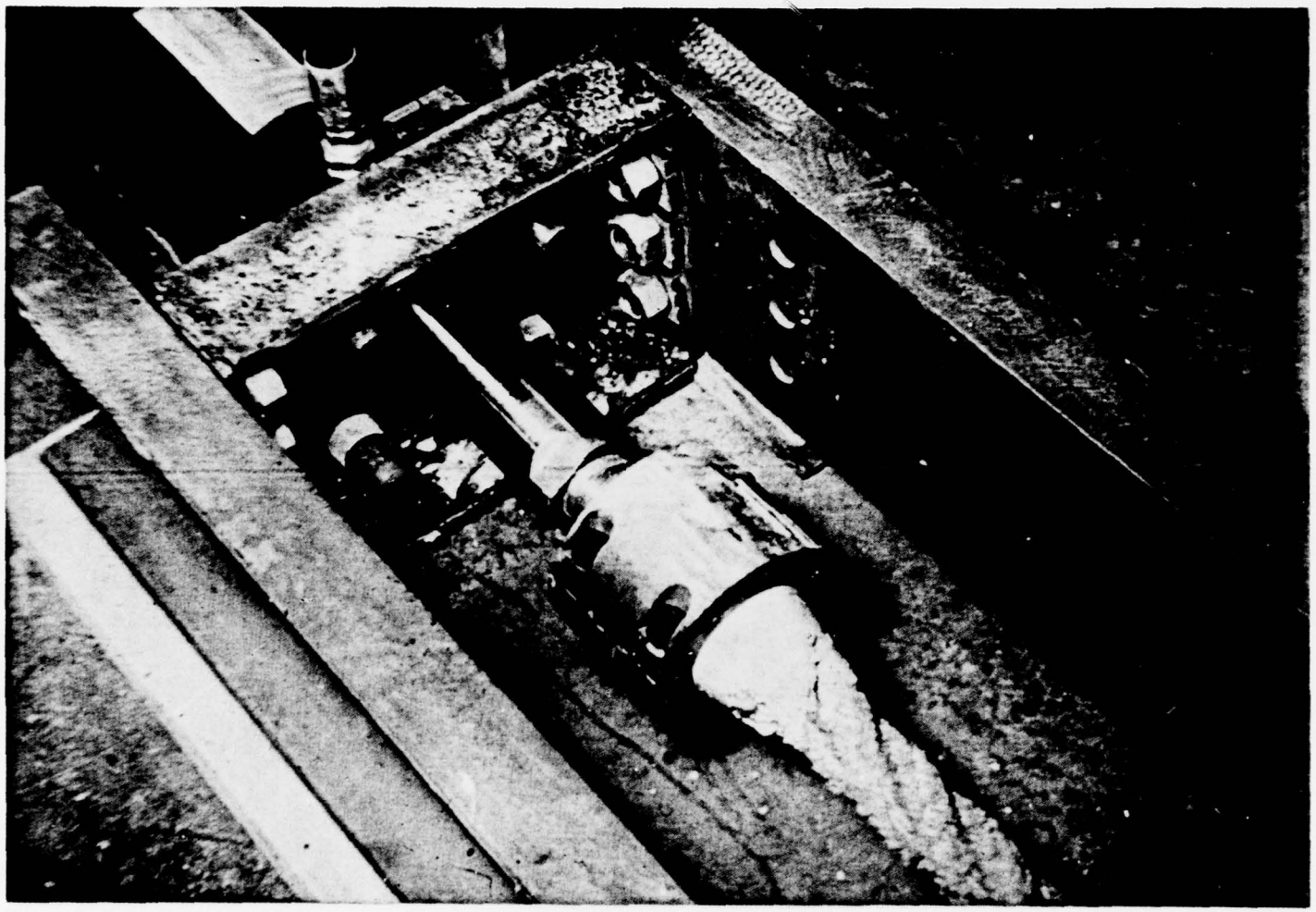

FIGURE 28 PHOTOGRAPHIC REPRESENTATION OF THE TEST TECHNIQUE TO SYNTHETIC ROPES WITH END FITTINGS ON CYLINDER END

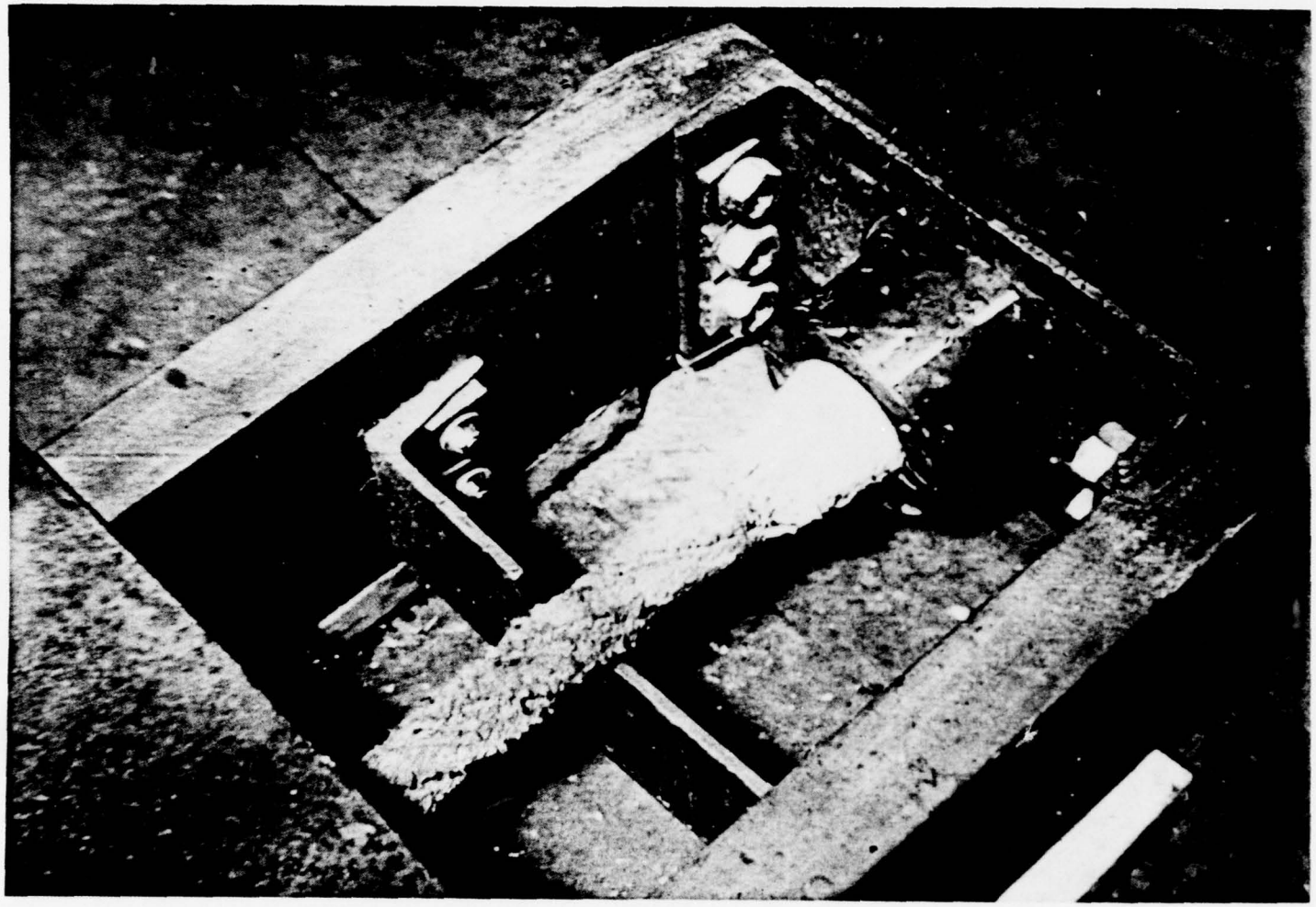

FIGURE 29 PHOTOGRAPHIC REPRESENTATION OF LOAD FRAME WITH END FITTINGS ON FIXED END

data was acquired. This requirement extends from the viscoelastic behavior of the synthetic rope material. This is discussed in detail in Section 4.3. Specific damping capacity values are recorded for each of the rope specimens to define this time parameter. After this time equilibrium has been reached, the specific damping capacity value is obtained from the Polaroid™ photograph taken of the attenuated decay curve from the CRT of the storage oscilloscope. Figure 30 depicts the expected full screen display of a typical decay curve for synthetic rope specimens as tested in the electrohydraulic loading device. The various data analysis and statistical analysis procedures are included in Appendix B of this report.

3.6 Data Analysis

3.6.1 Introduction to Data Analysis

The output decay of the IFD-NDE technique is a logarithmic decay of the system response resulting from the input pulse. From the record of the output decay, a reference amplitude (A_o) is measured. $A_{n(1-5)}$ is defined at five equal cycle intervals of the decay interval. The ratio of the relative amplitudes (A_o/A_n) is determined for the five amplitudes. The logarithmic decrement is determined from equation [4] which provides $\alpha_{n(1-5)}$. The specific damping capacity is determined from equation [5] and provides $\left(\frac{\Delta W}{W}\right)_{n(1-5)}$. These five logarithmic decrements are averaged from the mean of the sample. However, since the decay is logarithmic, the variance of the sample of the specific damping capacity must be determined. In order to convert the logarithmic decay to a linear straight line, decay of the linear least-squares curve fit is calculated. The linear least-squares curve fit provides the slope of the linear decay. The specific damping capacity is determined from the estimated slope of the linear decay.

3.6.2 Data Reduction Program

The program associated with the calculation

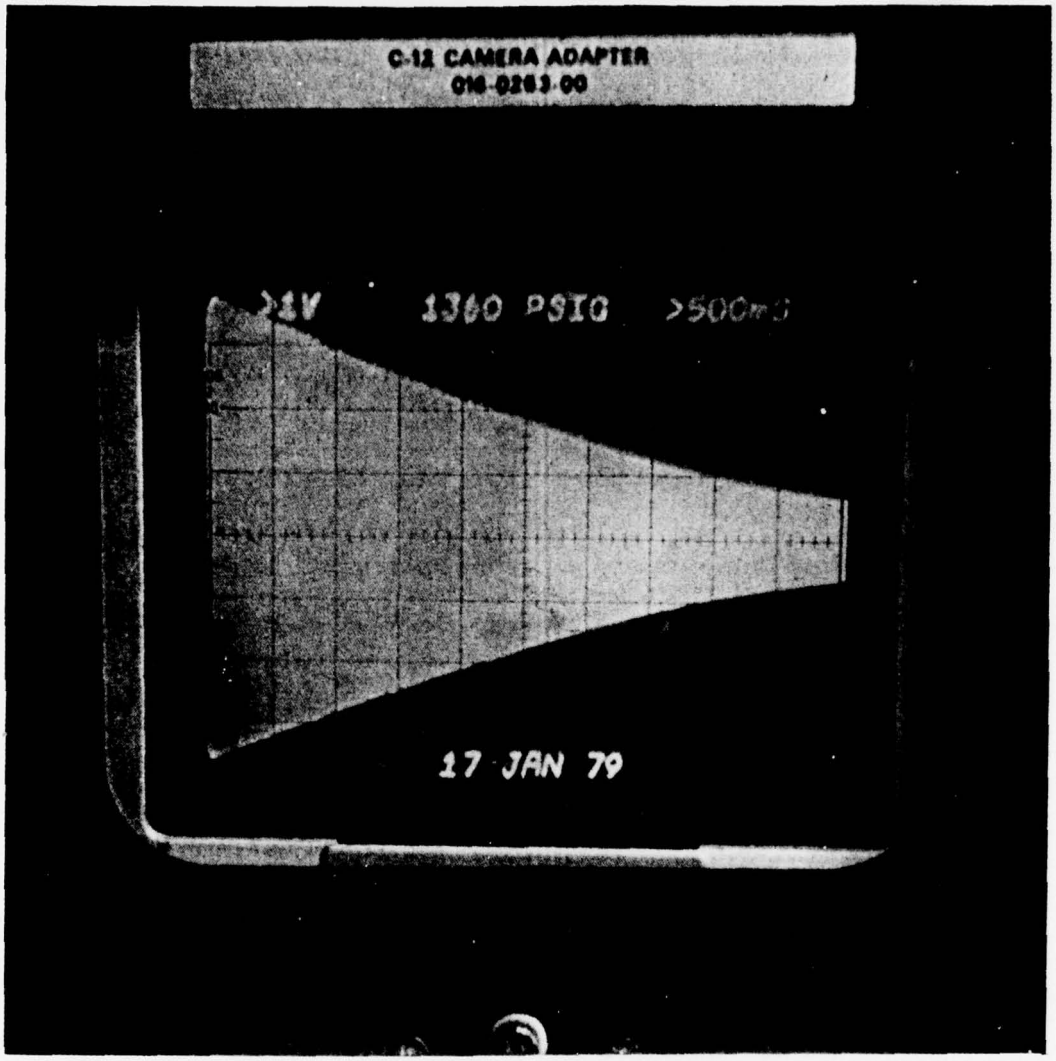

FIGURE 30 FULL SCREEN CRT DISPLAY OF THE RESPONSE (DECAY) OF A SYNTHETIC ROPE SPECIMEN SHOWING A SAMPLE DECAY ENVELOPE

of the specific damping capacity is found in Appendix B. The initial procedure sets the memory bank to zero and the reference amplitude (A_o) is entered into the program. The number of decay cycles between subsequent relative amplitude measurements (A_n) is entered into the program. Equal number of decay cycle intervals (LC_n) providing the decay interval are computed. The output of the decay cycle interval defines the $A_{n(1-5)}$. The logarithmic decrement is calculated and the least-squares linear curve fit is performed on the data. The specific damping capacity is determined along with the standard deviation of the least-squares linear fit. The data reduction program is found in Appendix C along with the definition of the sample mean, sample variance, and least-squares curve fit.

3.7 Viscoelastic Measurement for Synthetic Ropes

The dynamic modulus is related to the specific damping capacity as a dynamic response of the material exhibiting viscoelastic behavior. (27) Synthetic hawsers exhibit this viscoelastic nature and respond to the input load with some phase lag angle. The full discussion of the relationship between the specific damping capacity as a function of the applied load will be taken up in the results and discussion of results. However, the specific damping capacity will be discussed in this section as it relates to the time (viscoelastic response); the load (viscoelastic and mechanical response); and the temperature (viscoelastic response).

The evaluation of the fundamental relationship between stress and strain of a viscoelastic material is known as the "complex modulus." The complex modulus defines the relationship between stress and strain for a linear viscoelastic material subjected to a sinusoidal loading. When a linear viscoelastic material is subjected to a loading stress of the form $\sigma = \sigma_o \sin(wt)$, the resulting strain response is of the form $\varepsilon = \varepsilon_o \sin(wt-\phi)$ which lags the stress by the phase angle, ϕ. The complex modulus E* is defined by:

$$E^* = E' + jE'' \qquad [13]$$

where:

E^* = complex modulus

$E' = \frac{\sigma_o}{\varepsilon_o} \cos \phi$

$E'' = \frac{\sigma_o}{\varepsilon_o} \sin \phi$

j = imaginary number

σ_o = maximum stress applied - psi

ε_o = maximum recoverable strain experienced during test - in/in.

ϕ = phase lag angle - degrees

Based on this definition, the absolute value of the complex modulus, $|E^*|$, is a measure of the material's elasticity while the phase lag angle, ϕ, is a measure of the viscous response.

The absolute value of the complex modulus is commonly referred to as the dynamic modulus and is defined by the equation:

$$|E^*| = \frac{\sigma_o}{\varepsilon_o} \qquad [14]$$

where:

$|E^*|$ = dynamic modulus - psi

σ_o = maximum stress applied - psi

ε_o = maximum recoverable strain experienced during test - in/in.

The strain in the viscoelastic rope lags the stress by a time dependent phase angle ϕ. This phase angle was determined from the time dependency of the specific damping capacity measurements. Specific damping capacity measurements were made as a function of time for the rope under load. The specific damping capacity measurements were made periodically

until two consecutive values were identical in amplitude at different time periods.

3.8 General Mathematical Model for Specific Failure Mechanisms

A general mathematical model has been developed which relates the specific damping capacity to amount of rope use. This model takes into consideration that there are two apparent failure mechanisms working simultaneously: the first mechanism is the internal stress caused by the tensile, bending, and torsional forces experienced by the rope under field application; the second mechanism is the effect of chemical exposure due to the environmental effects such as brine, ultraviolet light, etc. The general effect of these forces on the specific damping capacity values are surmised to be as noted below.

1. The ropes are viscoelastic when subjected to high stresses; therefore, the effect of the mechanical forces will be to leave a residual internal stress. If this effect is significant, it should be observable in the rope after minimal usage.
2. After the initial residual stress is in place, one would expect a stable behavior (no large change in $\Delta W/W$) until one or both failure mechanisms bring the rope to the state of incipient failure. In highly corrosive environments, one would expect a smaller stable region (less time of use to incipient failure) than in noncorrosive environments.
3. When one or both failure mechanisms have created a state of incipient failure, a large increase in specific damping capacity is expected.

Based on the above observations, we expect the relationship between $\Delta W/W$ and time of use where $Y \equiv \Delta W/W \times 10^{-4}$ and X = time of use to possess the following features.

If Y = f(x) expresses the functional relationship between X and Y, then

(i) $f(X) \geq 0$ for $X \geq 0$

(ii) $f(0) \simeq 400$ = the value of Y for a new rope

(iii) f(X) is a monotonic increasing function. If f is assumed to be a differentiable function, then $f'(X) \geq 0$ for $X \geq 0$.

(iv) There is a value $X_s > 0$ such that the internal residual stress increases with X in the interval $0 \leq X \leq X_s$, but remains fairly constant for larger values of X than X_s. If this has a significant effect on the specific damping capacity, one should notice that $f''(X) < 0$ for $X < X_s$. We expect $X_s \leq 10$ load cycles.

(v) There is a value $X_f \geq X_s$ such that the relation Y = f(X) is linear or very nearly so for $X_s < X < X_f$ the interval $X_s \leq X \leq X_f$ is the stability region. In this region, f'(X) is expected to be small but positive, and f''(X) to be zero.

(vi) For $X \geq X_f$ one or both failure mechanisms have created an incipient failure condition and the values of Y should increase rapidly with X. This would be observed by noting that $f''(X) > 0$ for $X > Xf$. Incipient failure is detected when the value of Y has increased beyond the upper confidence limit for the linear region of the function.

The general nature of the expected graph is shown in Figure 31.

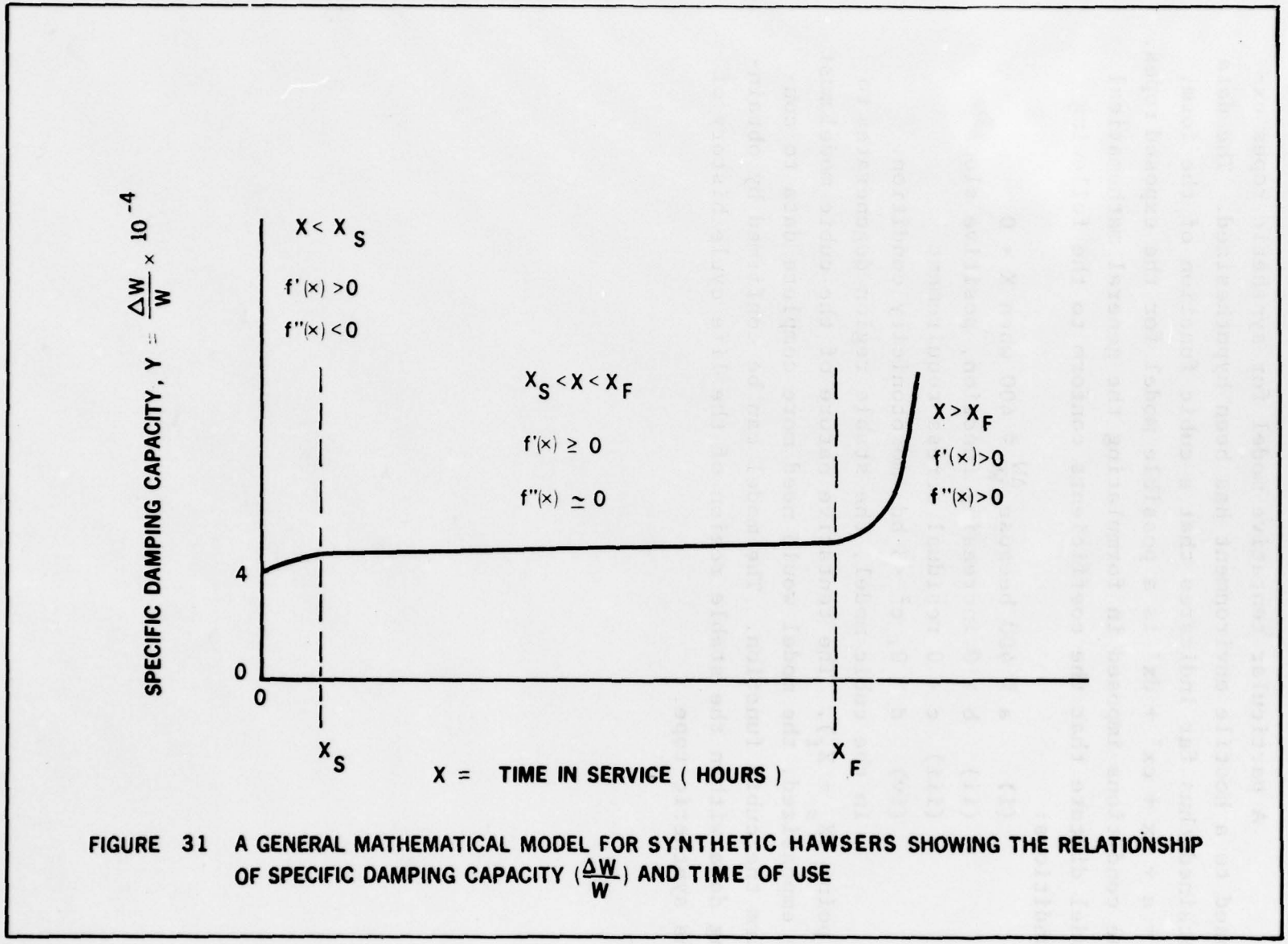

FIGURE 31 A GENERAL MATHEMATICAL MODEL FOR SYNTHETIC HAWSERS SHOWING THE RELATIONSHIP OF SPECIFIC DAMPING CAPACITY ($\frac{\Delta W}{W}$) AND TIME OF USE

A particular tentative model for synthetic ropes exposed to a hostile environment has been hypothesized. The data obtained thus far indicates that a cubic function of the form, $Y = a + bx + cx^2 + dx^3$ is a possible model for the exposed ropes. The conditions imposed in formulating the general mathematical model dictate that the coefficients conform to the following conditions:

(i) $a \cong 400$ because $\frac{\Delta W}{W} \cong 400$ when $X = 0$

(ii) $b > 0$ increasing function, positive slope

(iii) $c < 0$ residual stress requirement

(iv) $d > 0$, $c^2 < 3\,bd$ monotonicity condition.

In the cubic model, the stable region degenerates to a point ($X_s = X_f$). The tentative nature of the cubic model must be emphasized; the model would need more complete data to confirm the cubic function. The model can be confirmed by obtaining data within the stable region of the life cycle history of the synthetic rope.

4.0 EXPERIMENTAL RESULTS AND DISCUSSION

4.1 Test Matrix

Table I shows the test matrix of new and used ropes obtained. To summarize the table, 24 samples of new ropes were obtained; 14 of the six inch circumference size, and 10 of the eight inch circumference. The 14 rope samples of the six inch size contain nine different types of rope based on material and construction. The 10 samples of eight inch circumference contain eight different types; giving a total of 17 different types of new rope among 24 samples.

The variety of used rope types in the six inch and eight inch circumferences include eight different samples. Three of the samples are six inch circumference, and five are eight inch circumference. All eight used ropes are paired in matched sets with new ropes of the same types. Primary data collection was focused on the eight matched sets.

During the course of this program, over 620 specific damping capacity values were obtained. Each specific damping capacity value results from the analysis of six individual data points; therefore, a total of over 3,700 data points were analyzed.

4.1.1 Synthetic Rope Materials

Rope specimens of three different materials were studied under this program. These materials are nylon, polypropylene, and polyester. Polyester is also referred to as Dacron, which is a Dupont trade name for the material.

Four of the rope specimens were made of combinations of two materials. Two of these are six inch circumference, three strand polypropylene with the outer fibers of each strand composed of Dacron, referred to as POLY-DAC. The POLY-DAC ropes constitute a matched pair, one new and one used. There are also two new samples of double-braided rope which have a multi-filament polypropylene inner core and a nylon outer covering. These are designated Power-Braid™ by

TABLE I

TEST MATRIX

A. NEW ROPES

1) 6" CIRCUMFERENCE

AMERICAN

3 STRAND	8 STRAND
POLYPRO NYLON	NYLON

COLUMBIA

3 STRAND	8 STRAND
DACRON NYLON	NYLON

SOUTHWESTERN*

3 STRAND	8 STRAND
POLYPRO-DAC NYLON POLYPRO DACRON	POLYPRO

SAMSON

DOUBLE BRAIDED**

NYLON - NYLON
NYLON - POLYPRO
DACRON - DACRON

2) 8" CIRCUMFERENCE

AMERICAN

3 STRAND	8 STRAND
—	DACRON POLYPRO

COLUMBIA

3 STRAND	8 STRAND
NYLON DACRON	—

SOUTHWESTERN*

3 STRAND	8 STRAND
POLYPRO NYLON DACRON	—

SAMSON

DOUBLE BRAIDED**

NYLON - NYLON
NYLON - POLYPRO
DACRON - DACRON †

TABLE 1 - Cont'd.

TEST MATRIX

B. USED ROPES

1) 6" CIRCUMFERENCE

3 STRAND	8 STRAND	DOUBLE BRAIDED
NYLON POLYPRO POLY-DAC	—	—

2) 8" CIRCUMFERENCE

3 STRAND	8 STRAND	DOUBLE BRAIDED
POLYPRO NYLON DACRON	—	NYLON - NYLON DACRON - DACRON

* SOUTHWESTERN CORDAGE IS A BROKER FOR SHORT LENGTHS OF ROPE. MANUFACTURER OF ROPES SUPPLIED IS NOT DOCUMENTED.

** DOUBLE BRAIDED ROPES HAVE TWO MATERIAL DESIGNATIONS. FIRST MATERIAL IS OUTER COVERING, SECOND MATERIAL IS INNER CORE.

† DACRON IS DUPONT TRADE NAME FOR POLYESTER. SAMSON ROPES ARE NOT OF DUPONT MATERIAL.

Samson Ocean Systems, Inc., the manufacturer. One of these Power-Braid ropes is six inch circumference, the other is eight inch circumference.

4.1.2 Synthetic Rope Construction

The rope specimens evaluated are included in three categories of construction: three-strand twisted, eight-strand braided, and double-braided, the "rope inside a rope." New ropes were obtained in all three construction categories; used ropes were obtained of three-strand twisted construction and double-braided construction.

4.1.3 Rope Specimen Suppliers

All new double-braided ropes were manufactured by Samson Ocean Systems, Inc. New three-strand twisted and eight-strand braided ropes were obtained from three sources: American Manufacturing, Inc., Columbia Cordage Co., and Southwestern Cordage, Inc. American Manufacturing, Inc. and Columbia Cordage Co. manufacture synthetic rope; Southwestern Cordage is a broker for short lengths of synthetic rope.

Used ropes were obtained from various sources including marine towing companies in Baltimore, Md., McCallister Drydock Company in Philadelphia, Pa., the Curtis Bay Coast Guard Station, Curtis Bay, Md., and the U. S. Navy, Cheatham Annex near Williamsburg, Va. In most cases, the used ropes were acquired from scrap piles and no documentation of their use history was available. The condition of the used ropes as received visually ranged from excellent, with no visible signs of deterioration, to ropes of very poor appearance, with numerous broken strands, frayed and abraided outer fibers, melted areas due to friction and apparent strain hardening. Figures 32 through 39 are the photographic representations of the used rope specimens and the associated matching new ropes. The pairs of new and used rope sections are identical in construction, material and circumference. A detailed discussion of the correlations between visual assessment of

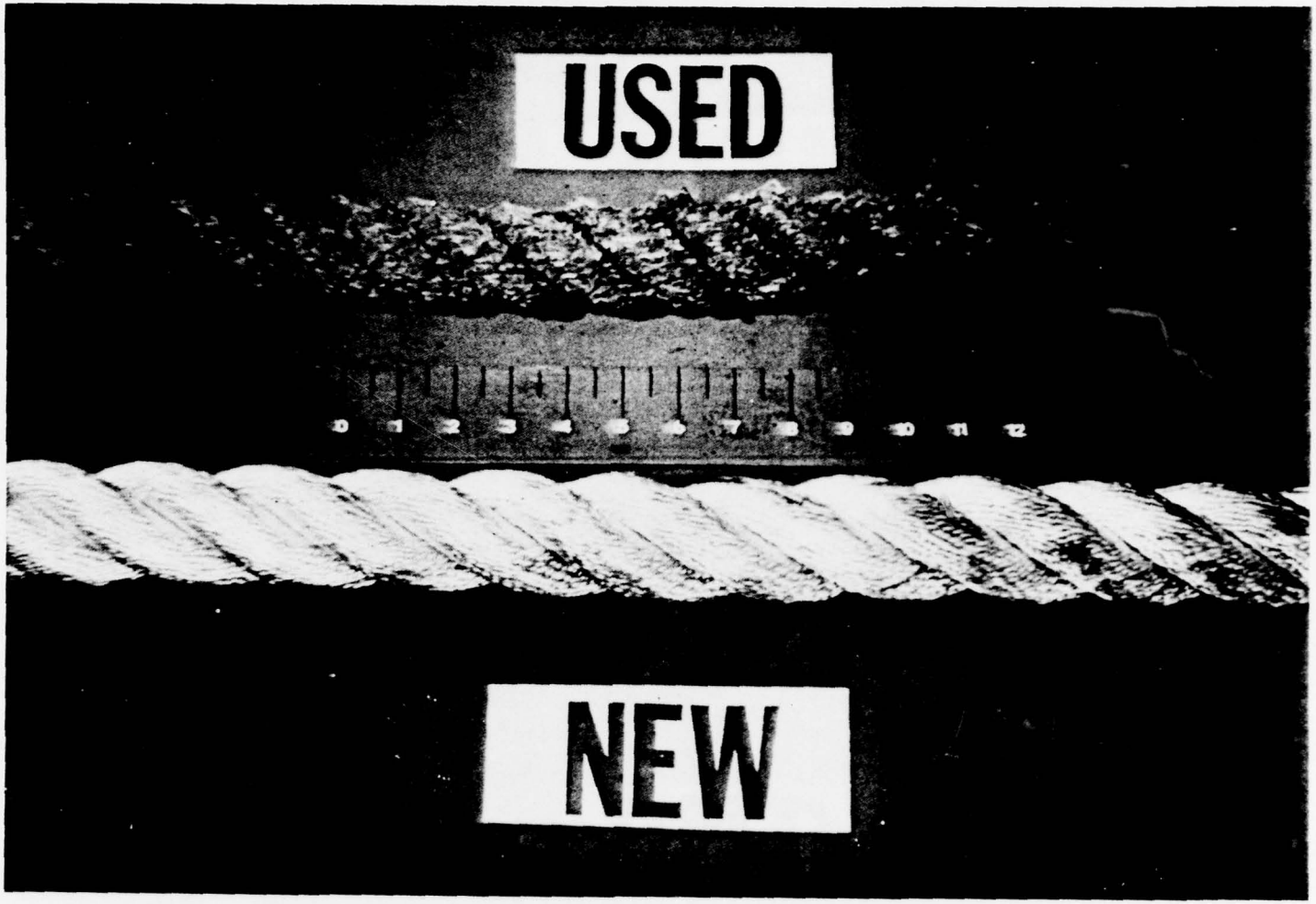

FIGURE 32 PHOTOGRAPHIC REPRESENTATION OF 6 INCH 3 STRAND NYLON ROPE

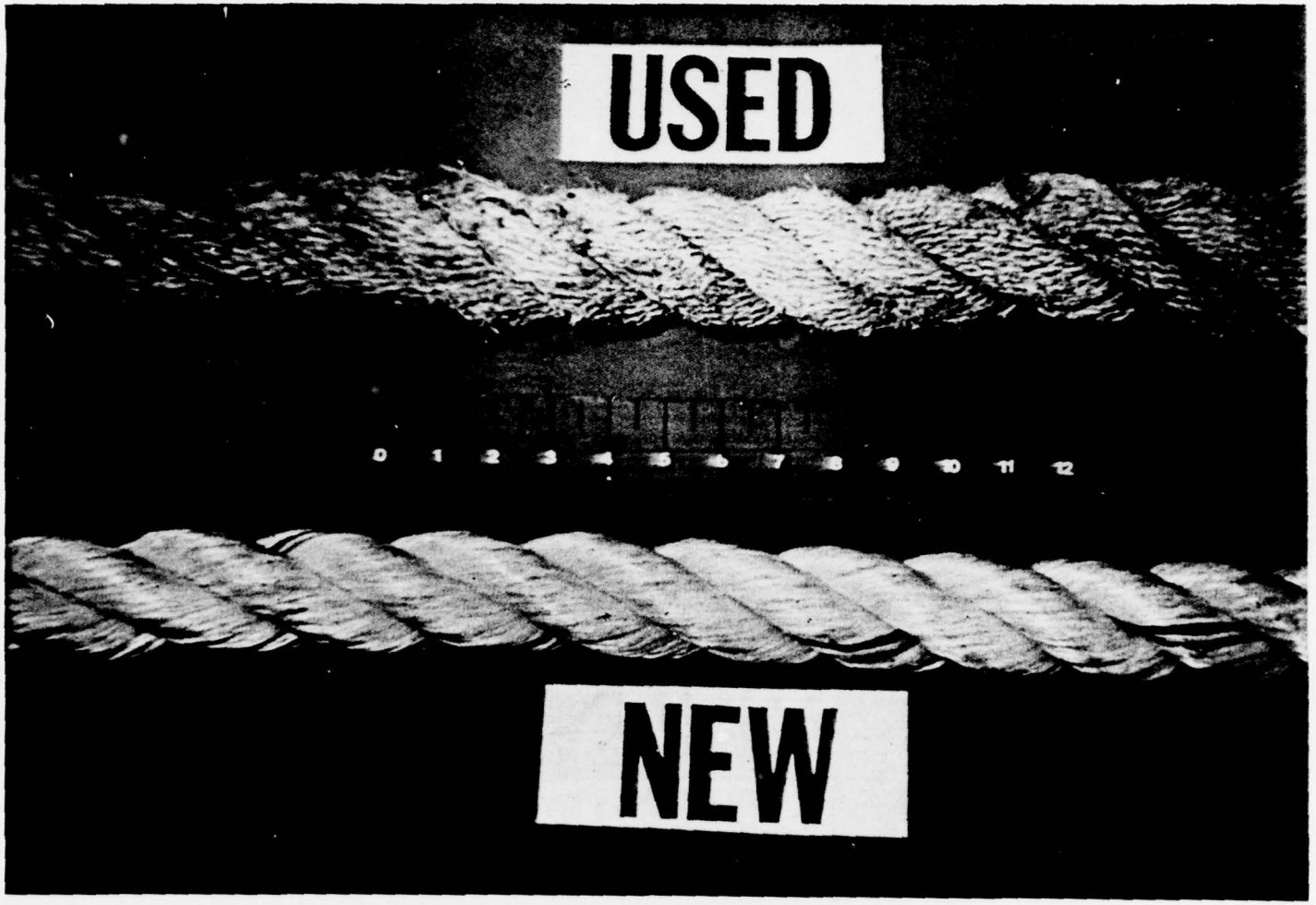

FIGURE 33 PHOTOGRAPHIC REPRESENTATION OF 6 INCH 3 STRAND POLYPROPYLENE ROPE

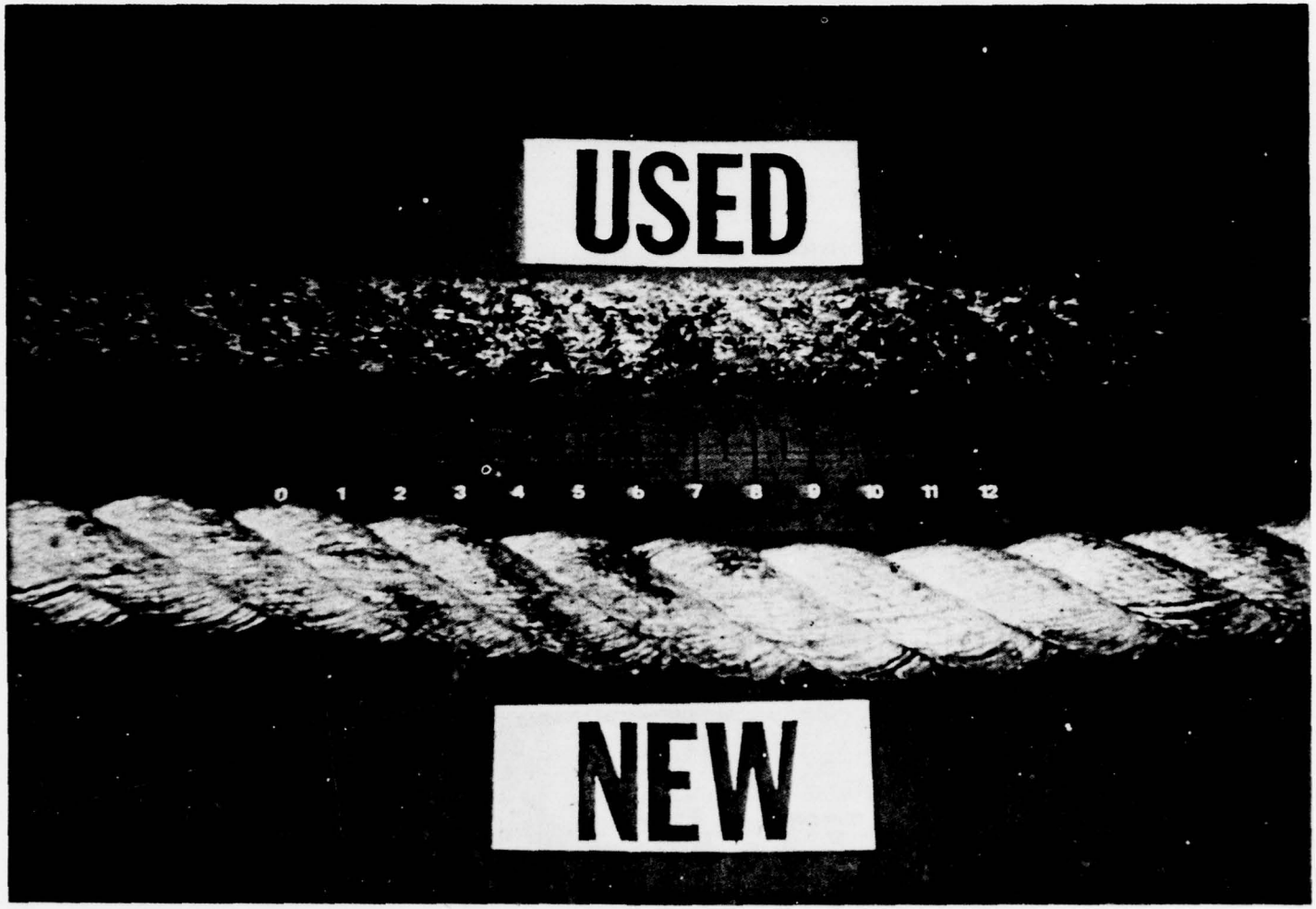

FIGURE 34 PHOTOGRAPHIC REPRESENTATION OF 6 INCH 3 STRAND POLY-DAC ROPE

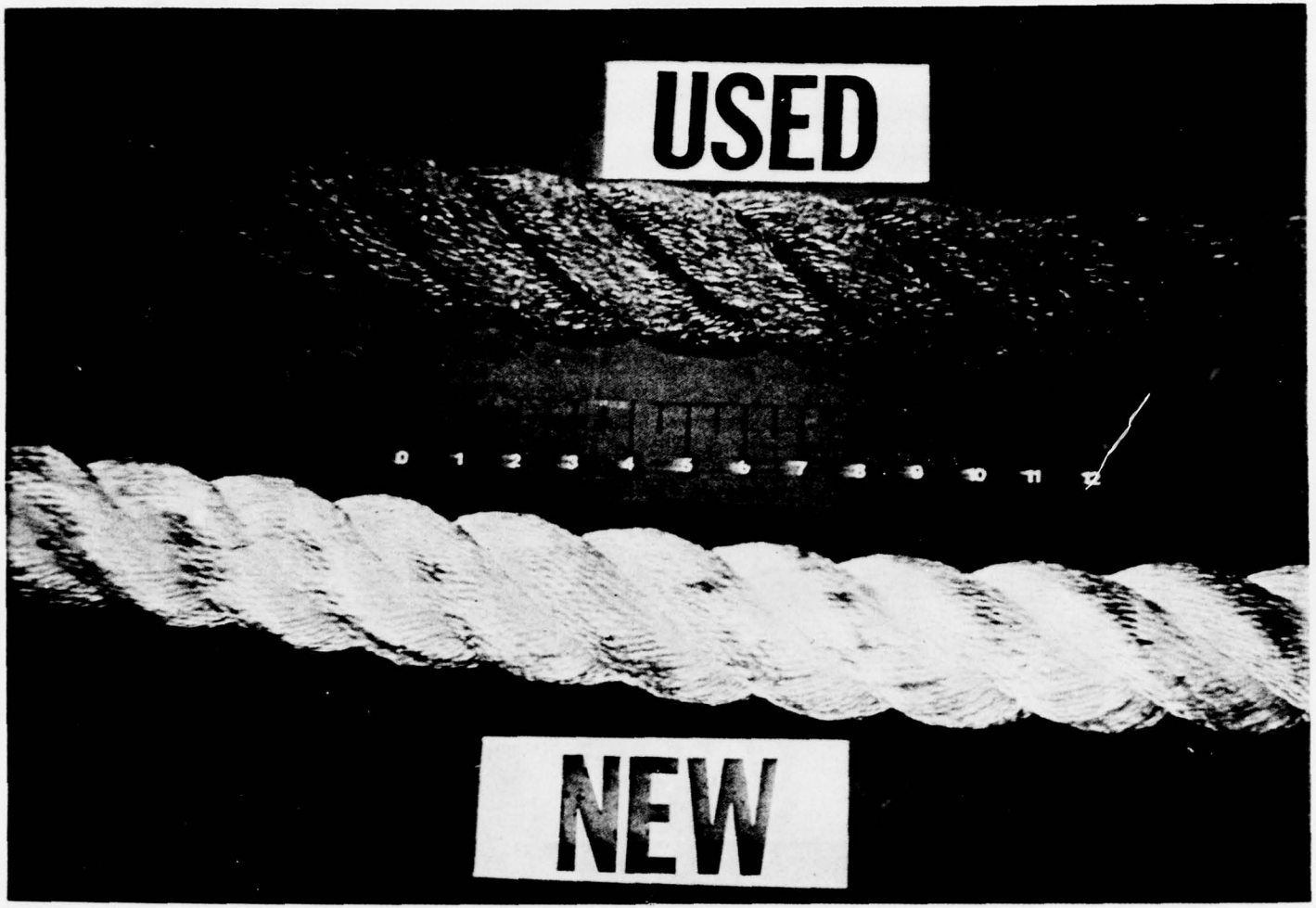

FIGURE 35 PHOTOGRAPHIC REPRESENTATION OF 8 INCH 3 STRAND NYLON ROPE

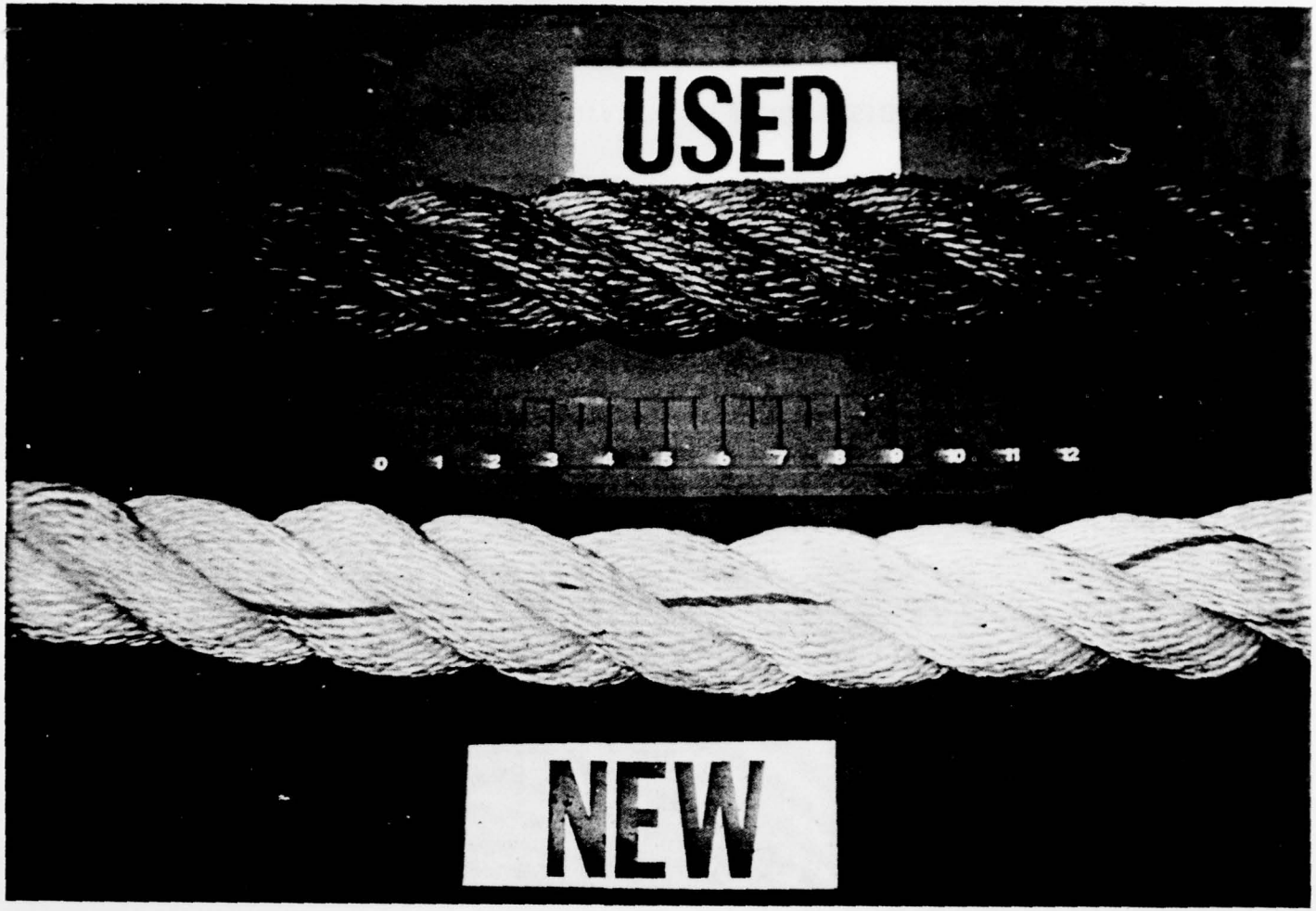

FIGURE 36 PHOTOGRAPHIC REPRESENTATION OF 8 INCH 3 STRAND POLYPROPYLENE ROPE

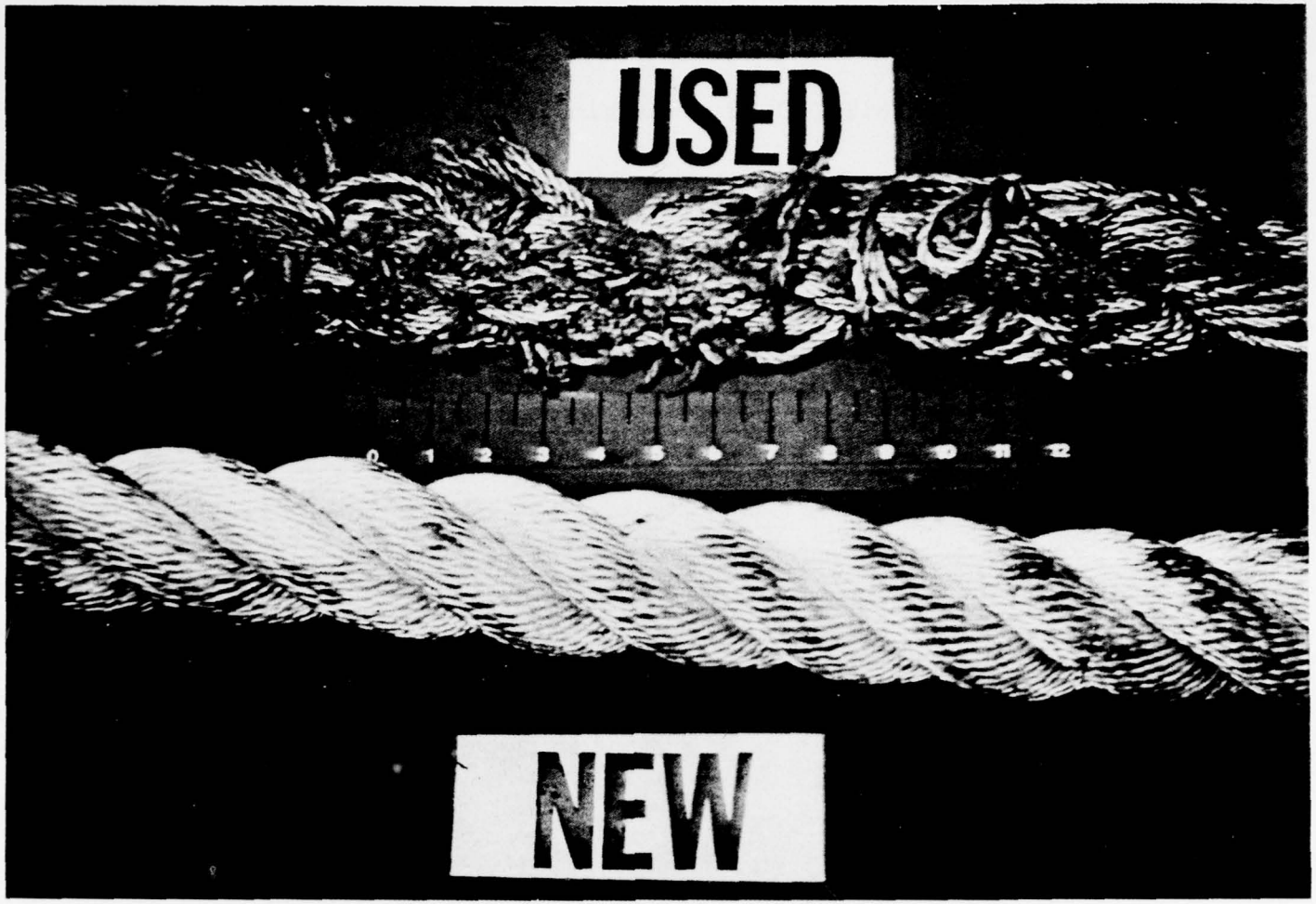

FIGURE 37 PHOTOGRAPHIC REPRESENTATION OF 8 INCH 3 STRAND DACRON ROPE

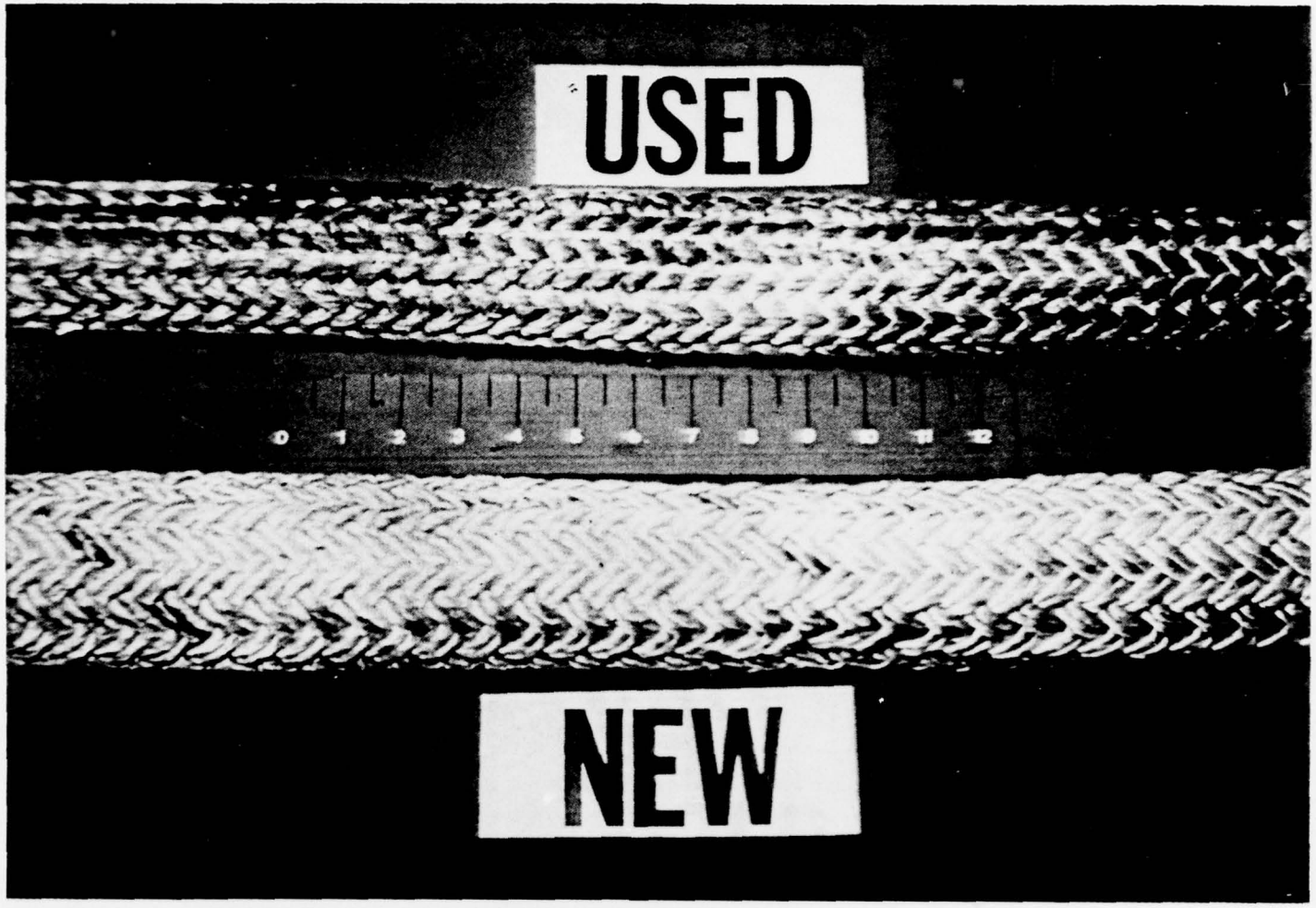

FIGURE 38 PHOTOGRAPHIC REPRESENTATION OF 8 INCH DOUBLE-BRAIDED NYLON ROPE

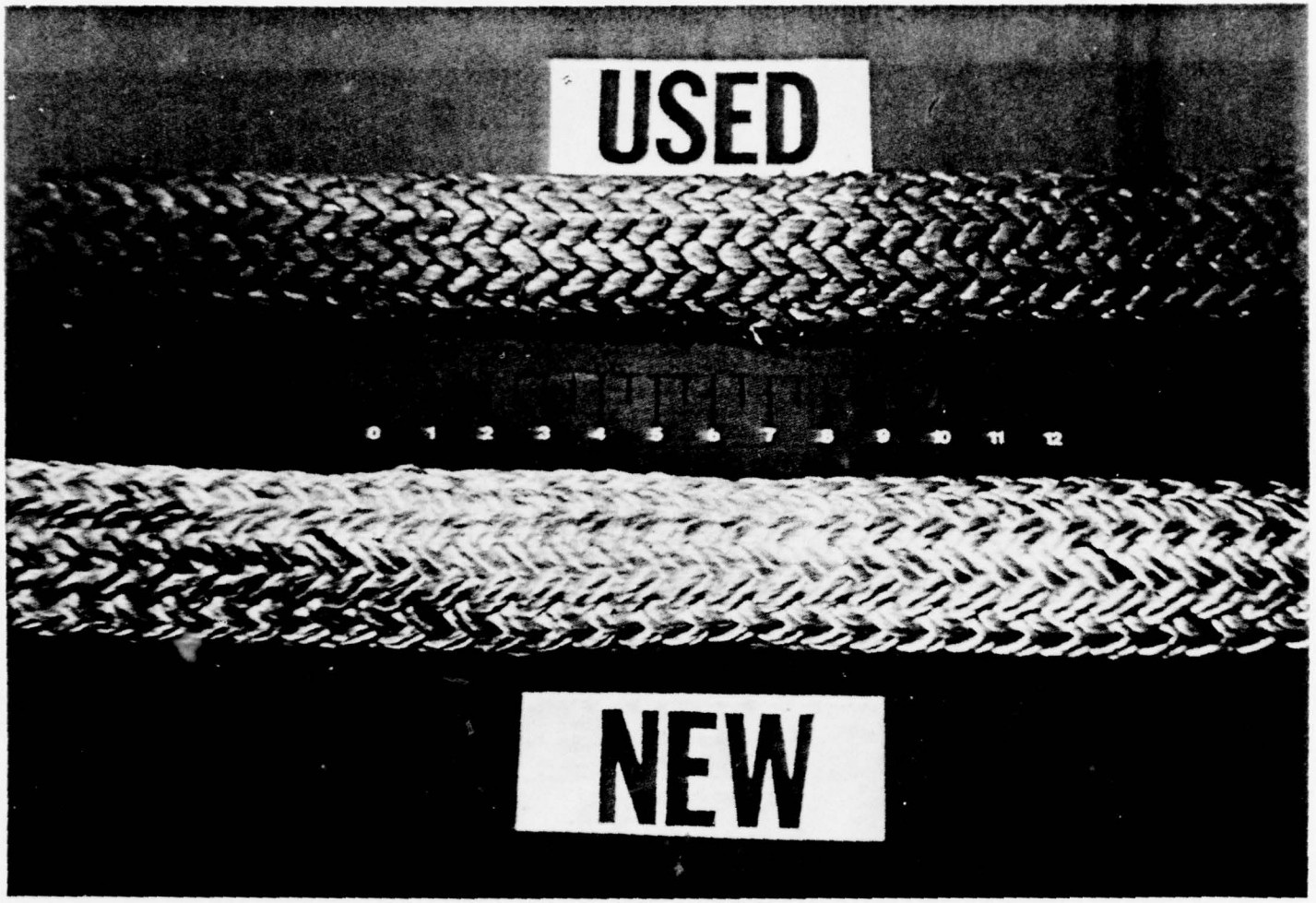

FIGURE 39 PHOTOGRAPHIC REPRESENTATION OF 8 INCH DOUBLE-BRAIDED DACRON ROPE

wear and specific damping capacity measurements will be found in Sections 4.6 and 4.7.

4.2 Characteristics of Ropes Studied

Synthetic ropes exhibit viscoelastic behavior as discussed in Section 3.7 of this report. Two aspects of this behavior are pertinent to the present program. The first of these is the finding that when a constant level of tension was kept on the rope specimen, the specific damping capacity decreased to a stable minimum value over time. The second aspect of viscoelastic behavior found pertinent to this study is the relationship between applied load and elongation. These two aspects are discussed later in this section, after a chronological discussion of the intermediate results leading to these findings.

4.2.1 Length of Rope to Radius of Gyration

As discussed in Section 3, "Experimental Apparatus and Techniques," the first testing conducted used three foot long rope specimens. This approach was modified in favor of a six foot long excited section due to the difficulty of forcing vibration in the three foot sections because of their low length to radius of gyration (l/r) ratios. The radius of gyration (r) is equal to the square root of moment of inertia (I) divided by cross sectional area, ($r = \sqrt{\frac{I}{A}}$). For a circular cross section, the radius of gyration reduces to half the radius of the circle ($R'/2$) as follows:

$$r = \sqrt{\frac{I}{A}} = \sqrt{\frac{\frac{\pi R'^4}{4}}{\pi R'^2}} = \frac{R'}{2} \qquad [15]$$

The l/r ratio for three foot sections is approximately 72 for six inch circumference ropes and approximately 55 for eight inch circumference ropes. Changing to a six foot vibrated length double the l/r ratios to approximately 144 and 110, respectively, which physically results in a lesser energy input requirement to obtain a given amplitude of vibration.

4.2.1.1 Application to Hawsers

For a typical hawser of approximately 21 inches in circumference, the minimum length to radius of gyration ratio will define the minimum length of hawser section that can be tested with the existing instrumentation and technique. Utilizing equation [15] to compute r for a 21 inch circumference hawser, the minimum test length is approximately 14 feet, for an 1/r ratio of $\sim$ 100.

4.2.2 Results of Initial Testing

The first functional relationship determined in early testing of six foot sections was that as the tension on the rope increased in the range of one to three percent of breaking strength, the specific damping capacity tended to decrease; which means physically that less energy was lost per vibration cycle at the higher levels of tension. This evaluation, based initially on the analysis of 192 data points representing 32 specific damping capacity measurements, indicated that the behavior of rope specimens at higher levels of tension should be investigated. It was also noted at this time that more meaningful results would be obtained if the specific damping capacity measurements were made with the rope tension in the range of the working load of the ropes. Design working loads for synthetic ropes are between 10 percent and 17 percent of breaking strength (2).

A new rope specimen support and tensioning apparatus was then designed and fabricated as discussed in Section 2.2 of this report. The new system permitted tension levels up to 65,000 pounds. The breaking strength of new six inch circumference ropes in laboratory tests ranges from 75,000 to 131,000 pounds, for eight inch circumference ropes the range of breaking strength is 160,000 to 230,000 pounds (2).

4.2.3 Specific Damping Capacity Measurements with Tension in Working Load Range

The next phase of testing initiated specific

damping measurements with tension levels of approximately 5, 10, 15 and 20 percent of breaking strength. One hundred six (106) specific damping capacity values were obtained from 636 data points. These values were obtained from 16 different rope specimens; six of the rope specimens were tested under both dry and laboratory salt water wet conditions. The wet ropes were tested after soaking for 24 hours in a solution of synthetic sea water.

It was expected, based on the viscoelastic model, that specific damping capacity values $\left(\frac{\Delta W}{W}\right)$ should decrease as the tension was increased up to a finite limit, then the damping values should remain constant regardless of applied load above that limit. The data obtained generally showed a decrease in $\frac{\Delta W}{W}$ as tension increased from the five percent to the 10 percent level; but there was variation in behavior above that level on tension, some specimens exhibited a decrease in $\frac{\Delta W}{W}$ as tension was increased to 15 percent and 20 percent of breaking strength, some exhibited stable damping capacity values, while others showed an increase in $\frac{\Delta W}{W}$ at either the 15 percent or 20 percent level.

These results prompted a more thorough investigation using three rope specimens. The rope sections were new six inch circumference three-strand twisted nylon: one from Columbia Cordage, one from American Manufacturing and one used specimen.

4.2.4 Detailed Investigation of Six Inch Circumference Three Strand Twisted Nylon Rope Specimens

Each of these rope specimens was studied in detail, and specific damping capacity measurements were made with the tension varying from 2,500 pounds to 25,000 pounds in increments of 2,500 pounds. There were a total of 131 specific damping capacity measurements made using 786 data points. Each rope specimen was taken through the series of applied loads at least three times in order to document the variability in the data.

4.2.4.1 Transducer Offset Distance Measurements

Measurements were made of the air gaps between the transducers and the magnetic discs attached to the ropes, along with the output voltage level, to assess what effect variation in transducer offset might have on the data. Particularly during these tests, several measurements of specific damping capacity were made at each level of tension before increasing tension to the next level. For each measurement, either the input transducer, output transducer or both were readjusted to vary the size of the gap (transducer offset). It was found that the transducer offset did not affect the specific damping capacity measurements except for the extreme conditions where a transducer was so close that it contacted the magnetic disc, or so far away ($\gtrsim$ 0.125") that the signal/noise ratio was reduced significantly. This is an important finding with respect to both the immediate phase of the program and any future field phase, as transducer offset distance is found not critical to the measurement of internal friction damping in synthetic ropes.

4.2.4.2 Time Dependent Relationship of Measured $\frac{\Delta W}{W}$

Another finding of at least equal significance was that when a constant level of tension was kept on the rope specimen, the specific damping capacity decreased to a stable minimum value over time. This is the first of the two relationships pertaining to rope behavior mentioned at the beginning of this section, and will be discussed more fully in Section 4.3.

4.2.4.3 Load-Strain Behavior

During this detailed study of the six inch circumference three-strand twisted nylon ropes, measurements were also made of rope elongation as tension was increased. This led to the second pertinent relationship mentioned

at the beginning of this section, the relationship between load and elongation. Figure 40 graphically depicts this relationship. As can be seen in the figure, the rope exhibits nonlinear behavior at stress levels up to about 9,000 pounds. There is a range of linear elasticity from 9,000 to approximately 14,000 pounds. Beyond this limit, it appears that plastic deformation begins to occur. As might be expected, the range of linear elasticity roughly corresponds to the working load range of the rope.

4.2.4.4 Summary

To summarize the important findings just discussed, transducer offset distance was found to have no significant effect on specific damping capacity measurements, measured specific damping capacity is dependent upon the length of time the rope specimen has been under tension, and the rope specimens exhibit a range of linear elasticity corresponding to the working load range.

With these findings in mind, the next step taken in the program was to evaluate, using the same rope specimens, the time dependency of the measured specific damping capacity in order to arrive at the correct functional relationship between level of tension and specific damping capacity.

4.3 Time Dependency of Measured Specific Damping Capacity

The next step of the program involved 83 specific damping capacity measurements, involving 498 data points. These measurements were made on the two specimens of new six inch circumference three strand nylon, and on another new section of three strand nylon from Columbia Cordage which had not yet been tested. The virgin specimen was included purposefully to check the values obtained for the other two specimens. The other two specimens had each been tested, at least once, at tension levels well in excess of the upper limit of linear elastic behavior.

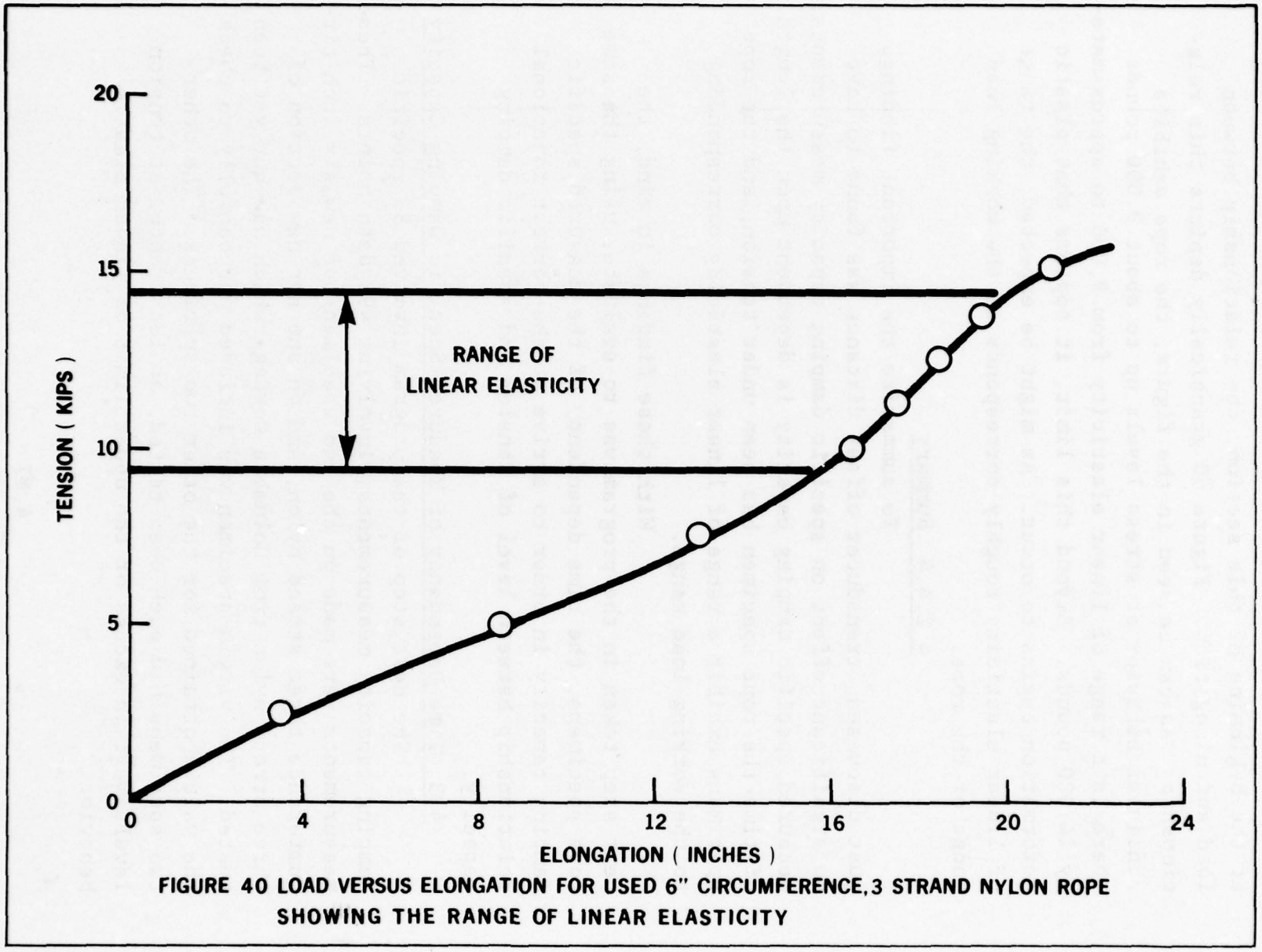

FIGURE 40 LOAD VERSUS ELONGATION FOR USED 6" CIRCUMFERENCE, 3 STRAND NYLON ROPE SHOWING THE RANGE OF LINEAR ELASTICITY

4.3.1 Procedure for Time Dependency Tests

Specific damping capacity measurements were made with rope tension varying from 2,500 pounds to 17,500 pounds generally in 2,500 pounds increments, with particular emphasis on the 10,000 to 15,000 pound region.

Testing was conducted in the following manner:

1. The rope specimen was brought to an initial level of tension.
2. Input and output transducer were positioned and an initial measurement of specific damping capacity $\left(\frac{\Delta W}{W}\right)$ was made.
3. Measurements of $\frac{\Delta W}{W}$ were made at intervals until the measured value stopped decreasing and reached a constant level.
4. Tension was increased and steps 2 and 3 were repeated.

4.3.2 Results of Time Dependency Tests

4.3.2.1 Less Than 5,000 Pounds Tension

For tensions of 5,000 pounds and less, final specific damping capacities ranged between 6.85×10^{-2} and 10.20×10^{-2}. A large variability was noticed in this data, and the decay curves were not always closely fitting the exponential decay theoretically expected of a vibrating element. The variability in the data of this stress region is due to the nonlinear rope response at low tensions.

4.3.2.2 Tension Between 7,500 Pounds and 17,500 Pounds

When the tension was in the region from 7,500 pounds to 17,500 pounds, the decay curves fit the theoretical exponential within the normal limits of experimental accuracy. As had been noted previously, when rope tension was brought from zero to a level within this range, the $\frac{\Delta W}{W}$ value always decreased over time until a stable value was obtained after 60 to 100 minutes. The time dependency is shown in Figure 41.

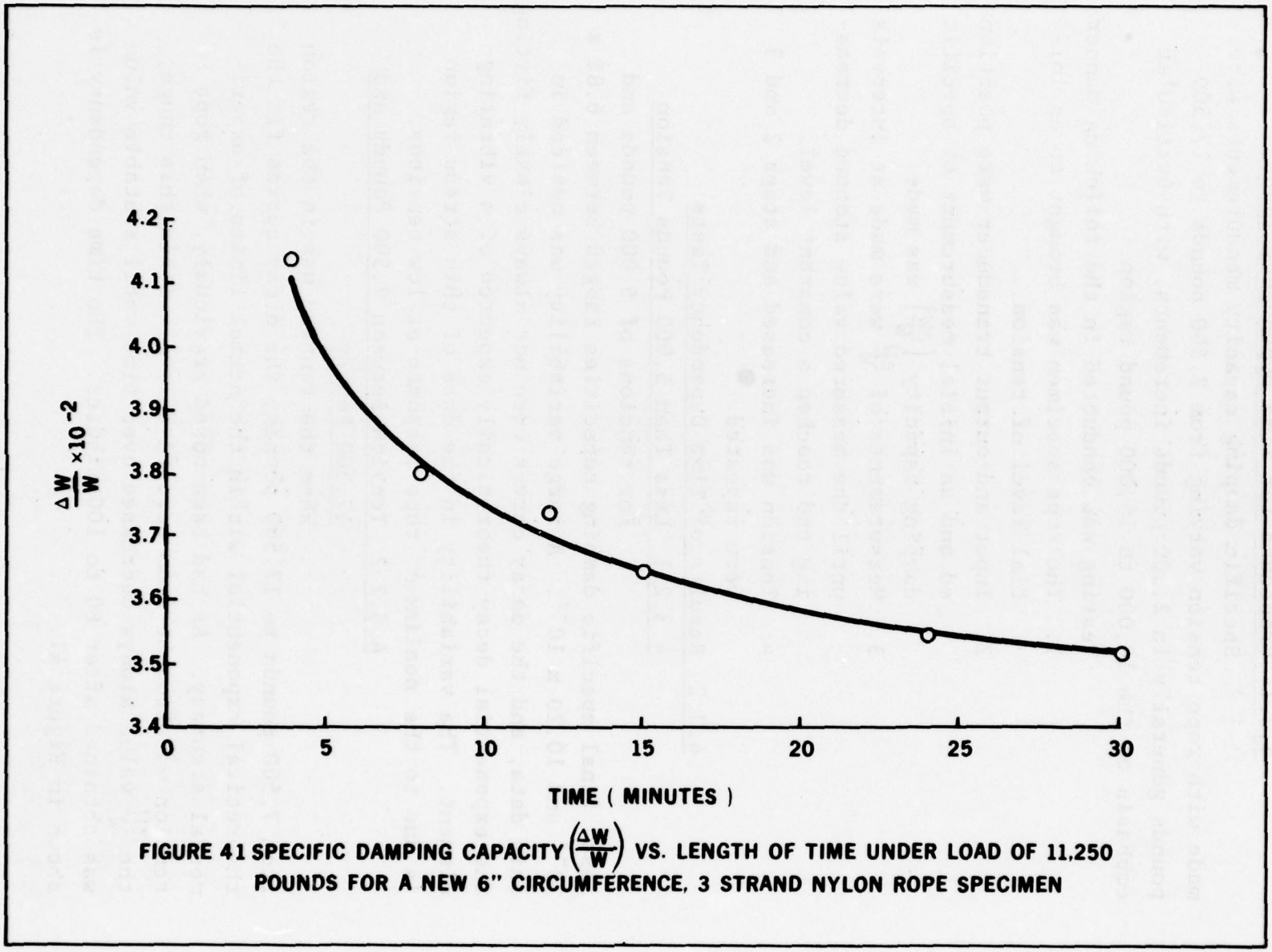

FIGURE 41 SPECIFIC DAMPING CAPACITY $\left(\frac{\Delta W}{W}\right)$ VS. LENGTH OF TIME UNDER LOAD OF 11,250 POUNDS FOR A NEW 6" CIRCUMFERENCE, 3 STRAND NYLON ROPE SPECIMEN

4.3.3 Stress Level Independence of $\frac{\Delta W}{W}$

Of importance to the program was the fact that stable specific damping capacity values remained at an essentially constant level throughout the tension region of 7,500 to 17,500 pounds. The stress level independence is shown in Figures 42 and 43.

4.3.3.1 Comparison of Virgin Specimen to Previously Tested Specimen

The stable measured specific damping capacity value for the specimen of Columbia Cordage rope which had been tested previously averaged 3.23×10^{-2} with a minimum value of 2.79×10^{-2} and a maximum value of 3.51×10^{-2}. The virgin specimen had a slightly lower and even more constant damping capacity value, averaging 2.64×10^{-2} with a minimum value of 2.61×10^{-2} and a maximum of 2.66×10^{-2}.

The general mathematical model relating specific damping capacity to material degradation predicts an increase in specific damping capacity as deterioration progresses. A material which has been stressed beyond the elastic limit experiences permanent deformation due to slippage at the molecular level, and would therefore be expected to show an increase in specific damping capacity.

Although the difference is not large, there is a consistent increase in specific damping capacity between the virgin specimen and the specimen which has been over-stressed. This is a preliminary indication of the ability of the internal friction damping NDE technique to detect material degradation in synthetic ropes.

4.3.3.2 Frequency of Resonance

With one exception to be discussed later, all internal friction measurements were made at the lowest (fundamental) resonance of vibration. The fundamental frequency of transverse vibration under tension is a function of the mass density and length of the specimen being vibrated

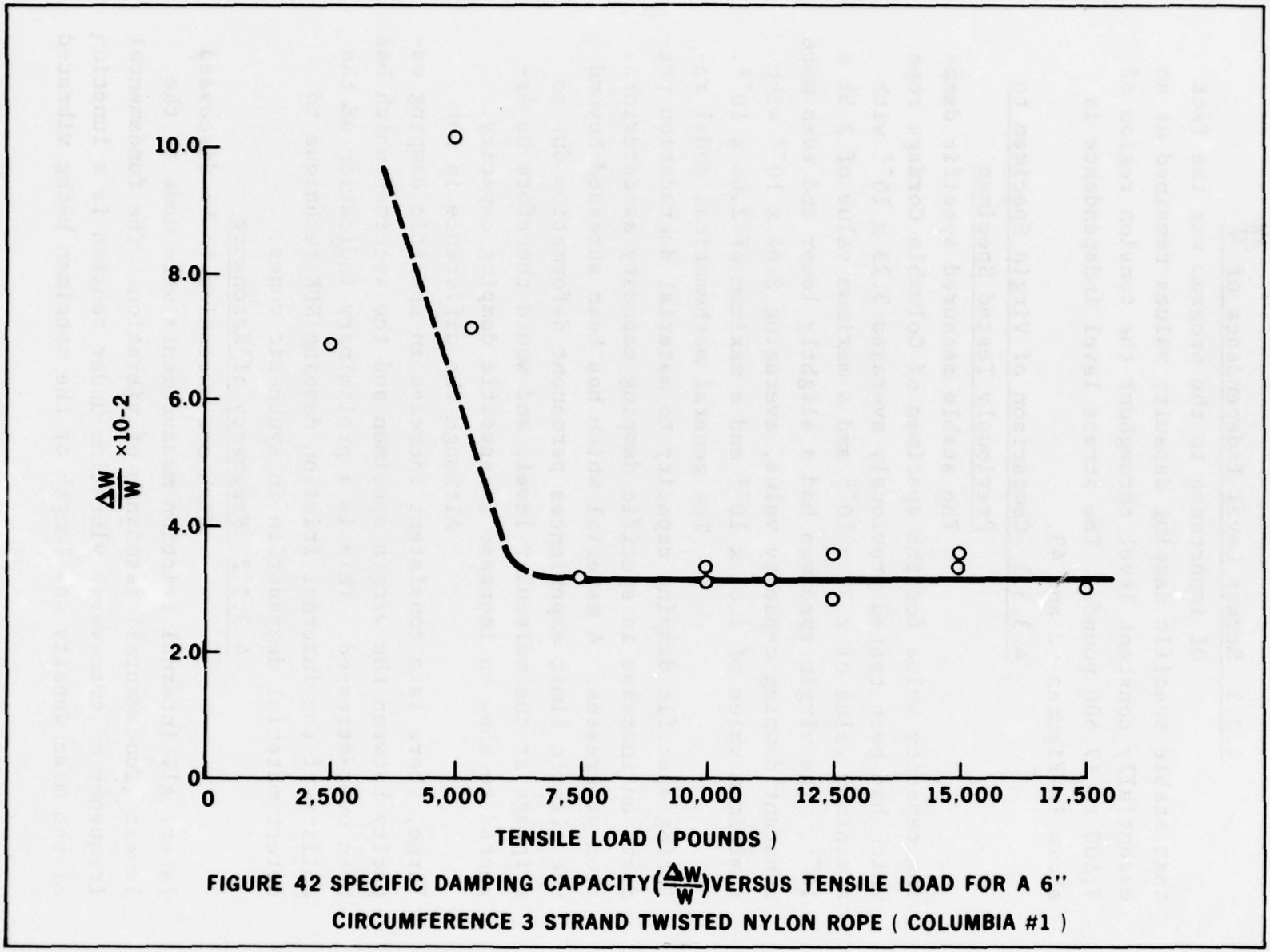

FIGURE 42 SPECIFIC DAMPING CAPACITY($\frac{\Delta W}{W}$)VERSUS TENSILE LOAD FOR A 6" CIRCUMFERENCE 3 STRAND TWISTED NYLON ROPE (COLUMBIA #1)

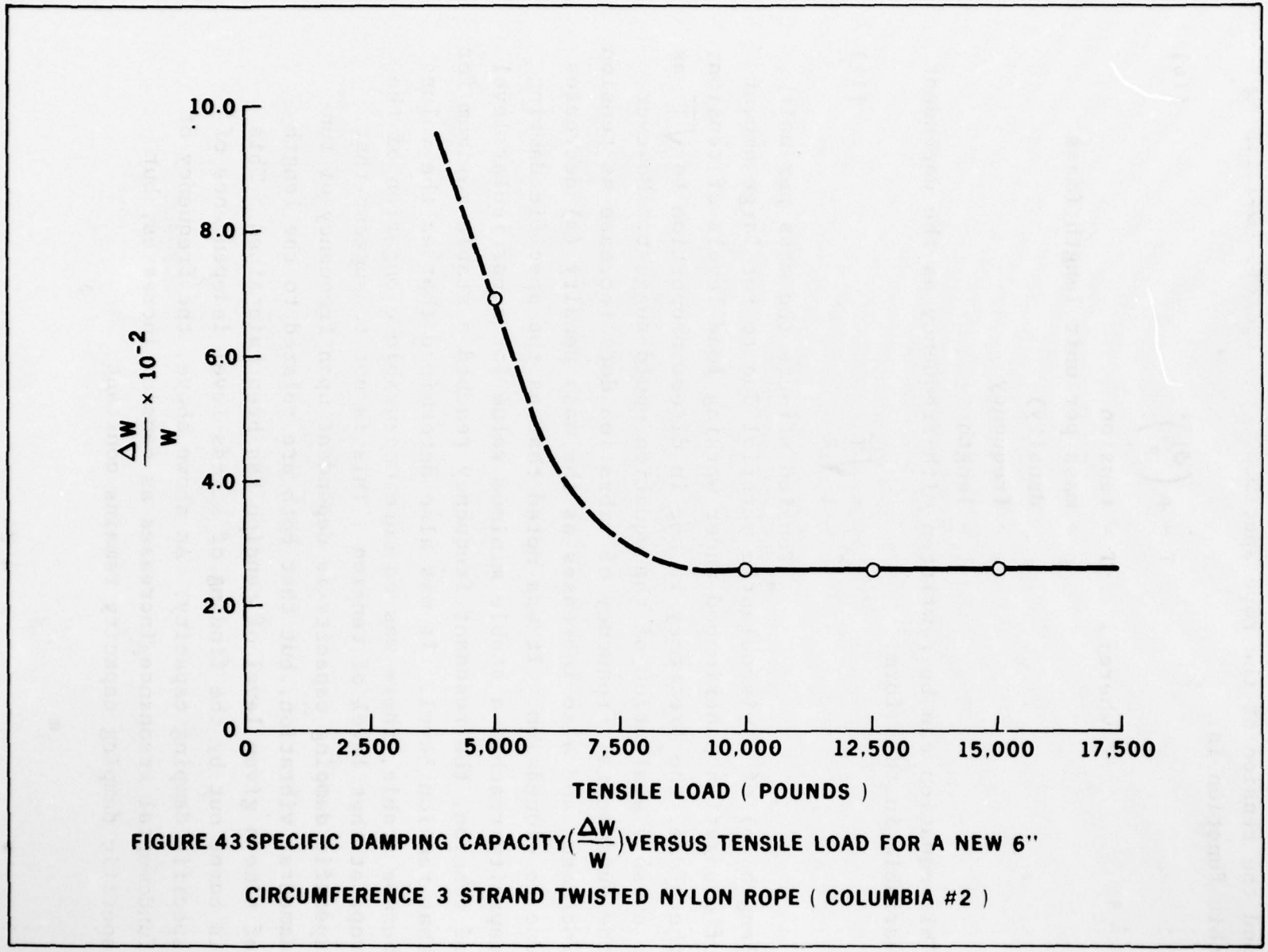

FIGURE 43 SPECIFIC DAMPING CAPACITY ($\frac{\Delta W}{W}$) VERSUS TENSILE LOAD FOR A NEW 6" CIRCUMFERENCE 3 STRAND TWISTED NYLON ROPE (COLUMBIA #2)

and the tension of the rope specimen. The equation describing this function is:

$$T = \rho \left(\frac{wl}{\pi} \right)^2 \qquad [16]$$

where: T = tension
ρ = mass per unit length (mass density)
w = frequency
l = length

This equation can be rewritten with frequency as the dependent variable in this form:

$$w = \frac{\pi}{l} \sqrt{\frac{T}{\rho}} \qquad [17]$$

Tension affects the mass per unit length (ρ) of a viscoelastic material due to the large amount of elongation experienced under working load levels of tension; therefore, the frequency is not in direct proportion to $\sqrt{T}$ as a cursory evaluation of the equation would suggest. However, the fundamental frequency of vibration does increase as tension increases and also increases as the mass density (ρ) decreases due to elongation. It was noted that as the specific damping capacity reached a stable minimum value for a particular level of tension, the resonant frequency reached a stable maximum for that tension level. It was also determined that as the values became stable, there was no more measurable elongation of the rope at that level of tension. This is not to suggest that specific damping capacity is dependent upon frequency of fundamental vibration, but that both are related to the length of time a given level of tension has been maintained. This is borne out by the finding of stress level independence of specific damping capacity. As shown above, the frequency of fundamental resonance increases as tension increases, but specific damping capacity remains constant.

4.3.3.3 Importance of Stress Level Independence

The measured specific damping capacity being independent of the level of tension above some minimum tension, has several important ramifications:

1. It agrees with the theoretical understanding of viscoelastic behavior.
2. It eliminated the need to test every rope specimen at a multitude of tension levels and therefore allowed more rope sections to be investigated under this program than may have been otherwise possible.
3. There were occasions during the course of the program when the fundamental frequency was very close to the 60 Hz power frequency, causing difficulty in data analysis because of interference and "beating" of the driven resonance and the 60 Hz noise provided by the electrohydraulic tensioning apparatus. Knowing that $\frac{\Delta W}{W}$ is independent of the level of tension, allowed the tension on the rope specimens to be increased or decreased in order to change the resonant frequency enough to allow the 60 Hz noise to be electronically filtered.

4. In future field applications, a precise level of tension will not be required so long as the tension is held fairly constant and is within the range of linear elasticity.
5. Stability of resonant frequency can be used as a secondary indicator that the required $\frac{\Delta W}{W}$ value has been obtained.

4.4 Comparison of Specific Damping Capacity Values on Dry and Saturated Samples

4.4.1 Polypropylene Rope Specimens

Three strand twisted polypropylene rope specimens of both six inch circumference and eight inch circumference were tested dry and after soaking for 24 hours in a synthetic sea water solution. One specimen, the used six inch three strand section, was impossible to test in the saturated state because it experienced failure during the dry testing.

The new six inch circumference specimen and the used eight inch circumference specimen both exhibited a decrease in $\frac{\Delta W}{W}$ of about 20% when tested in the saturated state as compared to the dry state (Table 2). It is hypothesized that because the polypropylene ropes are constructed of hard nonabsorbent, monofilament fibers, the water acts as a lubricant, reducing the friction between fibers and consequently reducing the damping.

The fact that the effect is consistent in both direction and magnitude of change is important in that it will facilitate the utilization of the internal friction damping nondestructive evaluation technique in the field. The results suggest that for polypropylene ropes, specific damping capacity measurements can be made, analyzed and correlated with previous measurements in either the dry or sea water saturated

TABLE 2 SPECIFIC DAMPING CAPACITY VALUES FOR MATCHED PAIRS OF NEW AND USED ROPE SPECIMENS

6" CIRCUMFERENCE, 3 STRAND SPECIMENS					
MATERIAL	SPECIMEN	DRY $\frac{\Delta W}{W} \times 10^{-2}$			SATURATED $\frac{\Delta W}{W} \times 10^{-2}$
		TEST 1	TEST 2	TEST 3	
NYLON	COLUMBIA #2 NEW	2.61	2.65	2.66	7.00
	COLUMBIA #1 NEW	3.13	3.16		8.25
	AMERICAN NEW	3.31	3.13		
	USED	3.01	2.53		8.45
POLYPROPYLENE	NEW	5.84	5.04		4.33
	USED	9.69			
POLY-DAC	NEW	4.04	4.05		5.69
	USED #1	3.72			5.99
	USED #2	5.97	5.06		8.09

8" CIRCUMFERENCE, 3 STRAND SPECIMENS					
NYLON	NEW	4.26	4.11		9.24
	USED	4.19			8.14
POLYPROPYLENE	NEW	5.04	4.33		7.08/4.83
	USED	5.35	5.04	7.24	4.15
DACRON	NEW	4.66	4.01	5.06	4.45
	USED	11.8	10.5		14.3

8" CIRCUMFERENCE, DOUBLE-BRAIDED SPECIMENS					
NYLON	NEW	5.37			8.33
	USED	4.35	3.15		6.20
DACRON	NEW	4.31	4.74		7.28
	USED	3.47	3.12		11.8

modes, so long as notation is made of which condition exists. The consistency of the change indicates that a coefficient of 0.8 can be applied to the measured specific damping capacity of a rope tested dry to obtain the value for the same specimen in the saturated state, or conversely, a factor of 1.25 can be applied to the saturated value to obtain the dry value.

In the field, ropes may often be wet but not completely saturated as in the laboratory. More data will be required to quantify the effect of partial saturation on the measured specific damping capacity.

4.4.2 Nylon Rope Specimens

Three strand twisted nylon rope specimens of both 6 inch circumference and 8 inch circumference, and 8 inch circumference double-braided nylon rope specimens were tested dry and after soaking for 24 hours in a synthetic sea water solution.

In all cases, the specific damping capacity was greater when rope specimens were saturated than when dry, indicating that the water absorbed by the nylon fibers increases the internal friction damping in the rope specimens. Specific damping capacity values of saturated ropes ranged from 1.55 to 2.65 times the respective dry rope values (Table 2).

4.4.2.1 Double-Braided 8 Inch Circumference Nylon Ropes

For the 8 inch circumference double-braided nylon, the percentage increase in $\frac{\Delta W}{W}$ was approximately the same for both new and used specimens. The specific damping capacity value increased by a factor of 1.55 for the wet new rope over the dry new rope, and increased by a factor of 1.7 for the wet used rope over its corresponding dry value.

4.4.2.2 8 Inch Circumference 3 Strand Nylon Ropes

Although the specific damping capacity increased for both new and used ropes in this category

when tested wet as compared to dry, the percentage increase was significantly larger for the new rope than the used rope specimen. The new rope value increased by a factor of 2.2 compared to a factor of 1.94 for the used rope. The net result of this was that where the used rope had a measured specific damping capacity equal to that of the new rope when tested dry, the measured specific damping capacity of the used rope was 12% lower than that of the new rope when both were tested wet.

This difference in the percentage increase between new and used ropes of the same type when tested dry and wet may be attributable to a difference in absorbency of the nylon fibers of the used rope due to age.

4.4.2.3 6 Inch Circumference 3 Strand Nylon Ropes

The specific damping capacity values for the new 6 inch circumference 3 strand nylon rope specimens when measured with the ropes saturated were 2.65 times the value when tested dry. There were two new rope specimens in this category which were tested both wet and dry. These were designated Columbia #1 and Columbia #2. Columbia #1 is the specimen which was subjected to a load of 26,000 pounds during the early testing previously described in Section 4.2.4 of this report. Columbia #2 was the virgin specimen which was brought into the program for the time dependency tests.

As was discussed in Section 4.3, the stable $\frac{\Delta W}{W}$ value for the virgin specimen in the dry state was 2.64×10^{-2} from three tests compared to 3.23×10^{-2} from nine tests for the specimen which had been overstressed; the $\frac{\Delta W}{W}$ value for Columbia #1 was then 1.18 times the $\frac{\Delta W}{W}$ value for Columbia #2. When tested wet, the same relationship was found to be true, the damping capacity for Columbia #1 measured 8.25×10^{-2}, which is 1.18 times the damping capacity value of 7.0×10^{-2} for Columbia #2. This result indicates that the internal friction damping technique is capable of detecting the difference

between a virgin three strand nylon specimen and one which nas been overstressed; and furthermore, the technique shows the same degree of difference between the specimens whether they are dry or saturated.

A used 6 inch circumference 3 strand nylon rope was tested both dry and in the saturated state. The specific damping capacity of the rope specimen was measured in the dry state during two separate test sequences. A specific damping capacity value of 3.01×10^{-2} was measured during the first test sequence. The second test sequence yielded a specific damping capacity value of 2.53×10^{-2}.

The value of 3.01×10^{-2} was obtained after the rope had been under 10,000 pounds of tension for 35 minutes, whereas, during the second sequence the value was obtained after 120 minutes of 10,000 pound tension. This indicates that the value of 3.01×10^{-2} was probably not the true value of $\frac{\Delta W}{W}$ because of the effect of phase lag of strain relative to applied stress, and the value would have stabilized at around 2.5×10^{-2} if testing had been continued for another 90 minutes.

The used rope specimen was of a tighter wind than the new specimens. This may be responsible for it having a lower specific damping capacity value.

When tested in the saturated condition, the specific damping capacity value increased to 8.45×10^{-2}, a factor of 3.34 times the dry value of 2.53×10^{-2}. This is slightly higher than the factor of 2.65 for the new specimens.

4.4.3 Dacron Rope Specimens

Dacron rope specimens of eight inch circumference 3 strand twisted construction and eight inch circumference double-braided construction were tested both dry and after 24 hours immersion in a synthetic sea water solution.

4.4.3.1 8 Inch Circumference 3 Strand Dacron Ropes

A new specimen of this category underwent three separate test sequences in the dry state. The specific damping capacity value for the three measurements averaged 4.58×10^{-2} and ranged between 4.01×10^{-2} and 5.06×10^{-2}. When tested in the saturated condition, the measured specific damping capacity was 4.45×10^{-2}, exhibiting essentially no change from the dry condition value.

A used specimen of this category also was tested dry and saturated. The measured specific damping capacity values for the dry state obtained during two separate test sequences were 10.5×10^{-2} and 11.8×10^{-2}. Testing the rope in the saturated condition yielded a $\frac{\Delta W}{W}$ value of 14.3×10^{-2}, an increase of about 1.3 times the dry value.

In both the wet and dry states, there was a large difference in measured specific damping capacity between the new and used specimens, indicating that the internal friction damping technique is sensitive to the failure mechanism acting on the used specimen. This will be discussed more fully in Section 4.5 of this report.

4.4.3.2 8 Inch Circumference Double-Braided Dacron Ropes

A new specimen of this category underwent three separate test sequences in the dry state. During the first test sequence 60 Hz noise interfered with the signal, causing a beating in the decay curve which prevented acquisition of a stable specific damping capacity value. During subsequent tests, the source of the noise was located and the problem was eliminated. The noise was caused by the fact that the hydraulic cylinder was cantilevered from the base plate. Pressure pulses created by the hydraulic pump caused the entire hydraulic cylinder unit to vibrate, inducing a forced vibration of 60 Hz into the rope specimen. Placing a support under the free end of the hydraulic cylinder eliminated the noise interference.

Two separate test sequences were then conducted on the new 8 inch circumference double-braided Dacron rope specimen. The specific damping capacity values obtained from the two test sequences were 4.3×10^{-2} and 4.74×10^{-2}

When the new specimen was tested in the saturated condition, the specific damping capacity increased by a factor of about 1.6 over the dry condition measurement to 7.3×10^{-2}.

A used specimen of 8 inch circumference, double-braided Dacron was also tested dry and saturated. Two test sequences were conducted in the dry state, giving $\frac{\Delta W}{W}$ values of 3.47×10^{-2} and 3.12×10^{-2}. When the specimen was tested in the saturated condition, the specific damping capacity increased by a factor of about 3.6 to 11.8 x 10^{-2}

4.4.4 Poly-Dac Rope Specimens

Poly-Dac is a copyrighted name for 3 strand twisted ropes which are constructed primarily of polypropylene with the outer fibers of each strand constructed of Dacron. New and used specimens of 6 inch circumference 3 strand Poly-Dac were tested both dry and saturated.

4.4.4.1 Specific Damping Capacity Measurements for New Poly-Dac Rope Specimen

Specific damping capacity of the dry new specimen was measured during two separate test sequences. The values obtained were 4.04×10^{-2} and 4.05×10^{-2}. When the new specimen was tested wet, the value increased by a factor of 1.4 to 5.69×10^{-2}.

4.4.4.2 Specific Damping Capacity Measurements for Used Poly-Dac Rope Specimens

Two sections of the used rope were tested in the dry state because the initial section was destroyed

after its dry and wet damping capacity values had been obtained, by an attempt at fatigue cycling. The specific damping capacity value for the initial section tested dry was 3.72×10^{-2}, approximating the value of the new rope. When tested in the saturated condition, the specific damping capacity value increased by a factor of 1.6 to 5.99×10^{-2} which is also within about 5% of the new rope value. The second section was evaluated through two test sequences in the dry condtion, yielding specific dampinc capacity values of 5.97×10^{-2} and 5.06×10^{-2}. Measurement of specific damping capacity for the second section in the saturated condition yielded a value of 8.09×10^{-2}, which is between 1.4 and 1.6 times the dry condition value.

4.4.4.3 Effect of Saturation on Specific Damping Capacity for Poly-Dac Rope Specimens

In all cases for both new and used specimens, saturating Poly-Dac ropes has exhibited the same effect on the value of the specific damping capacity, that is, an increase of 40 to 60 percent over the dry value.

4.5 Comparison of Specific Damping Capacity Values for New and Used Rope Specimens

This section reports and discusses the results of specific damping capacity measurements made on the eight matched pairs of new and used synthetic rope specimens. The focus of this section is on the comparison between new and used rope specimens of the same size, material, and construction, and on the correlation of the specific damping capacity measurements with visual observations of used rope condition.

Matched pairs of rope specimens are discussed in the order in which they are presented in Table I.

4.5.1 Six Inch Circumference Three Strand Specimens

Matched pairs of new and used six inch circumference three strand specimens were obtained in three materials. These are nylon, polypropylene and Poly-Dac. As mentioned before, Poly-Dac is an abbreviated name for a rope which is constructed primarily of polypropylene with the outer fibers of each strand constructed of Dacron.

4.5.1.1 Nylon

Three specimens of 6 inch circumference 3 strand nylon were evaluated, two were new and one used.

The rope designated Columbia No. 2 in Table I is the "as received" specimen which was used for the time dependence tests discussed in Section 4.3. Columbia No. 1 is the original specimen which had experienced a load of 26,000 pounds.

There was a distinct, reproducible difference between the measured specific damping capacity value of Columbia No. 2 and the measured specific damping capacity value of Columbia No. 1, both when tested dry and in the saturated condition. For all tests the measured specific damping capacity for Columbia No. 1 is 19% greater than that for Columbia No. 2. This difference can only be attributed to the overstressing of Columbia No. 1 during the early tests, as all other variables are the same for these two rope specimens.

The used rope specimen was a stiff, tightly wrapped rope. The outer surface was moderately rough from wear but there was not a significant amount of serious abrasion or broken strands. When tested dry, the $\frac{\Delta W}{W}$ values measured for this specimen were 3.01×10^{-2} and 2.53×10^{-2}, which are within the range of the values obtained for the new specimens. When tested in the saturated condition, the measured

specific damping capacity of the used rope was 21% higher than that of the new specimen. Figure 32 is a photographic representation of the new and used 6 inch circumference 3 strand nylon rope specimens.

4.5.1.2 Polypropylene

New and used rope specimens of 6 inch circumference 3 strand polypropylene were evaluated. The measured specific damping capacity values for the new rope tested dry were obtained from two test sequences. These values were 5.84×10^{-2} and 5.04×10^{-2}. While the variance between these two values may seem high, especially in view of the values obtained for the nylon specimens, it is an acceptable amount of variation when the value of 9.69×10^{-2} which was obtained for the used rope is considered.

The measured specific damping capacity value for the used rope was obtained during testing which preceded the investigation into time dependency. Based on the general trend of the time dependency phenomenon, it is expected that had the used specimen been tested after 60 minutes at load, the $\frac{\Delta W}{W}$ value would probably have decreased to approximately 8.5×10^{-2}. This would still be a significantly larger value than obtained for the new rope. The used 6 inch circumference 3 strand polypropylene rope was a severely abraded specimen having numerous broken yarns as shown in Figure 33. The condition of incipient failure was detected through the measurement of the internal friction damping, and confirmed by catastrophic failure when a tensile load in the range of 20,000 pounds was applied. Breaking strength for a new six inch circumference polypropylene rope is approximately 80,000 pounds. (2)

Due to failure of the used rope specimen, measurement of the $\frac{\Delta W}{W}$ value for the saturated condition could not be performed.

4.5.1.3 Poly-Dac

New and used rope specimens of 6 inch circumference 3 strand Poly-Dac were evaluated. The measured specific damping capacity values for the new rope specimen in the dry condition were obtained from two separate test sequences. These values showed excellent reproducibility, being 4.04×10^{-2} and 4.05×10^{-2}.

Two specimens of used Poly-Dac were tested. Specimen #1 had a measured specific damping capacity of 3.72×10^{-2}, which is not significantly different from the value obtained for the new rope specimen. When tested wet, used Specimen #1 had a $\frac{\Delta W}{W}$ value of 5.99×10^{-2} compared to 5.69×10^{-2} for the new specimen. This is also an insignificant difference. Used Specimen #1 had a good visual appearance, showing a moderate amount of wear on the outer surface and no kinks or other visible defects as shown in Figure 34. However, when fatigue cycling was attempted on this rope specimen, it broke when subjected to a load of 20,000 pounds. This indicates that either some failure mechanism was acting which is not detected by measurement of the internal friction damping of the material, or the measurement was faulty. Unfortunately, the specific damping capacity was measured during only one test sequence for each condition, so no second value is available to confirm the accuracy of the $\frac{\Delta W}{W}$ value.

A second specimen from the same used rope was prepared. Two test sequences were conducted on this specimen (# 2) in the dry condition. Specific damping capacity values obtained were 5.97×10^{-2} and 5.06×10^{-2}. This indicates a difference in the condition of the used specimens compared to the new specimen and suggests that the measurement obtained for used Specimen # 1 may have been faulty.

Used Specimen No. 2 was also tested in the saturated condition. A measured specific damping capacity value of 8.09×10^{-2} was obtained. This value is significantly higher than the measured value for the new rope, indicating again that the used rope has suffered degradation and suggesting that the measured value for used Specimen No. 1 may be incorrect.

4.5.2 Eight Inch Circumference Three Strand Specimens

Matched pairs of new and used eight inch circumference three strand synthetic rope specimens were obtained for three materials. The materials include nylon, polypropylene, and Dacron.

Specific damping capacity measurements were made and evaluated for each matched pair. Presentation and discussion of the results generated are included in the following subsections.

4.5.2.1 Nylon

New and used rope specimens of 8 inch circumference three strand nylon were evaluated. Figure 35 is a photographic representation of these rope specimens. The used nylon rope specimen visually appeared to be in excellent condition with virtually no evidence of wear or abrasion.

Measured specific damping capacity values for the new rope specimen in the dry condition were obtained from two separate test sequences. These values show excellent reproducibility of measurements being 4.26×10^{-2} and 4.11×10^{-2}.

A specific damping capacity value of 4.19×10^{-2} was measured for the used specimen in the dry condition. The equivalence of this value to the value measured for the new specimen confirms the visual assessment of the used specimen.

The measured specific damping capacity value of the new specimen in the saturated condition is 9.24×10^{-2}, compared to 8.14×10^{-2} for the used specimen. The difference may be attributable to a difference in the amount of water absorbed by each specimen. This hypothesis has not been tested but could be considered in a future phase of the program. The fact that the value for the used specimen is not greater than that obtained for the new specimen is an indication of the condition of the used specimen showing no evidence of wear or abrasion.

4.5.2.2 Polypropylene

New and used rope specimens of 8 inch circumference three strand polypropylene were evaluated. Figure 36 is a photographic representation of these rope specimens. The used polypropylene rope specimen visually appeared to be in very good condition, showing no serious abrasion or broken strands. Measured specific damping capacity values for the new rope specimen in the dry condition were 5.04×10^{-2} for the first test sequence and 4.33×10^{-2} for the second test sequence. These values compare to 5.35×10^{-2}, 5.04×10^{-2} and 7.24×10^{-2} for the used rope specimen in the dry condition. In checking the test sequence history, it is found that the values 5.35×10^{-2} and 5.04×10^{-2} were both obtained on the same day, and that all measurements that day were affected by noise. The value of 7.24×10^{-2} was obtained on a later date after the noise problem had been eliminated.

When the rope specimens were tested in the wet condition, two test sequences on the new rope yielded the values of 7.08×10^{-2} and 4.83×10^{-2}. The value of 7.08×10^{-2} was obtained after 66 minutes at load, whereas the value of 4.83×10^{-2} was obtained after 165 minutes under load. It is therefore expected that had the first test been carried out after 100 more minutes at load, the values would have been closer.

4.5.2.3 Dacron

New and used specimens of eight inch circumference three strand Dacron were evaluated.

Measured specific damping capacity values for the new specimen in the dry condition were generated during three separate test sequences. The values obtained were 4.66×10^{-2}, 4.01×10^{-2}, and 5.06×10^{-2}. When tested in the saturated condition, a $\frac{\Delta W}{W}$ value of 4.45×10^{-2} was measured.

The condition of the used Dacron specimen as visually assessed was very poor, with severe abrasion and many broken strands evident. There are indications of cutting of outer fibers by some hardware.

The used specimen was evaluated during two separate test sequences in the dry condition. The measured specific damping capacity values obtained from these test sequences were 11.8×10^{-2} and 10.5×10^{-2}. The average of these measurements is 2.43 times the average measurement of the new rope, indicating incipient failure. The $\frac{\Delta W}{W}$ value obtained for the used rope in the saturated condition was 14.3×10^{-2}, which is 3.2 times the value for the new rope. This is a further indication of incipient failure. It is pertinent to note that five minutes after the specific damping capacity value was obtained for the used rope in the saturated condition, the rope experienced catastrophic failure, without any increase in tensile load on the specimen. Figure 37 shows the 8 inch circumference three strand Dacron specimens.

4.5.3 Eight Inch Circumference Double-Braided Specimens

Matched pairs of new and used eight inch circumference double braided rope specimens were obtained

for two materials: nylon and Dacron. The following two subsections report and discuss the results of the specific damping capacity measurements for these rope specimens.

4.5.3.1 Nylon

New and used specimens of eight inch circumference double braided nylon were evaluated in both dry and saturated states. Figure 38 is a photographic representation of these rope specimens.

The new rope specimen, when tested in the dry condition, had a measured specific damping capacity of 5.37×10^{-2}. The measured specific damping capacity value for the new specimen in the wet condition was 8.33×10^{-2}.

The used rope specimen was visually evaluated as being in very good condition, with no visible deterioration of any sort. The measured specific damping capacity values for the used rope specimen were actually lower than those of the new specimen, being 4.35×10^{-2} and 3.15×10^{-2} when tested in the dry state and 6.20×10^{-2} when saturated. It is extremely unlikely that the used specimen is in better condition than the new specimen. However, there is a difference in construction between the new and used specimens which may be responsible for this result. Figure 44 illustrates the outer strands of these two specimens. As shown in the illustration, the outer cover of the new rope is constructed of pairs of strands braided into a herringbone-type pattern, whereas the outer cover of the used rope is constructed of single strands braided into a herringbone-type pattern.

4.5.3.2 Dacron

New and used specimens of eight inch circumference double braided Dacron were evaluated in both dry and saturated states. Figure 39 is a photographic representation of these rope specimens.

The specific damping capacity value for the new rope specimen in the dry state was measured during

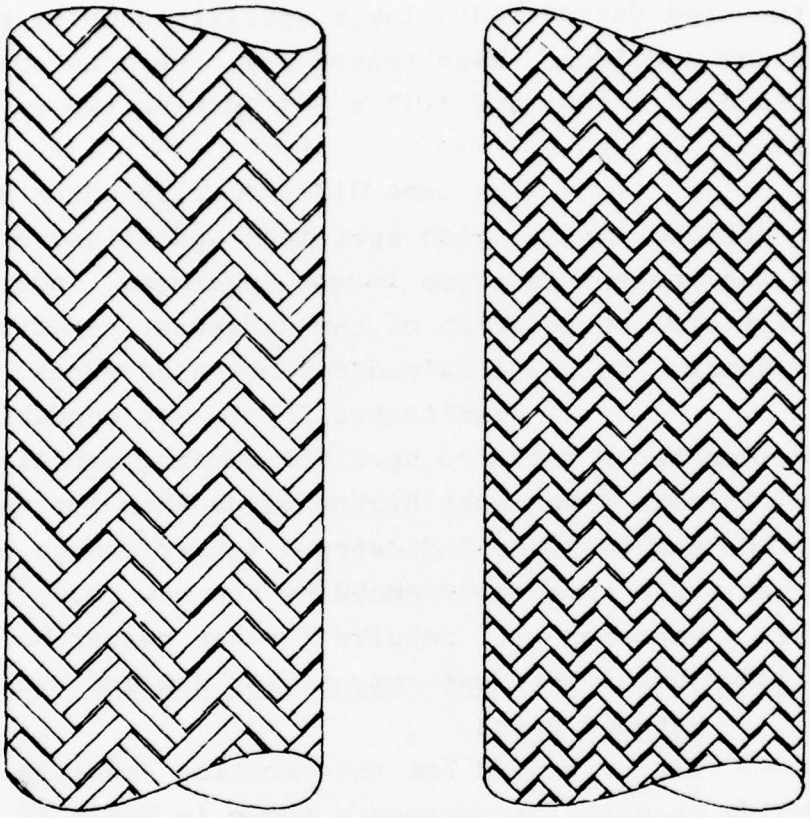

NEW SPECIMENS

USED SPECIMENS

FIGURE 44 ILLUSTRATION OF OUTER COVERING CONSTRUCTION FOR NEW AND USED DOUBLE-BRAIDED ROPE SPECIMENS

two separate test sequences. The values obtained were 4.31×10^{-2} and 4.74×10^{-2}. Measurement of the specific damping capacity for the new rope when saturated yielded a value of 7.28×10^{-2}.

The used rope specimen was visually evaluated as being in very good condition, with no visible deterioration of any sort. Similar to the nylon double braided specimens, the used Dacron had a lower specific damping capacity than the new specimen. When tested dry, the used specimen value measured 3.47×10^{-2} and 3.12×10^{-2} during two separate test sequences.

The same difference in outer cover construction noticed in the nylon specimens and illustrated in Figure 44 was present in these Dacron specimens, indicating the probability of a correlation of the different construction to the lower damping values obtained for the used ropes.

When tested in the wet condition, the used specimen had a measured specific damping capacity of 11.8×10^{-2}. This is a somewhat higher value than the value obtained for the new rope and indicates a larger change between the dry and wet state than experienced by the new rope. Explanation of this phenomenon will require further research.

4.5.4 Summary of Measurements for New and Used Matched Pairs

The core data for this section consists of 55 specific damping capacity measurements shown in Table II. These 55 measurements resulted from the analysis of 330 individual data points. These core data values represent the stable specific damping capacity measurements. Approximately 600 more measurements representing approximately 3,500 individual data points were made in order to determine the time at which each rope specimen reached the equilibrium state.

Of the eight matched pairs of new and used rope specimens, three contained used specimens which showed no visible

signs of deterioration. These three are:

1) Eight inch circumference three strand nylon,
2) Eight inch circumference double-braid nylon, and
3) Eight inch circumference double-braid Dacron.

In all three cases, measurement of the specific damping capacity also indicated no evidence of deterioration. There was only one anomaly in these measurements, the used eight inch circumference double braid Dacron specimen when tested in the saturated state had a significantly higher measured specific damping capacity than the new specimen. It is believed this effect may be due to a difference in the mass of water absorbed by the two specimens.

In one case the measurements of specific damping capacity showed great variability. This occurred with the eight inch circumference three strand polypropylene specimens. There was 60Hz background noise during some of the measurements which was later eliminated. It is believed that more testing of these two specimens would reduce the variability of values.

The measurements of specific damping capacity for the six inch circumference three strand Poly-Dac specimens showed an anomaly in that the first used specimen to be tested showed no difference in $\Delta W/W$ from the new specimen. Visually, the specimen was only moderately abraded however, it failed under a load of 20,000 pounds when fatigue cycling was attempted. There was no check made on the reproducibility of the values for this specimen as only one test sequence in the dry condition and one test sequence in the saturated condition were conducted before the specimen failed. However, another specimen was prepared from an adjacent section of the same rope. Two dry and one saturated test sequences

were conducted on this specimen, and in all cases, the presence of an incipient failure mechanism was detected through a significant increase in $\Delta W/W$ as compared to the new specimen.

Measurements of specific damping capacity for the remaining three matched pairs confirmed the existence of failure mechanisms. The remaining three matched pairs referred to are:

1) Six inch circumference three strand nylon,
2) Six inch circumference three strand polypropylene, and
3) Eight inch circumference three strand Dacron.

Measurements of specific damping capacity were made for four specimens of six inch circumference three strand nylon. Two of these were new specimens from Columbia Cordage Co., one of which had been overstressed (stressed above the upper limit of the linear elastic range) during early testing, the other was not overstressed. One new specimen from American Manufacturing, Inc. which had also been overstressed was tested. The damping values for this specimen were equivalent to the values obtained for the Columbia specimen which had been overstressed. Testing was not as extensive on this specimen as on the other two new specimens, therefore it was omitted from the discussion of Section 4.5.1.1. However, it is pertinent to note here that new specimens from two different manufacturers which had both experienced a stress level of 26,000 pounds had equivalent values of specific damping capacity. The most significant finding resulting from measurements made on the six inch circumference three strand nylon specimens was a consistent increase in specific damping capacity from the virgin state to a condition of having been overstressed. Further investigation along these lines was conducted, and will be discussed in Section 4.6.

The second case where a failure mechanism was detected through the measured specific damping capacity was in the matched pair of new and used six inch circumference three strand polypropylene specimens. In this case, the used specimen showed visible evidence of deterioration with numerous abrasions and broken strands. The specific damping capacity measurements detected this deterioration; the used specimen had a $\Delta W/W$ value approximately 80% higher than the average of the two $\Delta W/W$ values obtained for the new specimen. The existence of an active failure mechanism was confirmed when the rope specimen failed at around 20,000 pounds tensile load.

A similar situation prevailed for the third case, where measurement of the specific damping capacity predicted incipient failure. The used eight inch circumference three strand Dacron rope specimen showed visible evidence of very serious deterioration with numerous cuts and abrasions evident, as well as a large percentage of broken strands. The specific damping capacity measurements detected this deterioration through an average $\Delta W/W$ value approximately 140% larger than the measured value for the new specimen. Based on the general mathematical model relating specific damping capacity to incipient failure, it is surmised that the used Dacron specimen was closer to failure than the used polypropylens specimen just discussed. This was confirmed by the failure of the Dacron specimen without the application of additional load above that used for testing. Both the used six inch circumference three strand polypropylene specimen and the eight inch circumference three strand Dacron specimen failed under a tensile load of 20,000 pounds. However, for the six inch polypropylene that load represents about 20% of new rope breaking strength, whereas for the eight inch Dacron the 20,000 pound load is about 10% of new rope breaking strength.

Therefore, the specific damping capacity measurements not only detected incipient failure, but also, through the magnitude of the changes between new and used specimens, gave an indication of the actual breaking strength of the used specimens.

4.6 Changes in Specific Damping Capacity Resulting From Stress Cycling

After completing the testing of the eight matched pairs of ropes as discussed in the foregoing sections, a six inch circumference, three strand rope identified as Columbia #2 was mounted in the rope support and tensioning apparatus and subjected to stress cycling using a tensile load in excess of the upper limit of the range of linear elasticity.

The rope specimen was loaded to 25,000 pounds in tension for 10 minutes, then returned to zero load for 10 minutes. This cyclic loading was repeated four times and after the fourth cycle, the rope tension was brought to 10,000 pounds load. At 75 minutes after the 10,000 pound loading was begun, the measured specific damping capacity was 6.12×10^{-2}. This is 2.32 times the initial value of 2.64×10^{-2} obtained before stress cycling was initiated. At 90 minutes, the form of the decay curve began to deteriorate, probably from the rope beginning to recover the elastic strain which had resulted from the 25,000 pound load.

The rope was then stress cycled eight times in the same manner and returned to zero load for 16 hours so that all the elastic strain could be recovered.

Tension of 10,000 pounds was applied to the rope and sustained for two hours. At two hours, the $\Delta W/W$ had stabilized in the range of 4.9×10^{-2} to 5.5×10^{-2}. This is approximately twice the $\Delta W/W$ value obtained for the "as received" specimen.

4.7 Comparison of the Internal Friction Damping Technique to Ultrasonic Detection and Acoustic Emission Inspection Techniques

A comparison of the IFD-NDE technique to acoustic emission and ultrasonic detection inspection techniques is listed in this section. Examples of various parameters that enable IFD measurements to be successfully applied to synthetic rope specimens are enumerated in the following sections.

4.7.1 Coupling Pressure for Input-Output Response

The output response as a function of test technique can be dependent on a function of the method of attaching the output transducer to the synthetic rope being tested. The ultrasonic detection inspection technique is most sensitive to coupling pressure and must have discrete contact with the specimen being tested. An irregular surface with corrosion or pits could completely mask the ultrasonic signal response of the synthetic rope. The design of synthetic ropes which includes braided, double braided, and twisted sections would preclude reasonable responses from ultrasonic inputs. The rough texture and numerous rope strand interfaces with corresponding void spaces would be identified as crack initiation locations with ultrasonic detection inspection techniques. Moreover, the requirement of positive coupling pressure for ultrasonic inspection would critically damp the response of the synthetic rope in such a way that response would be difficult if not impossible to obtain.

The coupling pressure required for output responses from acoustic emmission (AE) devices would be even more critical than those required by ultrasonic inspection. AE coupling pressure must be maintained to insure the uninterrupted collection of output responses. The synthetic ropes would thus be critically damped and yield erroneous results, if any could be obtained. Since the acoustic emission technique measures an absolute input to absolute output response, the coupling

pressure would have to circumferentially contact the rope. Any anomaly in the rope surface could produce erroneous results.

The internal friction damping technique does not rely on the transducers being placed in discrete contact with the synthetic ropes. The close proximity of the input and output transducers has been discussed in another section. The advantage of a coupling method that is insensitive to pressure of coupling would simplify the applicability and increase the reliability of the inspection technique without compromising the reproducibility of the data. The IFD-NDE inspection technique utilizes input and output transducers that do not come into contact with the synthetic rope and therefore are not sensitive to coupling pressure. This is a major advantage to the IFD-NDE technique.

4.7.2 Signal-to-Noise Ratio

The ability to obtain an output response mode in synthetic rope is predicated on the ability to produce an output signal that is significantly stronger than the inherent noise of the system. The signal-to-noise ratio would be a measure of the ability of an inspection technique to analyze only that portion of an output signal that contains no transient noise elements. The use of the acoustic emission inspection technique as applied to synthetic ropes does not attain a signal-to-noise ratio that would enable the technique to respond to the rope section. Typically, signal-to-noise ratios that approximate 10db are common when acoustic emission inspection techniques are applied to synthetic ropes. The presence of an inordinately large component of noise in the synthetic rope specimen's response to an input signal, necessitates special electronic conditioning equipment. The frequencies of interest for the analysis of the acoustic emission output signal are sufficiently

large which negates the possibility of narrow band filtering to reduce the noise level. The overall outcome of utilizing acoustic emission for inspecting synthetic ropes would be a very low signal-to-noise ratio.

Ultrasonic detection inspection techniques do not attain large signal-to-noise ratios when applied to synthetic ropes. The use of ultra high frequencies are not readily adaptable to narrow band filtering which eliminates transient noise frequencies in close proximity to the test frequency.

The IFD-NDE technique maintains the high (typically 50-100db) signal-to-noise ratio. The advantage of the high signal-to-noise ratio would enable the earliest indication of output response to be made and would identify the IFD-NDE technique as having this advantage over ultrasonic detection or acoustic emission inspection techniques.

4.7.3 Input-to-Output Signal Ratio

The ratio of the input signal to the output signal can be used to identify that point in the operating time where the synthetic rope has experienced degradation. The calibration of the ultrasonic detection device is necessary for that instrument to be used as a method for the detection of synthetic rope degradation. The amplitude of response as measured by the ultrasonic device can be correlated to a defect provided a specific calibration of the equipment to a known defect has been made.

The acoustic emission technique requires that an absolute amplitude output be measured and correlated to the known input amplitude. This input-to-output signal ratio is required for the purpose of defining the extent of crack formation.

The IFD-NDE technique does not require a specific signal ratio for input and output. The relative decay is a function of the structural integrity of the

material and the frequency of test. An absolute or calibrated input-output signal ratio is not necessary for measuring a relative amplitude decay which is obtained from the IFD-NDE technique. The primary advantage of using a relative amplitude decay that does not need to be absolute or calibrated would enable the user to perform the inspection technique in an efficient manner. The inspection technique would not necessarily require background or base line data for the early prediction of incipient degradation in synthetic ropes.

4.7.4 Test Duration of Various Inspection Techniques

The acoustic emission inspection technique relies on the ability to perform a continuous monitoring process. It is a passive system which must be in operation at the time the crack is growing. Should the AE technique be able to overcome the noise problem already discussed in this section, the constant or continuous monitoring process would have to be initiated. The AE method relies on the noise generated on the micro-structural level to identify crack formation. Should the initiation phase of a crack arrest itself and become a dormant site for future failure initiation, then the AE method would not be sensitive in locating or identifying the cracked mode. The AE system can identify a growing crack.

The ultrasonic detection technique requires periodic frequency monitoring for responses of interest for the geometric site in consideration. The disadvantages of scanning the specimen for a specified time become apparent when one attempts to correlate data on large synthetic ropes with failure mechanisms.

The IFD-NDE technique complete with digital processing equipment could perform the entire inspection technique in real time. The ability to define and locate specific failure mechanisms would have the distinct advantage of saving time and expense to predict the remaining service life of synthetic ropes. The analysis of data is performed in real time

and is complete after the full attenuated decay has been recorded. For the case of synthetic ropes, the decay time analysis time (by computer) and the listing of data could be performed in real time (approximately five seconds). This real time analysis has the secondary advantage of early prediction of incipient failure with an estimate of the remaining useful life of the synthetic rope deferred from an established $\Delta W/W$ to cyclic load data relationship.

4.7.5 Test Technique as Passive or Active

The inspection technique that relies on an input signal from the technique would be defined as an active technique. The ultrasonic detection inspection technique requires the periodic input of a signal that excites the specimen and enables an output signal to be acquired. The input signal and associated output signal are related in an active manner. The input signal actively excites an output response. As discussed earlier, the output may or may not be directly related or dependent on the input signal strength.

The IFD-NDE technique, like the UT, is an active test technique. The input pulse excites the synthetic rope specimen and generates an active output decay response.

The acoustic emission technique relies on the random generation of noise in the specimen as provided by the internal micro-structure movement. The technique passively listens to the micro-structure movement and identifies that point where the randomly generated noise exceeds the background noise. As was discussed earlier in the section, this aspect may not be possible in all cases. The passive nature of the test requires that the initiation of failure must be happening at the time of test for the definition of a failure mode to be made.

The advantages of an active test technique include the early detection of failure at an incipient stage. The IFD-NDE technique relies on the active aspect of the test

to define the prediction of failure. There is no advantage in defining initiation of failure after the fact as is the case with the passive techniques.

4.7.6 Effect of Geometry on Inspection Test

The use of ultrasonic detection techniques for applications that have inherent changes in geometry, in many cases, is unable to differentiate a defect from the change in geometry. The UT technique experiences a large number of false alarm indications of defects near areas that exhibit changing geometry. The initiation of a failure mode, in many cases, occurs near a change in geometry where stress concentrations are found. As the UT inspection nears the area of geometry change, the technique identifies that change as a defect. The increased complexity of design arising from the geometry problem in UT inspection adds to the time and cost of the overall technique.

Acoustic emission methods of inspection are also adversely affected by changes in geometry in the operating mode. The noise created by applying AE to synthetic rope could mask the acoustic data being emitted by the technique.

The IFD-NDE technique is not affected by changes in geometry with respect to obtaining output data. The response to the IFD input signal is a bulk modulus that enables the technique to locate and define approximately the location where the incipient failure mode has initiated. The degree of sensitivity of the technique is also related to the bulk response of the specimen. An advantage of using the IFD technique for synthetic rope specimens would be its ease of application to different materials (nylon, Dacron, polypropylene, etc.) in numerous different constructions (three strand, eight strand, and double braided). Secondary advantages of using the IFD technique instead of AE or UT include savings of time through an implied reduction in time of test.

4.7.7 Frequency of Test in Relation to Ability to Locate Small Crack

In both cases of acoustic emission and ultrasonic detection inspection techniques, the frequency of test is inversely proportional to the magnitude of defect. That is, the smaller defect to be found in a synthetic rope specimen implies a higher frequency rate of test. The decay response from AE and UT is also inversely proportional to the frequency of test. For very high frequencies (typically 100MHz and more), the attenuation of the response signal becomes so large that the signal is critically damped before the pickup transducer is able to record the response. Even with more sophisticated equipment, the chance of picking up response signals from UT and AE in the higher ranges of frequencies is quite small. For this reason the common defects that are identified by AE and UT are in the range of 0.1 inches to 1.0 inches in size at the point of discovery.

The IFD technique is capable of identifying small (typically 0.001") defects in materials. The small defects that are identified are not dependent or inversely proportional to frequency. Typical responses for synthetic ropes were in the range of 50 to 100Hz. Typical responses for most common materials tested using the IFD-NDE technique are in the range of 20-20,000Hz.

The relationship of the frequency of test to the size of defect has been discussed. Another aspect of an inspection technique that is important is the relationship of the test frequency to the identification of a failure mode in an incipient stage that is not a defect. Ultraviolet radiation from the sun will deteriorate synthetic ropes after a lengthy period of exposure. In the advanced stages of deterioration, the AE and UT techniques could possibly detect a change caused by broken strands as a result of UV deterioration. The IFD technique based on prior test experience is sensitive to all forms of failure including the UV deterioration mode. For

synthetic ropes, the IFD technique has the advantage of low frequency responses which enables an early detection of deterioration to be made. The primary advantage, however, is the ability to detect deterioration that does not originally occur as a microcrack (i.e. environmental deterioration). Moreover, the ability to distinguish small cracks at low frequencies (typically 1000Hz) provides the ultimate advantage of earliest detection in rope sections. Other secondary advantages include less expensive analysis equipment and a reduced inspection time which implies lower inspection costs.

4.7.8 Crack Growth Rate

The acoustic emission and ultrasonic detection techniques require that the instrumentation be applied and constant on-line monitoring be performed to insure the early detection of crack formation. The AE and UT techniques rely on the ability of monitoring the specimen in an on-line mode to predict and correlate the crack growth to a time period. As was mentioned earlier, the failure mechanism is not cracking in all cases. Therefore, the constant monitoring required by AE and UT are time consuming and may not identify the potential failure mode.

The IFD technique indicates with the initial data collected a direct correlation to the crack growth. (28) The relative measurements do not require that the IFD technique be used to monitor the synthetic ropes on-line. It is anticipated that the IFD technique will indicate a direct correlation of specific damping capacity values to the number of failed strands in the synthetic ropes over the entire useful life of the rope.

5.0 CONCLUSIONS

This report concludes that monitoring the dynamic response of synthetic ropes as a function of the work-cycle history is a viable nondestructive technique for predicting impending failure due to fatigue and abrasion. The results of this program are an important milestone in accomplishing the overall objective of utilizing the internal friction damping nondestructive evaluation technique in order to detect impending failure of SPM hawsers, mooring, towing and other marine lines.

5.1 Feasibility and Applicability

The results of this program show that the internal friction damping nondestructive evaluation technique is applicable to synthetic ropes of both six inch circumference and eight inch circumference. The first evidence supporting this conclusion consists of the discovery that the synthetic rope specimens could be induced to vibrate using a noncontact magnetic input transducer. The vibration decay function which was obtained when the forcing signal was removed conformed closely to the expected exponential decay. These two findings, coupled with reasonable repeatability of specific damping capacity values for individual rope specimens, indicates the applicability of the technique to synthetic ropes of both six inch circumference and eight inch circumference.

To further support this conclusion, the technique has demonstrated the capability to detect the impending failure of two specimens, a used six inch circumference three strand polypropylene specimen and a used eight inch circumference three strand dacron specimen. Both of these specimens failed at a fraction of their rated breaking loads subsequent to the application of the internal friction damping technique, thus confirming the detection of impending failure. Further support of this conclusion is provided by the results of stress cycle loading discussed in Section 4.6. A 25,000 pound load

was applied for 12 cycles at 10 minutes for each load cycle and allowing 10 minutes of load relaxation between load cycles, to a new specimen of six inch circumference three strand nylon. A significant increase in the measured specific damping capacity resulted, indicating detection of the degradation produced by overstressing the rope specimen.

There is also evidence to suggest that the measurement of the specific damping capacity will not only detect impending failure but can be correlated to the remaining strength of the rope specimen. This correlation could be used to reassign high use rope to jobs of lower working loads, thus extending even further the useful life of any given rope.

The results of the specific damping capacity measurements for the six inch circumference three strand polypropylene and the eight inch circumference three strand dacron rope specimens show that the used six inch circumference three strand polypropylene rope, which failed at approximately 20% of rated breaking strength, had a measured specific damping capacity prior to failure 80% higher than the measured specific damping capacity for a new specimen of the same type. Moreover, the used eight inch circumference three strand dacron rope failed at approximately 10% of breaking strength and had a measured specific damping capacity prior to failure 140% higher than the measured specific damping capacity for a new specimen of the same type. This indicates a probably correlation between percentage increase in $\Delta W/W$ and remaining strength.

Figure 45 shows the preliminary correlation between normalized specific damping capacity versus the percentage of rated breaking strength for abraided ropes. Normalization of $\Delta W/W$ is achieved by dividing the specific damping capacities of each matched pair by the specific damping capacity for the new rope specimen of that pair.

The technique has shown its applicability to all three synthetic materials, as all three materials are involved in the results just discussed. The fact that reproducible data was

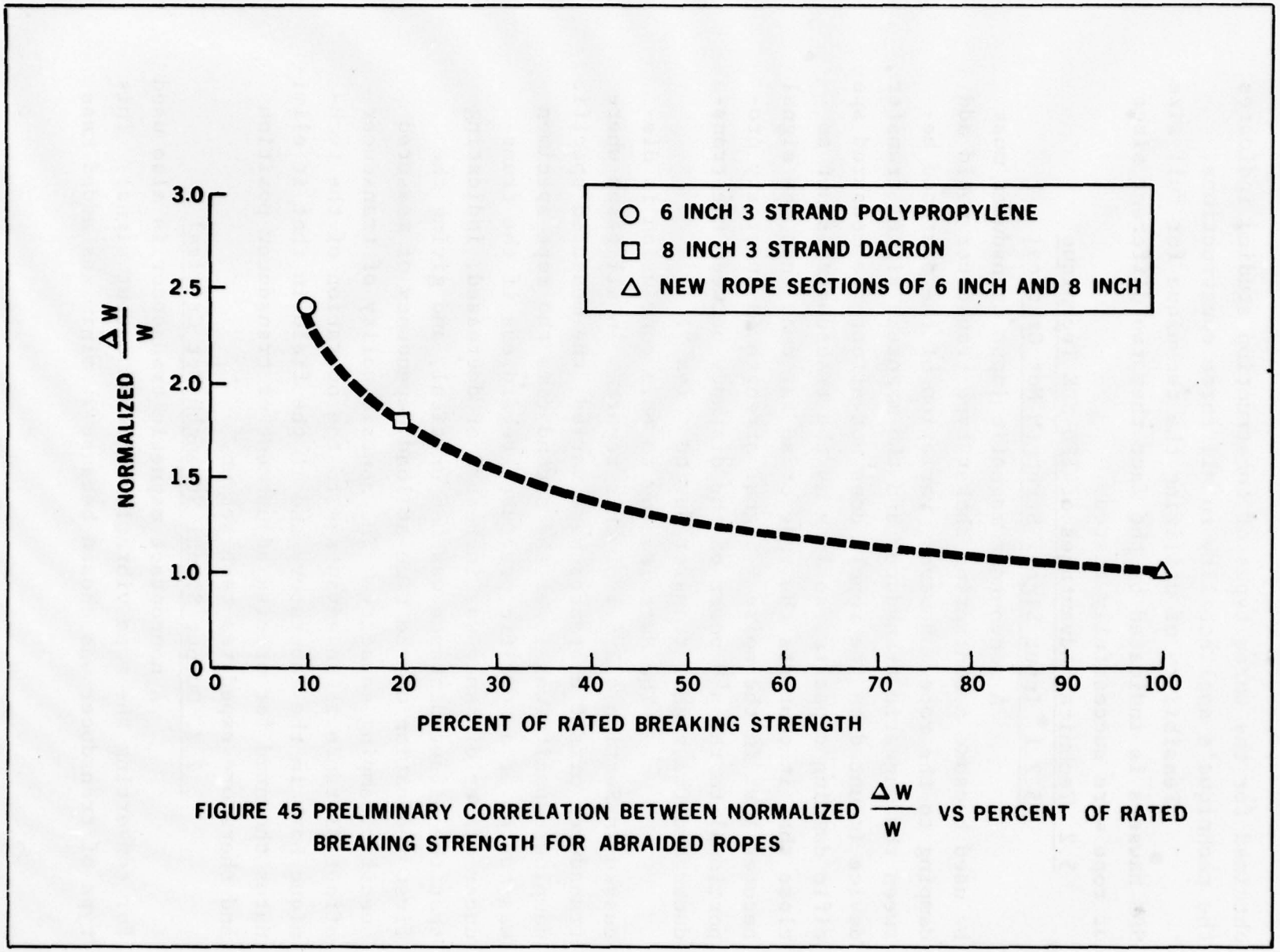

FIGURE 45 PRELIMINARY CORRELATION BETWEEN NORMALIZED $\frac{\Delta W}{W}$ VS PERCENT OF RATED BREAKING STRENGTH FOR ABRAIDED ROPES

obtained for the three types of construction studied indicates the technique's applicability to all three constructions.

Feasibility of utilizing the technique for full size SPM hawsers is indicated by the fact that two different sizes of rope were successfully tested.

5.2 Technical Advantages of IFD-NDE Technique

5.2.1 Input Signal Strength Not Critical

A noncontact magnetic input transducer must be used because a contacting shaker type transducer would add damping to the rope. However, variation of the distance between the magnetic transducer and the magnetic signal transfer device (mounted on the rope), does not affect the measured specific damping capacity, so long as the transducer is not so close that it contacts the rope or so far away that the signal becomes lost in the noise. Signal strength is inversely proportional to the a^{th} power of the distance between the transducer and the signal transfer device. ($\simeq x^{-a}$)

The data leading to this conclusion is discussed in Section 4.2.4.1 of this report. In all cases where transducer offset distances were varied, the measured specific damping capacity was lower the second time the rope specimen was tested at a specific pressure, regardless if the transducer offset distance was increased or decreased, indicating that the offset distance was not critical, and giving the first indication of the time at load dependency of measured specific damping capacity. The noncriticality of transducer offset distance is an advantage to the operation of the technique both in the laboratory and in the field in that it eliminates the need for precise adjustment of transducer position and therefore expedites test set up.

5.2.2 Output Signal Strength Not Critical

A noncontact magnetic transducer is also used for converting the rope vibration into an output signal. This type of transducer was chosen because it minimizes added mass

on the rope specimen, compared to other types of output transducers, such as accelerometers, which must be physically mounted on the rope. Offset distance of the output transducer is even less critical than for the input transducer. This is because it has no effect on the signal to noise ratio. Vibration in the rope is composed of two components. One is noise, which is a fixed quantity dependent upon such things as rigidity of supports, type of tensioning apparatus and the method of supporting the tensioning apparatus. The other vibration component is provided by the input transducer. The ratio between the amplitude of the component provided by the input transducer and the noise component is the signal to noise ratio. The output transducer simply converts the total vibration into an electronic signal without altering this ratio. Because the internal friction damping technique uses the measurement of the relative amplitude decay, as opposed to an absolute amplitude measurement, there is no restriction on output signal strength.

5.2.3 Independence of Specific Damping Capacity and Tensile Load in the Linear Elastic Range

This report concludes that the specific damping capacity is a constant value for any particular rope specimen and is independent of the level of tension, so long as the tensile load is within the range of linear elasticity. The range of linear elasticity is defined as that range of tension where an incremental increase of load produces a proportional increase in elongation. Figure 40 graphically illustrates the range of linear elasticity. Several rope specimens were investigated thoroughly, in order to quantify the time-dependence of measured $\Delta W/W$ and to evaluate the relationship between tensile load and $\Delta W/W$. Figures 42 and 43 show that the stable specific damping capacity values obtained on these rope specimens, once they have achieved static equilibrium, are constant throughout the linear elastic range.

There are three important advantages to the independence of specific damping capacity and tensile load. These are:

1. It eliminates the need to obtain a matrix of measurements of specific damping capacity at a multitude of tension levels.
2. If the resonant frequency is close to the frequency of a strong noise component, interference can occur which causes variation in the output signal amplitude. Because the specific damping capacity is independent of the level of tension, the tensile force can be increased or decreased to where the resonant frequency and the noise frequency are separated enough to filter out the noise using the frequency analyzer.
3. For possible future field applications a precise level of tension will not be required.

5.3 Technical Limitations of IFD-NDE Technique

5.3.1 Dependence of Measured Specific Damping Capacity on Time

This report concludes that the measured specific damping capacity is dependent upon the length of time that a constant tensile load has been maintained. The measured specific damping capacity decreases over time until the rope specimen reaches equilibrium, at which time a stable minimum value of specific damping capacity is obtained. Figure 41 graphically illustrates the relationship between time under load and measured specific damping capacity for a new six inch circumference, three strand nylon rope specimen. Some rope specimens showed considerably more scatter in the $\Delta W/W$ measurements made early in the load cycle than that illustrated. However,

the same general trend was evident, with the measured value settling down after some time. For six inch circumference and eight inch circumference, six foot long rope specimens, the time to equilibrium is between 30 and 100 minutes. This simply limits the number of specific damping capacity measurements which can be made in a given length of time.

5.3.2 Minimum Tensile Load Necessary

This report concludes that a minimum tensile load on the rope specimen is necessary for accurate measurements of specific damping capacity to be obtained. This load is equal to the load required to reach the lower bound of the range of linear elasticity.

The reason for this necessity is the finding early in the program, that specific damping capacity values generally decrease with increasing tension in the range below the linear elastic range. Figures 42 and 43 illustrate this effect. Figure 42 also illustrates the large variability in the measured specific damping capacity when the tensile load is less than that required to produce linear elastic behavior.

There are two material phenomena which act in combination to produce this effect. One is the viscoelastic behavior of synthetic materials, resulting in a phase lag of strain relative to stress. The other phenomenon is the fiber orientation effect. When the synthetic rope is under no load, individual fibers, due to their molecular structure, are not straight. As tension is applied to the rope, the fibers straighten out until, at the lower limit of the linear elastic range, they become aligned. Until that point is reached, the "curliness" of the fibers creates additional internal friction in the rope.

5.3.3 Maximum Allowable Tensile Load

Due to the nature of material behavior, it is necessary that the tensile load used in conjunction with the internal friction damping technique not exceed the upper

limit of the range of linear elasticity. This is because tensile loads above this limit will cause permanent elongation of the rope specimen which translates to permanent change in the internal structure. When this occurs, the value being measured is affected.

This effect is illustrated by the comparison between three specimens of new six inch circumference, three strand nylon rope. Specimens denoted American new and Columbia #1 new had both been overstressed during the early stages of the program. Columbia #2 was a virgin specimen. Table 2 lists the specific damping capacity values obtained for these specimens. The rope specimens which had been overstressed had a $\Delta W/W$ value approximately 20% greater than the virgin specimen.

5.3.4 Minimum 1/r Ratio

A preliminary conclusion of this report is that a minimum ratio between unsupported length of rope and radius of gyration of the rope cross-section (1/r) of approximately 100 is needed in order to produce the stable vibration necessary to utilize the internal friction damping technique.

This is a tentative conclusion which resulted, early in the program, in changing from testing three inch rope sections to testing six inch rope specimens. There were other factors at play during the early testing of three foot long specimens which may have also influenced the difficulty experienced in forcing the rope into resonant vibration. For this reason, the 1/r value of 100 may be modified through further research. For a 21 inch circumference hawser this would mean a minimum length between supports of about 14 feet would be required.

5.4 Dry Versus Saturated Rope Specimens

This report makes several general conclusions concerning measurement of specific damping capacity for dry specimens versus saturated specimens. These conclusions are enumerated below and discussed in detail in Section 4.4.

1. Saturated polypropylene ropes generally have a lower measured specific damping capacity than the same ropes tested dry. The single case where this did not occur was the first saturated test of the new eight inch circumference, three strand polypropylene specimen. As footnoted on Table 2, the $\Delta W/W$ value of 7.08×10^{-2} was obtained after 60 minutes at tension. The value of 4.83×10^{-2} was obtained during a second test after 165 minutes. During the second test, the $\Delta W/W$ value had not stabilized by 60 minutes, indicating that the value of 7.08×10^{-2} would have decreased if the test had been carried out later in the load cycle.
2. Saturated nylon and dacron ropes generally have a higher measured specific damping capacity than the same ropes tested dry.
3. It is feasible to conduct the technique under either condition, as the eight inch three strand dacron specimen which experienced failure had significantly higher specific damping capacity values than the new specimen under both conditions.
4. Correlation of specific damping capacity with remaining strength appears to be immediately feasible for dry rope specimens.
5. Correlation of specific damping capacity with remaining strength for saturated specimens appears to be feasible. However, further investigation is necessary in order to quantify all the effects of water saturation such that meaningful correlations can be made. Specific recommendations regarding further investigations are included in Section 6.

The conclusions listed above are qualitative and general. More specific, quantitative conclusions will be possible after a sufficient data base is obtained.

6.0 RECOMMENDATIONS FOR FURTHER WORK

Successful completion of this feasibility study has yielded indications for further work. Trends noted from data obtained during testing should be quantified with additional experimental work. The following work is recommended as a continuation of this feasibility program phase:

1. Additional data needs to be acquired to determine the feasibility of correlating synthetic rope conditions to remaining useful life.

The limited data acquired in the first phase of the program indicated that, for similar size, construction and wet/dry state, differences do exist between ropes of varying deterioration. However, insufficient data exists (and that for only a small sampling of rope type) so that specific correlations or standards for defining the remaining useful life of the rope cannot be made. Specifically, data beyond that obtained for eight matched pairs of rope is required in order to establish performance standards for mooring and towing lines. It is recommended that the correlation of $\Delta W/W$ to remaining useful life and the associated performance standards be conducted on six inch and eight inch circumference rope under cyclic loading with wet immersion.

2. Additional data is required to refine the length to radius of gyration constraint indicated in the results.

This constraint, which was obtained during preliminary tests in Phase I, needs to be correctly and accurately verified. The designing of any field test machine would be dependent upon the rope length requirement, as stated by this constraint. Specifically, the Phase I test indicated, for a length to radius of gyration ratio of 100, a six foot test section was required. Additional data for various other l/r ratios will allow the smallest, most economically viable, mobile test unit to be designed for "in-situ" testing.

3. A prototype design and working model of a field test machine is required to implement the field IFD-NDE technique.

The machines currently available for synthetic rope testing are designed for failure tests of full length rope and hawser specimens. The IFD-NDE technique application to synthetic rope, as indicated in the feasibility study, does not require breaking strength loads applied to the sample, specifically considering the smaller hawsers (six inches and eight inches) and lines used for towing and mooring. It is proposed that small, less costly field test equipment, used in the application of the NDE technique, be designed and a prototype unit be built. This prototype equipment could then be utilized in the field data acquisition phase proposed below.

4. The acquisition of a field data base would be required in any future work to be performed.

The acquisition of field data would be made in an "in-situ" state. For the purpose of the IFD-NDE tests, "in-situ" would include the specified test parameters of input, output, method of support, signal strength and output, method of support, signal strength and output analysis techniques. The proper evaluation of the field data would enable the large data base that was collected in the laboratory tests to be evaluated and correlated to the specific field tests. The correlation of specific damping capacity values to the degree of degradation for finite time intervals would enable the IFD-NDE technique to predict incipient failure in synthetic materials as a function of their remaining useful life. The proposed method of test for field evaluation of synthetic ropes would depend on the laboratory data gathered and would be included as a partial fulfillment of the prototype field design of the IFD nondestructive evaluation technique equipment package.

5. Other vibrational modes, materials, constructions and tests should be performed on laboratory specimens to define adequately the entire range of expected results for specific damping capacity measurements.

Rope and section degradation areas include environmentally assisted fatigue, cyclic fatigue, abrasion, salt water corrosion, and cutting of strands of the rope and sections of lines. The additional laboratory IFD-NDE tests would define the expected results for various failure modes that would also include the standard confidence limits for those tests. This failure criteria would establish the data base that would enable field tests to be performed on numerous constructions and types of lines and sections. Various ultimate uses of lines such as splices, braces, twists, terminations and eye splices would be included in the field evaluation tests. The field evaluation would, in part, be accomplished utilizing the established laboratory data base. Since the IFD-NDE technique utilizes laboratory baseline data to define certain input and output test parameters within the scope of the test procedure, the actual failure prediction indicated by field tests would be predicated upon a change in the IFD field data. The magnitude of the laboratory change could be scaled up to the magnitude of the field change and a correlation established for expected results.

6. Specific and major failure mechanisms of ropes, sections, lines, and hawsers should be adequately defined for the purpose of establishing quantitative failure guidelines.

The most common line failures should be specified for the purpose of establishing a correlation of the failure mechanism to the measured specific damping capacity of the

material. Specifications that include quantification of failure mechanisms and correlation to measured internal friction damping values would be the ultimate NDE test scenario for synthetic lines within the scope of present technology.

In order to develop the internal friction damping technique to full utilization for synthetic materials, other work outside the scope of the present program would be required. This includes:

1. Fatigue cycle monitoring of full size hawsers would accelerate the transfer of this technology to the SPM hawser safety program. The preliminary correlation made under this program between remaining strength and specific damping capacity should be refined. This work would permit a correlation to be made between specific damping capacity and remaining useful life for full size hawsers subject to cyclic fatigue. The inclusion of environmental degradation in the test matrix via exposure to ultraviolet radiation, salt water immersion, etc. of certain samples would permit quantifying the effects on the specific damping capacity value of the various environmental forces. This work may be expedited through interaction with Coordinated Equipment Company in California, as Coordinated Equipment has the apparatus for fatigue cycling full scale hawsers.
2. Acquisition of field data to provide adequate information on all Coast Guard approved lines, ropes, braces and hawsers, as well as spliced sections, eye splices, etc. This information would allow the determination of standard

regions of safe operation for these lines, based on the correlations which could be made to specific damping capacity.

3. Feasibility studies are suggested where other synthetic materials are used in marine applications. Some areas where feasibility studies should be performed are floating hoses used in conjunction with SPM systems, hovercraft skirts, buoy lines, and composite structural materials. Investigations should also be conducted to determine the feasibility of utilizing the internal friction damping technique as an aid to quality control at the point of manufacture for various items used in the marine industry. Synthetic ropes of different sizes and constructions and dockside vehicle tires are two areas where the IFD-NDE technique might prove to be a valuable quality control tool.

In conclusion, the successful contribution of the IFD-NDE technique to the investigation for a nondestructive test technique applied to synthetic materials has been defined. Specifically, the first study of applying the technique to six inch and eight inch circumference synthetic rope specimens has shown feasibility of application to synthetic ropes. Rope specimens have been found to have characteristic repeatable specific damping capacity values, which are affected by degradation due to fatigue and abrasion. Based upon the test data, the technique is applicable not only to small and medium size hawsers, but also full size SPM hawsers. Further work leading to utilizing this technique for full size SPM hawsers has been recommended and is strongly suggested. This technique may also be applicable to many other synthetic materials,

both for field evaluation of items in-service and for quality control of newly manufactured items.

All of the objectives of the synthetic rope feasibility study have been met. Ropes of various synthetic materials, constructions and sizes have been tested, both dry and in the saturated laboratory wet condition. The data was analyzed and specific damping capacity values were correlated with the visible condition of the ropes. Differences between new and used ropes of similar size, material and construction were noted. Differences between the values obtained in the dry and laboratory wet conditions were also noted.

Conclusions have been drawn from the results. Where firm conclusions could not be made but trends were noted, these were discussed and the work needed to arrive at firm conclusions was identified. Recommendations for further work needed to bring the IFD-NDE technique to full utilization in the evaluation of synthetic ropes and hawsers have been made. Recommendations for further work in related areas and for feasibility studies for other synthetic material marine applications have also been made.

REFERENCES

1. Flory, F., Benham, F. A., Marcello, J. T., Poranski, P. F., and Woehleke, S. P., "Guidelines for Deepwater Port Single Point Mooring Design," Final Draft Report, Exxon Research and Engineering Company, Florham Park, N. J., May 1977.

2. Special Technical Publication AR-6A, "Single vs Double Leg Hawsers for Single Point Moorings," Samson Cordage Works, Boston, Mass., 1978.

3. Zener, C., "Internal Friction in Solids, Theory of Internal Friction in Reeds," Physical Review, Vol. 52, p. 230, 1937.

4. Zener, C., "Elasticity and Anelasticity of Metals," The University of Chicago Press, Chicago, 1948.

5. Jenson, J. W., "Damping Capacity - Its Measurements and Significance," Bureau of Mines Report of Investigation 5441. United States Department of the Interior, 1959.

6. Grosskreutz, J. C., Fatigue an Interdisciplinary Approach, Syracuse University Press, Syracuse, New York, p. 27, 1964.

7. Roberts, J. T. A., and Barrand, P., "Model for the Low Temperature Grain Boundary Damping Peak in FCC Metals," TRANS. AIME 242, pp. 2299-2303, 1968.

8. Roberts, J. T. A., "Grain Boundary Damping in Substitutional Alloys," MET. TRANS. 1, pp. 2487-2493, 1979.

9. Peguin, P., Perez, J., and Gobin, P., "Amplitude—Dependent Part of the Internal Friction of Aluminum," TRANS AIME 239, pp. 438-451, 1967

10. Sachse, W., and Green, R. E. Jr., "Experimental Study of the Orientation Dependence of Dislocation Damping in Aluminum Crystals," TRANS. AIME 242, pp. 2185-2190, 1968.

11. Gibala, R., "Internal Friction in Hydrogen Charged Iron," TRANS. AIME 239, pp. 1574-1584, 1967.

12. Kalski, H., "Stress Waves in Solids," Dover Publications, New York, New York, 1963.

13. Zener, C., "Internal Friction in Solids, Theory of Internal Friction in Reeds," Physical Review, Vol. 52, p. 230, 1937.

14. Zener, C., "Internal Friction in Solids, General Theory of Thermoelastic Internal Friction," Physical Review, Vol. 53, p. 90, 1938.

15. Randall, R. H., Rose, F. C., Zenner, C., "Intercrystalline Thermal Currents as a Source of Internal Friction" Physical Review, Vol. 56, p. 343, 1939.

16. Ké, T. S., "Experimental Evidence of the Viscous Behavior of Grain Boundaries in Metals," Physical Review, Vol. 71, p. 533, 1947.

17. Orowan, I. E., "Mechanism of Viscous Flow in Solids," Proceedings West of Scotland Iron and Steel Institute, 1947.

18. King, R., Cahn, R. W., and Chalmer, B., "Mechanical Behavior of Crystal Boundaries in Metals," Nature, Vol. 161, p. 682, 1948.

19. Ké, T. S., "Stress Relaxation Across Grain Boundaries in Metals," Physical Review, Vol. 72, p. 41, 1947.

20. Seitz, F., Physics of Metals, Chapter X, McGraw-Hill Book Co., New York, New York, 1943.

21. Koehler, J. S., "The Influence of Dislocations and Impurities on the Damping and the Elastic Constants of Metal Crystals, Imperfections in Nearly Perfect Crystals, Edited by W. Shockley, John Wiley and Sons, Inc., New York, New York, p. 191, 1962.

22. Thompson, D. O., and Holmes, D. K., "Dependence of Young's Modulus and Internal Friction of Copper Upon Neutron Bombardment," Journal of Applied Physics, Vol. 27, p. 191, 1956.

23. Carson, K. R., and Weertman, J., "Dislocation Density in Single Crystals of Silicon-iron During Low Cycle Fatigue," TRANS. AIME 242, pp. 956-958, 1968.

24. Boettner, R. C., "Fatigue Crack Nucleation in a High Strength Low-Alloy Steel," TRANS. AIME 239, pp. 1030-1033, 1967.

25. Cottrell, A. H., The Mechanical Properties of Matter, John Wiley and Sons, Inc., New York, 1964.

26. Thiruvengadam, A. P., "On Corrosion Fatigue at High Frequencies," American Society for Testing and Materials, STP 503, pg. 171, 1970.

27. Yeager, L. L., and Wood, L. E., "Recommended Procedure for Determining the Dynamic Modulus of Asphalt Mixtures," Transportation Research Board, National Research Council, Washington, D. C., Transportation Research Record #549, 1975.

28. Fresch, D. C., Yeager, L. L., Hochrein, A. A. Jr., and Thiruvengadam, A. P., "Technical Feasibility for Measuring the Relative Amplitude Decay for the Internal Friction Nondestructive Evaluation Technique for the General Electric Pipe Test Fixture Assembly," DAI Technical Report DF-7748-001-TR, September 1978.

APPENDIX A

OPERATION OF NDE EQUIPMENT

A.0 INSTRUMENTATION SETTINGS AND INSTRUCTIONS FOR IFD-NDE TECHNIQUE

A.1 Instrument Operation

In order to operate the instrument package for dynamic response measurements, the following operational procedure has been developed. This procedure is used to obtain an output decay curve for a specific input signal.

A.1.1 Wiring

1. Transmit Section: Connect the "Attenuator Output" of the B & K Beat Frequency Oscillator to the "signal input" BNC connector on the back plate of the General Radio 1396-B Tone Burst Generator (gate). Connect the "signal output" of the Tone Burst Generator to the Mini-Shaker, B & K model 4810. Connect the "sync output" of the gate to the lower "ext trig" of the Tektronix type 564 storage oscilloscope. The BNC connection from the gate connects to a banana plug-in, and then into the scope if a BNC/banana adapter is needed. The ground is marked on the banana plug by the word "ground" and has a raised shoulder.
2. Receive Section: Connect the accelerometer, B & K model 4334, to "Amplifier Input"

of B & K type 2107 frequency analyzer. Connect the "Recorder" output of the analyzer to the Channel 1 input of the oscilloscope.

A.1.2 Fixed Instrument Controls:

The instrument controls detailed in this section are set prior to the initiation of the test sequence.

1. Gate:

Trigger level/+ slope	"0"/"+"
Cycle Count	"Normal"
Power	"On"

2. Beat Frequency Oscillator:

Power	"On"
Power Frequency Beat	See calibration instructions in manual.
Automatic Scanning	"Off"
Modulation Frequency	"Mod Off"
Frequency Deviation	"0"
Compressor Speed	"Comp. Off"
Frequency Scale Alignment	See "Power Frequency Beat" above.
Compressor Voltage	"0"

Oscillator Stop	Normal or Out
Matching Impedance	"ATT"/"12V"
Attenuator Output	"12,000 MV"/"0dB"

3. Frequency Analyzer:

Input Potentiometer	"10"
Power	"On"
Input	"Direct"
"Weighting Network"	"Linear 2-40000"
"Meter Switch"	"Fast RMS"
"Frequency Rejection Balance"	12 o'clock
"Frequency Analysis Octave Selectivity"	"MAX"
Oscilloscope	Contained in instructions

A.1.3 Test Procedure:

1. Tuning Section:

Goal: Structural resonance at a predetermined frequency.

Method: Set oscillator main tuning knob (center of frequency scale) to the specified resonance frequency. Turn up "Output Level Control" until a full scale meter deflection is obtained (12 V).

Set gate "Output On" control to "Cont" and "Output Off" control to "Sec."

Set analyzer, "Function Selector" to "Selection Section Off." Set the "Meter Range" to "10V." Set the "Range Multiplier" to "X1." Lower the "Meter Range" voltage settings until a small deflection is obtained on the Frequency Analyzer meter.

NOTE:
At any time, the "Range Multiplier" can be used as a fine adjustment of the meter deflection.

Rotate the oscillator "Frequency Increment" knob in the direction which increases the analyzer meter deflection.

NOTE:
Reduce the sensitivity of the analyzer meter as necessary using the "Meter Range" or "Range Multiplier" and/or adjust the main frequency knob on the oscillator if the "Frequency Increment" goes off the scale (scale is located in lower portion of the main scale, -50 to +50 hz).

Set the analyzer "Function Selector" to "Frequency Analysis" after the maximum deflection has been obtained.

CAUTION:
Do not readjust oscillator.

Set "Frequency Range" of the analyzer to the range containing the resonance. Set "Frequency Tuning" knob to the resonant frequency. Readjust the analyzer "Meter Range" and/or "Range Multiplier" to give a 25% - 75% meter deflection on the analyzer meter. Fine tune the analyzer with the Frequency Tuning Knob to a maximum deflection.

NOTE:
Use only the Frequency Tuning knob and if necessary the "Meter Range" and/or "Range Multiplier" to set the "Frequency Range."

The transmitting section is now tuned. The analyzer is sending the resonant frequency from the signal pickup to the oscilloscope.

2. Oscilloscope Operation Section (Tektronix Type 564 Storage Oscilloscope or equivalent)

Goal: Visual representation of the output signal of the frequency analyzer.

General: The oscilloscope controls may be grouped in three sections, the mainframe consisting of the controls to the right of the cathode ray tube (CRT), the vertical amplifier or dual trace amplifier (left plug in compartment) (Type 3A1/3A72) and the horizontal sweep (Type 3B3).

Initial Operation: Set the "Display" on the mainframe area as follows: "Locate" and "Integrate" push buttons out, "Upper" and "Lower" traces to "Nonstore" and "Writing Rate" to 12 o'clock. Set the "Calibrate" knob to "Off." Set the "CRT" area controls to 12 o'clock. (The power indicator light to the right of the "Scale Illumination" knob should come on.)

Set the "Delayed Sweep Triggering" on the time base to: "Level", knob to 12 o'clock, slope to "+", "Coupling" to "AC" and "Source" to "Int." Set the "Normal or Delaying Sweep Triggering" area as

follows: "Delay Time: to "000", "Level" to 12 o'clock, trigger select to "Norm," "Slope" to "+", "Coupling" to "Auto," "Source" to "Int." On the left-center portion of the time base, set the "Mode" (grey knob) to "Norm," horizontal position (red knob) to 12 o'clock, "Time/Div and Delay Time Range" to "1 mSec" and the variable (red knob) to full clockwise (calibrated).

Disconnect the Channel 1 input on the vertical amp/"Dual Trace Amplifier" plug. Set the "Volts/Div" (grey knob) on Channel 1 to "1", "Mode" (grey knob) to "Ch 1 Only," red knob concentric to "Mode" knob to "Ch 1 Norm."

At this time a trace should be observed, if not raise the "Intensity" (on mainframe) and/or adjust the Channel 1 "Position" knobs until a straight line trace is obtained on the center of the CRT (the red horizontal position knob in the left center area of the time base may be used to laterally center the trace and the grey "Position" knob on the vertical amp may be used to vertically center the trace). Now, adjust the "focus" "Intensity" and "astigmatism" knobs until a sharp trace of moderate intensity is obtained.

NOTE:
The intensity may be varied at any time to obtain a usable trace. A continuous high intensity will damage the CRT screen.

AD-A078 461 DAEDALEAN ASSOCIATES INC WOODBINE MD F/G 11/5
ENGINEERING FEASIBILITY OF INTERNAL FRICTION DAMPING AS A NONDE--ETC(U)
FEB 79 D C FRESCH , L L YEAGER DOT-CG-828271-A

UNCLASSIFIED USCG-D-51-79 NL

3 OF 3
AD
A078461

END
DATE FILMED
1 — 80
DDC

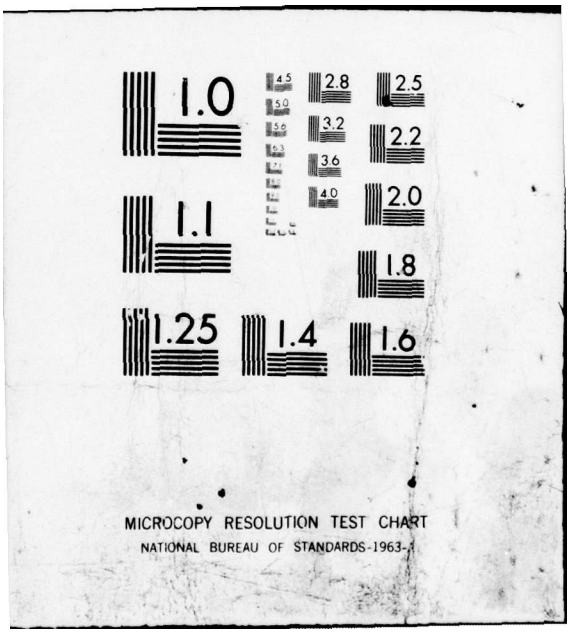
1.0
1.1
1.25
1.4
1.6
1.8
2.0
2.2
2.5
2.8
3.2
3.6
4.0
4.5
5.0
5.6
6.3
7.1
MICROCOPY RESOLUTION TEST CHART
NATIONAL BUREAU OF STANDARDS-1963-A

Once completed, this procedure or a part thereof need only be repeated as it becomes necessary. The above procedure was to familiarize the operator with the controls of a 564 Storage Oscilloscope.

Reconnect the input to Channel 1 and adjust the Channel 1 "Volts/Div" and "Time/Div" until the sine wave displayed is within the bounds of the screen.

NOTE:
Adjust the "Time/Div" knob and observe the changes in the wave form.

3. Decay Curve Section

Goal: Display and photograph the exponential decay of the output pulse.

Set the "Output On" control of the gate to "128" cycles and the "Output Off" to "Sec" with the inner vernier knob set to a time off long enough for the specimen to stop vibrating before the next pulse. Set the oscilloscope mainframe "Display" controls (upper and lower) to "Store" and the time base "Normal" or Delaying Sweep Triggering" as follows: "Coupling" to "DC" "Source" to "Ext" and "Slope" to "-". Adjust the sweep rate (Time/Div) and Vertical Deflection "Volts/Div" controls until a decaying sweep is obtained.

NOTE:
The Ch 1 "Volts/Div" "Variable" control (red knob) may be adjusted as necessary but the "Time/Div" vernier (red knob) ("Variable") should not be touched.

APPENDIX B

ANALYSIS OF NDE RESPONSES

B.0 DATA ANALYSIS TECHNIQUE

The measured values of the specific damping capacity are used in a point by point determination of the base line equation for synthetic rope specimens. Each data point consists of a finite number of measurements (five for this data program) taken on the instant photograph. These data points are converted to a single specific damping capacity number by statistical averaging and analytical methods. The statistical averaging method performed on the numerous measurements taken from the output decay enables the average specific damping capacity value to be calculated from the "least squares linear curve fit." The statistical methods used to calculate the specific damping capacity are predicated upon the definition of elements that combine to provide analytically the existence of a "best" fit of a line through the measurements taken from the output decay. The confidence limit (defined as a function of the standard deviation of the set of measurements) is a measure of the logarithmic decay. The elements that are utilized for the determination of the specific damping capacity are defined in the following sections. The standard error of estimates (Section B.4) and the confidence limits (Section B.5) are included to identify the analysis for the data scatter under cyclic loading fatigue conditions. Section B.6 addresses the analytical method used to determine the effect of different

operators on the specific damping capacity measurements. Section B.7 is the software program for data reduction and generation of the specific damping capacity value.

B.1 Mean of a Sample

The arithmetic mean, $\bar{x}$, of a sample set containing n pieces of data is:

$$\bar{x} = \frac{1}{n} \sum_{i=1}^{n} x_i \qquad [B-1]$$

The arithmetic mean (denoted "mean") is assumed to be a stable average, not unduly affected by moderately large or small data points.

B.2 Variance of a Sample

The variance, s^2, of a sample set containing n pieces of data, with sample mean, $\bar{x}$, is:

$$s^2 = \frac{1}{n} \left[\sum_{i=1}^{n} (x^2{}_i) - n \bar{x}^2 \right] \qquad [B-2]$$

The variance is the minimum of the sum of the squares of the deviations taken with respect to the mean, and is a measure of the dispersion of the data about the sample mean.

B.3 Least-Squares Curve Fit

The linear least-squares fit of input data points (x_i, y_i) is calculated using the following:

$$\text{Slope} = m = \frac{\dfrac{\sum_{i=1}^{n} x_i \sum_{i=1}^{n} y_i}{n} - \sum_{i=1}^{n} x_i y_i}{\dfrac{\left(\sum_{i=1}^{n} x_i\right)^2}{n} - \sum_{i=1}^{n} x_i^2}$$

and

$$\text{Intercept} = b = \frac{\sum_{i=1}^{n} y_i - m \sum_{i=1}^{n} x_i}{n} \qquad \text{[B-3]}$$

where y_i is the measured specific damping $\frac{\Delta W}{W}$ and x_i is the corresponding number of load cycles (LC_n). The estimated value of specific damping $\left[\frac{\Delta W}{W}\right]_{est}$ is found by solving the equation:

$$\left[\frac{\Delta W}{W}\right]_{est} \equiv y_{est} = mx + b \qquad \text{[B-4]}$$

The correlation coefficient (r^2) is the fraction of the total variation which is explained by the least-squares regression line or how well the least-squares regression line fits the sample data, i.e.,

$$r^2 = \frac{\text{Explained Variation}}{\text{Total Variation}} \qquad [B\text{-}5]$$

The correlation coefficient can be computed from:

$$r^2 = m \left[\frac{\dfrac{\sum_{i=1}^{n} x_i \sum_{i=1}^{n} y_i}{n} - \sum_{i=1}^{n} x_i\, y_i}{\sum_{i=1}^{n} y_i^{\,2} - \dfrac{\left(\sum_{i=1}^{n} y_i\right)^2}{n}} \right] \qquad [B\text{-}6]$$

In practice, r^2 lies between 0 and 1.

B.4 Standard Error of Estimate

A measure of the scatter about the regression curve, $y_{est} = f(x)$ is:

$$S_{y \cdot x} = \left[\frac{1}{n} \left(\sum_{i=1}^{n} (y_i)^2 - b \sum_{i=1}^{n} y_i - m \sum_{i=1}^{n} x_i\, y_i \right) \right]^{\frac{1}{2}} \qquad [B\text{-}7]$$

which is the standard error of estimate of y on x.

B.5 Confidence Limits

The estimated value of the sample y at a corresponding $x = x_o$ is $y_{est} = f(x_o)$. At a specified probability level, σ, a degree of confidence for the estimated parameter can be calculated. An estimate of the interval in which the estimate of the sample value y will be found at the specified probability level is given by:

$$y_p = y_{est} \pm \left[\frac{t.\ S_{y\text{-}x}}{(n-2)^{\frac{1}{2}}} \right] \left[n + 1 + \left(\frac{n(x_o - \bar{x})^2}{S_x^{\ 2}} \right) \right]^{\frac{1}{2}} \quad [B\text{-}8]$$

where t is the Student's statistic with n-2 degrees of freedom (df). The value of the t statistic can be found in tables. The estimated values define the confidence limits of the dependent variable at the specified probability level.

B.6 Operator Significance

The possibility of using data obtained by two operators exists providing the differences between the two sets of data can be proven nonsignificant. This can be accomplished by determining whether the correlation coefficients r and r_2 drawn from samples n and n_2 differ significantly from each other.

To prove the differences nonsignificant, a null hypothesis (H_o:) is formulated that any observed differences are due to chance fluctuations in two operators sampling from the same population. The null hypothesis is:

$$H_o: \quad (\mu_{z_1} = \mu_{z_2}) \qquad \text{[B-9]}$$

i.e., there is no significant difference between the two sample means. The alternate hypothesis is:

$$H_1: \quad (\mu_{z_1} \neq \mu_{z_2}) \qquad \text{[B-10]}$$

i.e., the difference between the two sample means is significant.

To test the null hypothesis, use is made of Fisher's Z transformation given by:

$$Z = \frac{1}{2} \ln \left[\frac{1 + r}{1 - r} \right] \qquad \text{[B-11]}$$

The statistic, z, given by:

$$z = \frac{Z_1 - Z_2 - \mu_{z_1 - z_2}}{\sigma_{z_1 - z_2}} \qquad \text{[B-12]}$$

is calculated and used in a two-tailed test to determine whether the value falls within the region of nonsignificance at the specified probability level. Z_1 and Z_2 are calculated for corresponding values of r and r_2. For the statistic

$$\sigma_{z_1 - z_2} = \left[\frac{1}{n_1 - 3} + \frac{1}{n_2 - 3} \right]^{\frac{1}{2}} \qquad \text{[B-13]}$$

and

$$\mu_{z_1 - z_2} = \mu_{z_1} - \mu_{z_2} \qquad \text{[B-14]}$$

The null hypothesis, H_o:, is accepted if A lies within the critical region specified by the preassigned probability level; i.e., the observed differences in the data are not significant at the specified probability level. If, however, z lies outside the critical region, then reject H_o: and accept H_1:; i.e., the observed differences in the data are significant at the specified probability level.

B.7 Specific Damping Capacity Program

The software program that utilizes the foregoing definitions and combine to establish the analytical and statistical method of converting a discrete number of measurements into a single specific damping capacity value is presented in this section. The first page lists the output selection of variables displayed through the completion of the analysis of measurements taken from the output decay. The other pages list the data reduction program for converting a discrete number of measurements into a single specific damping capacity number.

TITLE NDE Data Reduction PAGE 1 OF 2

◀A▶				
N		σ_{α_i}		
A_0	α_i	$\bar{\alpha}$	$\Delta W/W$	INIT

◀B▶				

STEP	PROCEDURE	ENTER	PRESS			DISPLAY
1	INITIALIZE		E			0.000
2.	STORE A_0	A_0	A			A_0
3.	STORE N	N	*	A'		N
4.	LOAD A_i	A_i	B			$\Sigma \alpha_i$
5	CALCULATE $\bar{\alpha}$		C			$\bar{\alpha}$
6.	CALCULATE σ_{α_i}		*	C		σ_α
7.	CALCULATE $\Delta W/W$		D			$\Delta W/W$

Part No. [illegible]

TITLE _____ PAGE 1 OF 2

PROGRAMMER _____ DATE _____

SR-52 Coding Form

LOC	CODE	KEY	COMMENTS	LOC	CODE	KEY	COMMENTS	LOC	CODE	KEY	COMMENTS	LABELS
000 112	46	*LBL			01	1			75	−		A
	11	A			54	)			53	(		B
	42	STO		040 152	95	=			43	RCL		C
	00	0			65	×			00	0		D
	02	2			01	1		080 192	07	7		E
005 117	56	*rtn			52	EE				*x²		A'
	46	*LBL			95	=			65	×		B'
	16	*A		045 157	44	SUM			43	RCL		C'
	42	STO			00	0			00	0		D'
	00	0			05	5		085 197	01	1		E'
010 122	03	3			96	*x²			54	)		REGISTERS
	56	*rtn			44	SUM			54	)		00
	46	*LBL		050 162	00	0			55	÷		01
	12	B			06	6			43	RCL		02
	42	STO			43	RCL		090 202	00	0		03
015 127	00	0			00	0			01	1		04
	04	4			05	5			95	=		05
	01	1		055 167		*rtn			30	*√		06
	44	SUM			46	*LBL			56	*rtn		07
	00	0			13	C		095 207	46	*LBL		08
020 132	01	1			43	RCL			14	D		09
	43	RCL			00	0			53	(		10
	00	0		060 172	05	5			01	1		11
	02	2			55	÷			75	−		12
	55	÷			43	RCL		100 212	53	(		13
025 137	43	RCL			00	0			02	2		14
	00	0			01	1			65	×		15
	04	4		065 177	95	=			43	RCL		16
	95	=			42	STO			00	0		17
	23	ln x			00	0		105 217	07	7		18
030 142	55	÷			07	7			54	)		19
	53	(				*rtn			94	+/−		FLAGS
	43	RCL		070 182	46	*LBL			22	INV		0
	00	0				*C			23	ln x		1
	03	3			53	(		110 222	54	)		2
035 147	65	×			43	RCL			56	*rtn		3
	43	RCL			00	0		TEXAS INSTRUMENTS INCORPORATED				4
	00	0		075 187	06	6						

TITLE NDE Data Reduction PAGE 2 OF 2
PROGRAMMER _____ DATE _____

SR-52 Coding Form

LOC	CODE	KEY	COMMENTS	LOC	CODE	KEY	COMMENTS	LOC	CODE	KEY	COMMENTS	LABELS
000 112	16	*LBL										A A_0
	15	E										B a_i
	25	CLR		040 152								C J
	47	*CMS										D ΔW
	57	*fix						080 192				E INIT
005 117	03	3										A N
	56	*rtn										B
				045 157								C σ_{a_i}
												D
								085 197				E
010 122												REGISTERS
												00
				050 162								01 USED
												02 A_0
								090 202				03 N
015 127												04 USED
												05 Σa_i
				055 167								06 $\Sigma(a_i)^2$
												07 $\bar{a}_i$
								095 207				08
020 132												09
												10
				060 172								11
												12
								100 212				13
025 137												14
												15
				065 177								16
												17
								105 217				18
030 142												19
												FLAGS
				070 182								0
												1
								110 222				2
035 147												3
												4
				075 187								

TEXAS INSTRUMENTS
INCORPORATED

APPENDIX C
DIGITAL EQUIPMENT SELECTION

C.0 SELECTION OF AN APPROPRIATE SYSTEM

C.1 System Evaluation

Many configurations of digital processing equipment have been evaluated as a means of assisting the Internal Friction (IF) Nondestructive Evaluation (NDE) technique in predicting incipient failure. Numerous systems are listed along with the results of the evaluation.

C.1.1 Texas Instrument

A Texas Instrument SR52 programmable calculator and a P-100 printer were evaluated as the digital processor for the IF-NDE technique. The calculator was sufficient for data reduction but was not capable of being programmed for the more complex data analysis techniques. There was no interface capability with the IF-NDE equipment which would mean that the data could not be acquired by the processor automatically. This manual step of transferring the data and the lack of data analysis eliminated this system as the automated digital processing system.

C.1.2 Brüel & Kjaer (B & K)

The B & K IF-NDE equipment as it is presently configured could be used as a supporting system for a digital processor. The B & K equipment can be interfaced with a digital processor that could automatically acquire the data, analyze it, store the reduced data and retrieve it at a later time for comparative purposes. The B & K equipment would

supplement the digital processor with its ability to record the log decrement decay of the material being tested. The B & K equipment has no capability to reduce the data on its own.

C.1.3 Nicolet Scientific Corp.

The Nicolet Model 660 digital oscilloscope with built-in microprocessor was evaluated as a digital processing system for use with other NDE equipment. The Nicolet system was capable of analyzing the signals at very low frequencies, but did not have an analog-to-digital convertor that could transform the signal fast enough at higher (about 1,000 Hz) frequencies. Since most signals are analyzed between 20 Hz and 20,000 Hz, this Nicolet system becomes impractical.

C.1.4 Hewlett Packard (HP)

The H. P. 9825A programmable desk-top calculator was evaluated for suitability as the digital processor to be used in conjunction with the present IF-NDE equipment. Its main disadvantage was the slow analog-to-digital convertor, its lack of memory storage, and the resultant loss in high frequency capability. The H. P. system would require that additional storage be made available to handle most IF-NDE testing. This additional cost in memory and storage brings the configured price of this system very close to the minicomputer range.

C.1.5 Mini-Computer Systems

The following systems are all of the mini-computer variety and were evaluated differently based on their superiority to the less sophisticated digital programmable calculators. The mini-computers all have the capability of intelligently controlling lab peripherals that include the present NDE equipment. The storage, analysis and retrieval capability of these systems are very fast. The systems evaluated are:

Varian V77

Data General Eclipse S/130

IBM Series I (4900)

Honeywell

Digital Equipment Corp. PDP 11/34

All of these systems were evaluated with the same basic configuration including peripherals. The basic system consisted of a central processor with 64K of memory, an analog-to-digital convertor, an input/output controller, addressable memory storage, lab controlling package, a terminal, and a line printer. The system was also configured to include operating software and scientific subroutines. The selection of the digital processor was based on the ability of the various mentioned systems to perform the necessary NDE functions. The automatic acquisition of data was an essential feature that each system could perform. The final choice

was based on price, options that were included at no extra charge, and the fact that the systems manufacturer that was selected has a history of successes primarily in the scientific field of computer assistance. Digital Equipment Corporation's (DEC) PDP 11/34 (Figure 1) was selected as the final configuration that would assist the present IF-NDE equipment in evaluating critical components in U. S. Navy vessels.

C.2 Advantages of the DEC PDP 11/34 System

The DEC PDP 11/34 system has capabilities that other mini-computers cannot match such as the fast A-to-D, the addressable memory, and the intelligent laboratory controller I/O. The entire scientific package, as configured by DEC, includes such items as a bi-directional parallel transfer, intelligent laboratory control systems, fast line printer, priority interrupt system, and multiple user input for the intelligent I/O controller. Varian, IBM, Data General and Honeywell did not include these variables and others in their price quotation. The Digital Equipment Corporation routinely includes the scientific peripherials, such as the intelligent laboratory controller I/O and the direct access memory, as standard features on their mini-computers. The Digital Equipment Corporation has demonstrated the portability of their mini-computer systems which makes them ideal for field use. The versatility of configuration offered by

the Digital Equipment Corporation enables the mini-computer to be packaged in various ways.

C.3 System Description

The Digital Equipment Corporation PDP 11/34 mini-computer consists of the following:

C.3.1 PDP-11/34

The PDP-11/34 is a midsize microprogrammed processor. The CPU is compact and contained on two circuit boards. This provides greater flexibility during later system expansion by making additional chassis space available.

The Memory Management is an advanced memory extension, relocation and protection feature. The Memory Management provides extended memory space from 28K to 124K words; plus, segmentation, and effective protection of memory segments in multi-user environments.

Self-test Diagnostic Routines are automatically executed every time the processor is powered up, the console emulator routine is initiated, or the bootstrap routine is initiated.

Operator front panel with built-in CPU console emulator allows control from any terminal without the need for the conventional front panel with display lights and switches.

Automatic bootstrap loader allows system restart from a variety of peripheral devices without manual switch toggling or key pad-operations.

The central processor contains eight general registers which can be used for a variety of purposes. The registers can be used as accumulators, index register, auto-increment or auto-decrement registers, as well as stack pointers for temporary storage of data. The instruction complement uses the flexibility of the general purpose registers to provide hard-wired instructions.

The Extended Instruction Set (EIS) provides the capability of performing hardware fixed-point arithmetic and allows direct implementation of multiply, divide and multiple shifting.

The FP11-A floating-point is an arithmetic processor which fits integrally into the PDP-11/34 central processor. It performs all floating-point arithmetic operations and converts data between integer and floating-point formats. This option provides flexible addressing in addition to single and double precision (32 or 64 bit) floating-point modes, and it is fully program compatible with all double precision PDP-11 floating-point processor options.

C.3.2 DECpack Disk

This disk subsystem includes a disk controller and two drives. It is a complete mass storage system for random access data storage. One drive utilizes a removable disk cartridge with 2.4 million bytes (8 bit bytes) capacity. The

other drive utilizes a fixed disk drive with an additional 4.8 million bytes.

The DECpack features a transfer time of 11.1 microseconds/word. Average total access time on a disk drive is 70 milliseconds. All data transfers are DMA (direct memory access).

C.3.3 VT55 Graphic Terminal and AKD11-KT Real-Time Analog

The VT55 is an on-line interactive CRT terminal that offers waveform graphics capability. Two graphs of 512 (maximum) data points each can be displayed with a screen resolution of 512 points (x) by 236 points (y). Cursors (20 point vertical lines) are available (one per data point) to facilitate data editing and graph generation. In addition, the VT55 allows simultaneous display of any combination of text and graphics. The VT55 supplies a hardcopy reproduction of the display screen for both characters and graphs. The VT55 can hold up to 1,920 characters in 24 lines of an 80 character-per-line matrix.

The real-time Analog Data Acquisition Package consists of the necessary logic and listed hardware for interfacing to laboratory analog instrumentation. The package contains a 12 bit, 16 channel, single ended (or 8 channel differential) analog-to-digital convertor, a dual programmable real-time clock, cable, and a distribution panel to provide a complete instrumentation interface package.

C.3.4 AD11-K Analog-to-Digital (A/D) Convertor

The 12 bit A/D convertor can be switch selected to operate as a 16 channel, single ended, 16 channel psuedo differential or 8 channel true differential A/D convertor. The A/D convertor will convert an analog voltage from within one of the specified input ranges of ± 5V, ± 5.12V, ± 10V, ± 10.24V, 0 to 10V, or 0 to 10.24V to a digital number for processing. These input ranges are jumper selectable. The A/D convertor contains an input multiplexer, sample and hold, 12 bit successive approximation A/D convertor and UNIBUS interface logic. The A/D convertor can be started in one of three ways; under program control, on overflow of the programmable clock, or from external input. This versatility allows the adaption of the package to most individual applications.

C.3.5 KW11-K Programmable Clock

KW11-K is a dual, programmable real-time clock which interfaces directly with the DECLAB-11/34 UNIBUS.

Clock A is a 16 bit clock which can be program selected to operate at eight clock rates: five rates are crystal controlled frequencies (1 MHz, 100 KHz, 10 KHz, 1 KHz, and 100 Hz); the remaining three rates are an external (Schmitt Trigger One) input, line frequency or the overflow of the second clock (clock B).

Clock A operates in one of four programmable modes of operation: single interval, repeat interval, external event timing and external event timing from zero base.

Clock B is an 8 bit, programmable, real-time clock which can accurately count intervals of time or events. Clock B can be used to generate a program controlled interval or to provide an input frequency for clocking Clock A. Clock B operates in repeated interval mode. Seven clock rates can be program selected: five rates by crystal controlled frequencies (1 MHz, 100 KHz , 10 KH_z, 1 KHz, and 100 Hz); the remaining two rates are line frequency and external (Schmitt Trigger) input.

C.3.6 AA11-K D/A Convertor System

The AA11-K is a 4 channel, 12 bit digital-to-analog convertor (DAC). It has the control logic for displays such as the Tektronix 602, 604 display scopes and 611, 613 storage scopes. The four DAC channels are controlled by four independent registers directly addressable from the UNIBUS. This allows complete flexibility in programming the output of the DAC for a variety of applications. The 4 channel, 12 bit D/A convertor can be used with point plot display, analog X/Y or chart recorders, set point controller, programmable power supply and signal generators.

C.3.7 DR11-KT 16 Bit Digital I/O Interface

The DR11-KT general device interface is an integral logic module which forms a self-contained digital input/output interface between the DECLAB 11/34 UNIBUS and a user's peripheral. The general purpose interface performs all of the

necessary tasks to communicate with the processor so that the user may easily interface a device or devices.

Under program control, the general purpose interface permits bidirectional parallel transfer of up to 16 bits of information between the UNIBUS and a user's device or another general-purpose interface. All interfacing lines to and from the general-purpose interface are fused and have recoverable over-voltage protection.

Various options, which are hardware-selected by the user, are available for data input. Data can either be read off a user's device directly onto the UNIBUS or through the input register. The input register bits are transitionally set by its respective input line.

C.3.8 LPA11-K

The LPA11-K is a direct memory access (DMA) controller for Digital's laboratory data acquisition I/O devices. It is a fast microprocessor subsystem. The LPA11-K allows analog data acquisition rates up to 150,000 samples per second and is designed for applications requiring concurrent data acquisition and data reduction at high rates. Operating system support is provided under RT-11 and RSX11-M.

The LPA11-K allows multiple users to simultaneously control analog-to-digital convertors (ADC), digital-to-analog convertors (DAC), real-time clocks and digital input and output (Digital I/O). Interaction with these peripherals

is performed by the microprocessors; therefore, the host PDP-11 is freed from the overhead of the interrupt service routines normally associated with these devices.

To meet a variety of applications the LPA11-K operates in two distinct modes, dedicated and multirequest. In dedicated mode, the LPA11-K performs high speed data acquisition from analog-to-digital convertors for a single user. In multirequest mode, the LPA11-K allows up to eight simultaneous users to perform data acquisition at independent rates from any one of the supported device types.

Maintainability is an important part of the LPA11-K subsystem. Standard diagnostic capability is coupled with microcode dedicated to fault identification. The LPA11-K subsystem has the capability of diagnosing faults within the laboratory I/O peripherals. Request verification and error reporting are provided during data acquisition.

C.3.9 Languages for the DEC11/34

The RT-11 software as supplied by Digital Equipment Corp. is the operating language for the digital processor. Fortran IV and BASIC are included in the system. The Fortran IV software includes a full set of subroutines that supports real-time, reading analog signals, controlling a graphic terminal, and controlling I/O hardware. The last feature is the most important one, as it allows the user to automatically control other peripherals such as the frequency analyzer through the I/O.

APPENDIX D

SOFTWARE

D.0 DATA ACQUISITION AND REDUCTION PROGRAM FOR THE IFD-NDE SYSTEM

Software has been developed to acquire the analog signal from the frequency analyzer and to transform the analog signal to a digital signal that can be analyzed, stored and compared at a later time. The program lists the log decrement decay values, the specific damping capacity measurements, and the standard deviation of these measurements.

D.1 Data Acquisition Program

The computer printout is listed for the various programs that acquire, analyze, and calculate the log decrement decay in order to define the specific damping capacity number. The program, written in a machine language called "MACRO", acquires the various analog signals from the frequency analyzer and converts them into digital signals that can be stored in the memory of the digital processor. The data acquisition program also stores the digital values in eight buffers for analysis at a later time.

D.2 Data Reduction Program

The data reduction program analyzes the digital values stored in the buffers and reduces those values to average log decrement decay values. The program uses Fortran language to compile and reduce the various raw data to the average log decrement decays that are used in obtaining the final specific damping capacity value. The output from the data reduction

program is listed in both the short and long form. The longer form of data reduction includes intermediate digital values of specific damping capacity before the proper statistical averaging methods have been applied.

D.3 Statistical Program

The various elements of the statistical program are included in Section 3.5 that statistically combines all values of the calculated specific damping capacity for one data point. The data reduction enables the precise average of a data point predicated on numerous measurements to be added to the predictive program. The abbreviated form of data reduction will list as an output the specific damping capacity and the associated standard deviation for a single data point.

DATA ACQUISITION PROGRAM

```
; MACRO INVOCATIONS
;
        .MCALL  ..V2..,.REGDEF,.PRINT,.EXIT,.TTYIN
        .MCALL  .SYNCH,.INTEN,.ENTER,.WRITE,.CLOSE
        .MCALL  .WAIT,.PURGE,.DEVICE,.PROTECT
        ..V2..
        .REGDEF
;
; LOCAL DEFINITIONS
;
WIP=1
DONE=2
ALLDON=4
ADCHAN=1
BLKBF=1
NUMBF=20
RTCHAN=16
CLRATE=20000
BUFSZ=BLKBF*400
;
; HARDWARE DEFINITIONS
;
ADCSR=170400
ADBUF=ADCSR+2
KWCSR=170420
KWFRE=KWCSR+2

        .ASECT
        .=440
        .WORD   CLKINT  ;POINT TO ISR
        .WORD   340     ;SET HIGH PRIORITY
        .CSECT
;
; LOCAL STORAGE
;
BLOCK:  .WORD   0       ;CURRENT BLOCK WITHIN DISK FILE
BUFCTR: .WORD   0       ;COUNTER OF POSITION WITHIN BUFFER
BUFNUM: .WORD   0               ;CURRENT BLOCK WITHIN SAMPLE
BUFPTR: .WORD   0               ;POINTER TO CURRENT BUFFER
NXTPTR: .WORD   0               ;POINTER TO NEXT BUFFER
LSTPTR: .WORD   0               ;POINTER TO LAST BUFFER
WFLAG:  .WORD   0               ;FLAG OF CURRENT WRITE STATUS
BUFSIZ: .WORD   0               ;SIZE OF BUFFER IN WORDS (COMPUTED)
BLKBUF: .WORD   BLKBF           ;NUMBER OF BLOCKS PER BUFFER
NUMBUF: .WORD   NUMBF           ;NUMBER OF BUFFERS TO WRITE OUT
CHAN:   .WORD   ADCHAN          ;A/D CHANNEL TO SAMPLE
RATE:   .WORD   CLRATE          ;RATE TO RUN CLOCK
DEVBLK: .RAD50  /DX1SAMDATDAT/  ;NAME OF DISK FILE
EAREA:  .BLKW   5               ;ROOM FOR ENTER

;
; DATA BUFFERS
;

BUFA:   .BLKW   BUFSZ
BUFB:   .BLKW   BUFSZ
```

DATA ACQUISITION PROGRAM (Continued)

```
;+
; START OF A/D SAMPLING PROGRAM
;
; AS THE PROGRAM NOW STANDS, IT RUNS STAND ALONE, READING FROM
;       A/D CHANNEL 1 AND WRITING TO DISK ON RT CHANNEL 15 WITH
;       A FILE NAME OF DX1:SAMDAT.DAT.
;
; THE ROUTINE COULD BE MADE FORTRAN CALLABLE, WITH THE ADDITION
;       OF CODE TO COPY ARGUMENTS FROM THE FORTRAN ARGUMENT LIST
;       TO THE LOCAL STORAGE OF THIS ROUTINE.
;-
        .ENABL  LSB
START:
        MOV     BLKBUF,R1       ;FETCH THE NUMBER OF BLOCKS IN A BUFFER
        MUL     NUMBUF,R1       ;MULTIPLY BY THE NUMBER OF BUFFERS TO READ
        .ENTER  #EAREA,#RTCHAN,#DEVBLK,R1       ;ENTER THE FILE ON THE DISK
        CLR     BLOCK           ;INIT BLOCK NUMBER COUNTER
;
; INIT BUFFER POINTERS
;
        MOV     BLKBUF,R1       ;GET NUMBER OF BLOCKS PER BUFFER
        MUL     #400,R1         ;COMPUTE NUMBER OF BYTES
        MOV     R1,BUFSIZ       ;SAVE BUFSIZ
        MOV     R1,BUFCTR       ;INIT BUFFER LENGTH COUNTER
        MOV     #BUFA,LSTPTR    ;INIT POINTER TO LAST BUFFER
        MOV     #BUFB,NXTPTR    ;INIT POINTER TO NEXT BUFFER
        MOV     LSTPTR,BUFPTR   ;INIT POINTER TO CURRENT BUFFER
        MOV     NUMBUF,BUFNUM   ;INIT COUNTER OF BUFFERS
;
; INIT A/D AND CLOCK
;
        MOVB    CHAN,R0         ;GET A/D CHANNEL NUMBER
        SWAB    R0              ;PUT IN CORRECT BYTE
        BISB    #40,R0          ;SET A/D START COMMAND
        MOV     R0,@#ADCSR      ;START THE A/D
        MOV     RATE,R0         ;GET RATE OF A/D CLOCK
        NEG     R0              ;TAKE 2'S COMPLEMENT
        MOV     R0,@#KWPRE      ;SET CLOCK COUNTER
        MOV     #113,@#KWCSR    ;START CLOCK
        .TTYIN
        BR      WAIT                    ;NOW WAIT FOR ACTION
;
; CLOCK INTERRUPT SERVICE ROUTINE
;
CLKINT:
        MOV     @#ADBUF,@BUFPTR ;READ FROM A/D, MOVE TO BUFFER
        ADD     #2,BUFPTR       ;ADVANCE BUFFER POINTER
        DEC     BUFCTR          ;NOTE SAMPLE COLLECTED, CHECK FOR BUF END
        BNE     RET             ;IF NE NOT FULL, JUST RTI
;
; BUFFER IS FULL, SWITCH BUFFERS
;
        BIT     #WIP,WFLAG      ;CHECK FOR WRITE STILL IN PROGRESS (ERROR)
        BNE     ERR             ;IF NE ERROR, SAMPLING TOO FAST
        MOV     BUFSIZ,BUFCTR   ;RE-INIT BUFFER COUNTER
        MOV     NXTPTR,BUFPTR   ;RESET CURRENT BUFFER
        MOV     LSTPTR,NXTPTR   ;RESET NEXT BUFFER
        MOV     BUFPTR,LSTPTR   ;RESET PREVIOUS BUFFER
        BIS     #DONE,WFLAG     ;SET BUFFER DONE FLAG
```

DATA ACQUISTION PROGRAM (Concluded)

```
RET:
        BIC     #200,@#KWCSR    ;CLEAR OVERFLOW
        BIS     #113,@#KWCSR    ;RESTART CLOCK
        RTI                     ;RETURN FROM INTERRUPT
ERR:
        HALT                    ;ERROR !!! DATA OVERRUN!!!
;
; NOW ALLOW INTERRUPTS
;
;
; COMPLETE INTERRUPT PROCESSING
;       WRITE THE BLOCK(S) TO THE FILE
;
WRITE:
        BIS     #WIP,WFLAG              ;SET FLAG TO SHOW WRITE IN PROGRWSS
        .WRITE  #EAREA,#RTCHAN,NXTBTR,BUFSIZ,BLOCK ;WRITE THE BUFFER OUT
        .WAIT   #RTCHAN                 ;WAIT FOR WRITE TO COMPLETE
        DEC     BUFNUM          ;COUNT UP THE BUFFERS WRITTEN
        BEQ     FINISH          ;IF EQ FINISHED
        BIC     #WIP!DONE,WFLAG ;NOTE THAT WRITE IS COMPLETE
        ADD     BLKBUF,BLOCK            ;POINT TO NEXT BLOCK FOR NEXT WRITE
WAIT:
        BIT     #DONE,WFLAG     ;IS THE NEXT SAMPLE READY
        BEQ     WAIT            ;IF EQ NO, WAIT
        BR      WRITE                   ;WRITE THE BUFFER OUT

;
; SHUT DOWN THE A/D AND CALL IT A DAY
;
FINISH:
        CLR     @#KWCSR         ;STOP THE CLOCK
        .CLOSE  #RTCHAN                 ;CLOSE THE OUTPUT FILE
        .EXIT
        .END    START
*^C

.R PEG
   DATA ANALYSIS PROGRAM "PEG" FORTRAN PROGRAM
ENTER THE NAME OF DATA FILE /<DX0:SAMDAT.DAT> ?*DX1:DRPIPE.DAT
```

DATA REDUCTION PROGRAM

```
*TT:=PEG.FOR
        INTEGER*2 DATA(256)
        INTEGER NCYC(101),PEAK(101),COUNT,RECORD,PAGE,BUFSIZ,BLKBUF,RECSIZ
        INTEGER FATIG
        LOGICAL*1 NAME(15)
        LOGICAL*1 ICHR,YES
        REAL LDEC(101),SDAMP(101),FCYC(101)
        DATA DATA/512*0/,YES/'Y'/,INDEXR/1/,RECSIZ/256/
        DATA STAT3/0./,STAT4/0./
C
C NUMBUF IS THE NUMBER OF DATA BUFFERS COLLECTED
C BLKBUF IS THE NUMBER OF DISK BLOCKS PER BUFFER
C BUFSIZ IS THE NUMBER OF SAMPLES PER PER BUFFER (RECSIZ*BLKBUF)
C NUMREC IS THE NUMBER OF RECORDS (NUMBUF*BLKBUF)
C RECSIZ IS THE NUMBER OF SAMPLES PER DISK BLOCK (256)
C
C
C ENTER TEST PARAMETERS OF THE DATA COLLECTED BY "SAM" MACRO PROGRAM
C
        TYPE 5
        TYPE 5
        TYPE 5
        TYPE 5
5       FORMAT('1')
        TYPE 10
10      FORMAT('1','   DATA ANALYSIS PROGRAM "PEG" FORTRAN PROGRAM')
        TYPE 20
20      FORMAT(' ENTER THE NAME OF DATA FILE /<DX0:SAMDAT.DAT> ?',$)
        CALL ASSIGN(3,'DX:SAMDAT.DAT',-1)
        TYPE 21
21      FORMAT(' ENTER THE NAME OF THE TEST MATERIAL (15 LETTERS) ?',$)
        ACCEPT 28,NAME
28      FORMAT(15A1)
        TYPE 27
27      FORMAT(' ENTER THE NUMBER OF FATIGUE CYCLES (1 TO 10E6) ?',$)
        ACCEPT 23,FATIG
        TYPE 22
22      FORMAT(' ENTER THE NUMBER OF DATA BUFFERS COLLECTED (16) ? ',$)
        ACCEPT 23,NUMBUF
23      FORMAT(I6)
        TYPE 24
24      FORMAT(' ENTER THE NUMBER OF DISK BLOCKS PER BUFFER (1) ? ',$)
        ACCEPT 25,BLKBUF
25      FORMAT(I6)
        NUMREC=NUMBUF*BLKBUF
26      TYPE 30
30      FORMAT(' ENTER THE FREQUENCY OF OSCILLATION RECORDED (.0001 KHZ
        1 TO 2.5 KHZ) (.340)  ?',$)
        ACCEPT 35,FREQ
35      FORMAT(F7.4)
        IF (FREQ.GT.2.5) GO TO 37
        IF (FREQ.GE..0001) GO TO 42
37      TYPE 40
40      FORMAT('+FREQUENCY NOT IN ACCEPTABLE RANGE, <CR> TO REENTER',$)
        ACCEPT 190,ICHR
        GO TO 26
```

DATA REDUCTION PROGRAM (Continued)

```
42      TYPE 45
45      FORMAT(' ENTER THE DATA COLLECTION RATE OF THE A/D CONVERTER
        1(.256 KHZ) ? ',$)
        ACCEPT 47,RATE
47      FORMAT(F7.4)
        IF(RATE.NE.0.0) GO TO 49
        RATE=.256
49      TYPE 50
50      FORMAT(' ENTER DURATION OF DAMPED OSCILLATION TEST (0.1 SEC
        1 TO 120.0 SEC) (16.0) ?',$)
        ACCEPT 55,TIME
55      FORMAT(F7.4)
        IF (TIME.GT.120.0) GO TO 57
        IF (TIME.GE.0.1) GO TO 59
57      TYPE 58
58      FORMAT('+TIME NOT IN ACCEPTABLE RANGE, <CR> TO REENTER',$)
        ACCEPT 190,ICHR
        GO TO 49
59      TYPE 60
60      FORMAT(' ENTER NUMBER OF SPECIFIC DAMPING VALUES TO BE COMPUTED
        1 (MAX OF 100) ? ',$)
        ACCEPT 65,N
65      FORMAT(I6)
C CHECK THE NUMBER OF SPECIFIC DAMPING VALUES TO BE COMPUTED
C FOR VALIDITY. MAX NUMBER OF VALUES THAT CAN BE
C COMPUTED DEPENDS ON SAMPLING RATE AND DURATION OF TEST
        NPTS=1000*RATE*TIME
        COUNT=NPTS/N
        IF(COUNT.GE.20) GO TO 82
        IF(COUNT.GE.10) GO TO 77
        TYPE 75
75      FORMAT('+NOT ENOUGH DATA COLLECTED FOR SPECIFIED COMPUTATIONS, <CR>
        1 TO REENTER',$)
        ACCEPT 190,ICHR
        GO TO 59
77      TYPE 80
80      FORMAT(' WARNING-LESS THAN 20 POINTS USED PER  PEAK ESTIMATION')
82      TYPE 85,COUNT
85      FORMAT(' NUMBER OF POINTS/PEAK ESTIMATED =',I6)
C COMPUTE THE PEAK AND CYCLE VALUES
C
C NUMBUF IS TOTAL NUMBER OF RECORDS IN DATA FILE (NO. OF BUFFERS)
C BUFSIZ IS NUMBER OF WORDS PER RECORD (NO. OF SAMPLES PER BUFFER)
        DEFINE FILE 3(NUMREC,RECSIZ,U,INDEXR)
        READ(3'INDEXR,END=160,ERR=170)(DATA(K),K=1,RECSIZ)
        DO 91 K=1,RECSIZ
91      DATA(K)=DATA(K)-2048
        PAGE=1
        RECORD=0
        TYPE 96
        ACCEPT 190,ICHR
        IF(ICHR.NE.YES) GO TO 93
        TYPE 97,PAGE
        WRITE(5,100)(DATA(K),K=1,RECSIZ)
93      DO 150 I=1,N+1
        PEAK(I)=0
        NCYC(I)=0
        DO 120 J=1,COUNT
```

DATA REDUCTION PROGRAM (Continued)

```
        IF (RECORD.LT.RECSIZ) GO TO 110
        READ(3'INDEXR,END=180,ERR=170)(DATA(K),K=1,RECSIZ)
        DO 94 K=1,RECSIZ
94      DATA(K)=DATA(K)-2048
95      PAGE=PAGE+1
        RECORD=0
96      FORMAT(' DO YOU WANT A LISTING OF DATA COLLECTED BY A/D  (Y/N) ?
        1',$)
        IF (ICHR.NE.YES) GO TO 110
        TYPE 97,PAGE
97      FORMAT(' RECORD NUMBER ',I6)
        WRITE(5,100)(DATA(K),K=1,RECSIZ)
100     FORMAT( 16(1H ,I6))
C FIND THE PEAK AND CYCLE NUMBER OF THIS GROUP OF POINTS
110     RECORD=RECORD+1
D       WRITE(5,115)I,J,RECORD,DATA(RECORD),PEAK(I)
115     FORMAT( 3(I3,3H   ),2(I6,2H   ))
        IF (DATA(RECORD).LE.PEAK(I)) GO TO 120
        PEAK(I)=DATA(RECORD)
        NCYC(I)=(I*COUNT+J)*FREQ/RATE
120     CONTINUE
150     CONTINUE
        GOTO 200
C COMPUTATION PROBLEMS
155     TYPE 157,N
157     FORMAT(' NUMBER OF PEAK ESTIMATES= ',I6)
160     TYPE 165
165     FORMAT(' END OF DATA FILE')
        GOTO 200
170     TYPE 175
175     FORMAT(' READ ERROR IN INPUT FILE')
        GO TO 200
180     DO 182 L=K,RECSIZ
182     DATA(L)=0
        GOTO 95
200     DO 203 I=2,N+1
203     NCYC(I)=NCYC(I)-NCYC(1)
        TYPE 205
205     FORMAT(' DO YOU WANT A PRINTOUT OF THE PEAK VALUES COMPUTED (Y/N)
        1 ?',$)
        ACCEPT 190,ICHR
190     FORMAT(A1)
        IF (ICHR.NE.YES) GO TO 210
        DO 207 I=2,N+1
        WRITE(5,209)NCYC(I),PEAK(I)
209     FORMAT(' CYCLES FROM INITIAL PEAK #=',I6,'  PEAK VALUE=',I6)
207     CONTINUE
C
C
C COMPUTE THE LOGARITHMIC DECREMENTS
C
C
C COMPUTE LOG DECREMENTS AND SPECIFIC DAMPING VALUES
C
210     STAT1=0
        STAT2=0
        K=0
        LDEC(1)=FLOAT(PEAK(1))
        WRITE(5,215)LDEC(1),NCYC(1)
```

DATA REDUCTION PROGRAM (Concluded)

```
215     FORMAT(' INITIAL PEAK =',F7.1,'  CYCLE OF PEAK VALUE =',I6)
        DO 250 I=2,N+1
        LDEC(I)=FLOAT(PEAK(I))
        FCYC(I)=FLOAT(NCYC(I))
        IF(LDEC(I).GE.0.0) GOTO  220
        K=K+1
C COUNT THE NUMBER OF ZERO PEAK VALUES
        GOTO 250
220     LDEC(I)=(1.0/FCYC(I))*ALOG(LDEC(1)/LDEC(I))
        SDAMP(I)=1.0-EXP((-2.0)*LDEC(I))
        STAT1=STAT1+SDAMP(I)
        STAT2=STAT2+(SDAMP(I)*SDAMP(I))
250     CONTINUE
C
C PRINTOUT ROUTINES
C
C
        TYPE 260
260     FORMAT(' DO YOU WANT A PRINTOUT OF IMTERMEDIATE VALUES (Y/N) /',$)
        ACCEPT 265,ICHR
265     FORMAT(A1)
        IF(ICHR.NE.YES) GO TO 300
        N=N-K
        DO 275 I=2,N+1
        LDEC(I)=10000.*LDEC(I)
        SDAMP(I)=10000.*SDAMP(I)
        WRITE(5,270)I,LDEC(I),SDAMP(I)
270     FORMAT(' EST # ',I3,' LOG DEC =',F5.1,'*E4   SDAMP =',F5.1,'*E4')
275     CONTINUE
C
C
300     STAT3=STAT1/N
        STAT4=(1.0/(N-1.0))*SQRT(STAT2-((1/N)*STAT1*STAT1))
        STAT3=STAT3*10000.
        STAT4=STAT4*10000.
        WRITE(5,305)NAME
305     FORMAT('0','***** TEST MATERIAL IS  ',15A1,'  *****')
        TYPE 307,FATIG
307     FORMAT(' NUMBER OF FATIGUE CYCLES IS ',I6)
        WRITE(5,310)STAT3,STAT4
310     FORMAT('0','MEAN SDAMP =',F5.1,'*E4  S.D. =',F5.1,'*E4')
        STOP
        END*
```

DATA REDUCTION ABBREVIATED

```
.^C

.R SAM


..R PEG
   DATA ANALYSIS PROGRAM 'PEG' FORTRAN PROGRAM
ENTER THE NAME OF DATA FILE /<DX0:SAMDAT.DAT> ?*DX1:SAMDAT.DAT

ENTER THE NAME OF THE TEST MATERIAL (15 LETTERS) ?PIPE

ENTER THE NUMBER OF FATIGUE CYCLES (1 TO 10E6) ?3

ENTER THE NUMBER OF DATA BUFFERS COLLECTED (16) ? 16

ENTER THE NUMBER OF DISK BLOCKS PER BUFFER (1) ? 1

ENTER THE FREQUENCY OF OSCILLATION RECORDED (.0001 KHZ TO 2.5 KHZ) (.340)  ?.461

ENTER THE DATA COLLECTION RATE OF THE A/D CONVE$TER (.256 KHZ) ? 0.122

ENTER DURATION OF DAMPED OSCILLATION TEST (0.1 SEC TO 120.0 SEC) (16.0)  ?16.

ENTER NUMBER OF SPECIFIC DAMPING VALUES TO BE COMPUTED (MAX OF 100) ? 100

WARNING-LESS THAN 20 POINTS USED PER  PEAK ESTIMATION
NUMBER OF POINTS/PEAK ESTIMATED =     19
DO YOU WANT A LISTING OF DATA COLLECTED BY A/D  (Y/N) ?

DO YOU WANT A PRINTOUT OF THE PEAK VALUES COMPUTED (Y/N) ?

INITIAL PEAK = 1886.0  CYCLE OF PEAK VALUE =     83
DO YOU WANT A PRINTOUT OF IMTERMEDIATE VALUES (Y/N) /


***** TEST MATERIAL IS  PIPE                *****
NUMBER OF FATIGUE CYCLES IS      3

MEAN SDAMP =  6.2*E4  S.D. =  0.6*E4
STOP --
```

APPENDIX E

GLOSSARY

Braided Rope	Rope constructed by braiding or interweaving strands together.
Breaking Strength	The axial load applied to a rope which results in rupture.
Design Load	The maximum load which should be applied to a rope consistent with the factor of safety for the type of rope use.
Directional Valve	Electro-mechanical system that provides for the diversion of flow of hydraulic fluid to either side of the power cylinder.
Double-Braid Rope	A rope consisting of a hollow core of many braided strands enclosed in a cover of many braided strands.
Eight-Strand Rope	A rope consisting of two pairs of strands twisted to the right and two pairs of strands twisted to the left and braided together such that pairs of strands of opposite twist alternately overlay one on another.
Electro-hydraulic Loading Apparatus	An electronically controlled mechanical system which actuates the power cylinder for loading the synthetic rope in tension.
End Fittings	Mechanical system for transferring axial loads from the loading frame to the synthetic rope specimens.
Epoxy	A class of synthetic resins characterized by having a highly active oxirane ring which incorporates into the two part mixture selected desirable mechanical properties.
Factor of Safety	The ratio of the rated breaking strength of a new rope to the design load.
Frequency Analyzer	Electronic equipment capable of conditioning an output signal from the magnetic transducer by selective filtering and amplification.

Frequency Counter	Electronic device for counting peak signals during specified interval.
Function Generator	Electronic instrument for generating a sine wave of specified frequency and amplitude.
Hawser	The mooring rope between an SPM and a moored vessel. Generally any large rope 40 mm or more in diameter (>5 inches circumference).
Internal Friction Damping	Phenomenon by which the total dislocation density in a specimen may be counted.
Log Decrement Decay	Output response of the full wave attenuated signal measured over a period of time.
Magnetic Transducers (Input and Output)	The electronic device for transferring the input impulse from the frequency oscillator to the synthetic rope specimen. Output transducer magnetically captures response signal from synthetic rope specimen and passes signal on to the frequency analyzer.
Moment of Inertia	With respect to an axis, the moment of inertia is the sum of the products obtained by multiplying each element of an area by the square of its distance from the axis.
Nylon	Generic name for long-chain polymeric amide molecules in which recurring amide groups are part of the main polymer chain.
Oscillator	Electronic equipment capable of producing a constant sine wave of varying frequency and amplitude.
Overstress	Load in excess of the upper limit of the linear elastic range of the material.
Polyester	A thermosetting synthetic resin made by esterification of polybasic organic acids with polyhydric acids.
Polypropylene	A crystalline, thermo-plastic resin made by the polymerization of propylene, C_3H_6.

Radius of Gyration	With respect to a given axis, the square root of the moment of inertia divided by the area.
Rope Size	In hawsers, the rope size is defined as the circumference rather than the diameter.
Rope Support and Tensioning Apparatus	The loading frame that supports the synthetic rope and applies the axial load through the special end fittings.
Specific Damping Capacity	The phenomenon of internal friction which is a thermal relaxation process.
Single Point Mooring (SPM)	A mooring and cargo transfer system for vessels including a mooring swivel and a cargo transfer swivel, in which at one point either the cargo transfer swivel is concentric with the mooring-load-carrying system or the mooring swivel is concentric with the cargo transfer system such that the moored vessel may swing completely around the mooring point while transferring cargo.
Three-Strand Rope	A rope consisting of three strands twisted together in a spiral pattern.
Viscoelasticity	Compound relationship of stress and the resultant strain wherein a phase lag angle of the response is noted. The mechanical model of viscoelasticity is a series of springs in parallel with dash pots.

APPENDIX F

MATERIAL PROPERTIES

PROPERTIES OF SYNTHETIC FIBERS	
Chemical Class	Nylon
Resin Type	Thermoplastic
Subclass or Modification	6/6
FORMS AVAILABLE Cs—castings, F—film, Fb—fibers, I—impregnants, L—laminations, Lq—lacquers, Mf—monofilaments, P—Powder, pellet, or granules, R—rods, tubes, or other extruded forms, S—sheets.	F, Fb, Mf, P, R, S
FABRICATION Cl—calendering, Cs—casting, E—extrusion, F—hot forming or drawing, I—impregnation, MB—blow molding, MC—compression molding, MI—injection molding, S—spreading.	E, F, MB, MC, MI
ELECTRICAL PROPERTIES	
D.C. Resistivity, ohm-cm	.....
Dielectric constant, 60 cps	4.0–4.6
Dielectric constant, 10^6 cps	3.4–3.6
Dissipation factor, 60 cps	0.014–0.04
Dissipation factor, 10^6 cps	0.04
MECHANICAL PROPERTIES	
Modulus of elasticity, 10^3 psi	.....
Tensile strength, psi	9,000–12,000
Ultimate elongation, %	60–300
Yield stress, psi	.....
Yield strain, %	.....
Rockwell hardness	R 108–R 120
Notched Izod impact strength, ft.lb/in	1.0–2.0
Specific gravity	1.13–1.15
THERMAL PROPERTIES	
Burning rate	Self extinguishing
Heat distortion 264 psi, °C	.....
Specific heat, cal/g	0.4
Linear thermal expansion coefficient, 10^{-5}, °C	8.0
Maximum continuous service temperature, °C	80–150
CHEMICAL RESISTANCE	
Mineral acids, weak	Very good
Mineral acids, strong	Poor
Oxidizing acids, concentrated	Poor
Alkalies, weak	No effect
Alkalies, strong	No effect
Alcohols	Good
Ketones	Good
Esters	Good
Hydrocarbons, aliphatic	Very good
Hydrocarbons, aromatic	Fair to good
Oils, vegetable, animal, mineral	Good

PROPERTIES OF SYNTHETIC FIBERS

Chemical Class	Polypropylene
Resin Type	Thermoplastic
Subclass or Modification	Copolymer
FORMS AVAILABLE Cs—castings, F—film, Fb—fibers, I—impregnants, L—laminations, Lq—lacquers, Mf—monofilaments, P—Powder, pellet, or granules, R—rods, tubes, or other extruded forms, S—sheets.	F, Fb, Mf, P, R, S
FABRICATION Cl—calendering, Cs—casting, E—extrusion, F—hot forming or drawing, I—impregnation, MB—blow molding, MC—compression molding, MI—injection molding, S—spreading	Cl, E, F, MB, MC, MI
ELECTRICAL PROPERTIES	
D.C. Resistivity, ohm-cm	10^{17}
Dielectric constant, 60 cps	2.3
Dielectric constant, 10^6 cps	2.3
Dissipation factor, 60 cps	0.0001–0.0005
Dissipation factor, 10^6 cps	0.0001–0.002
MECHANICAL PROPERTIES	
Modulus of elasticity, 10^3 psi	.....
Tensile strength, psi	2,900–4,500
Ultimate elongation, %	200–700
Yield stress, psi	.....
Yield strain, %	.....
Rockwell hardness	R 50–R 96
Notched Izod impact strength, ft.lb/in	1.1–12
Specific gravity	0.90
THERMAL PROPERTIES	
Burning rate	Medium
Heat distortion 264 psi, °C	.....
Specific heat, cal/g	0.5
Linear thermal expansion coefficient, 10^{-5}, °C	8–10
Maximum continuous service temperature, °C	190–240
CHEMICAL RESISTANCE	
Mineral acids, weak	Excellent
Mineral acids, strong	Excellent
Oxidizing acids, concentrated	Poor
Alkalies, weak	Excellent
Alkalies, strong	Good
Alcohols	Good below 80°C
Ketones	Good below 80°C
Esters	Good below 80°C
Hydrocarbons, aliphatic	Good below 80°C
Hydrocarbons, aromatic	Good below 80°C
Oils, vegetable, animal, mineral	.....

U.S. GOVERNMENT PRINTING OFFICE 1979 -633-019/303